

# Book of Abstracts



**CMPNC 2019**

Condensed Matter Physics  
National Conference



**8-10 May, 2019**

**Faculdade de Ciências, Universidade do Porto**

SPONSORS



Universidade do Minho



**COMMITTEES**

**ORGANIZING COMMITTEE**

JOAQUIM AGOSTINHO MOREIRA, CHAIRMAN – UNIVERSITY OF PORTO

BRNARDO GONÇALVES ALMEDIA, CHAIRMAN – UNIVERSITY OF MINHO

JOSÉ LUÍS MARTINS, CO-CHAIRMAN - UNIVERSIDADE DE LISBOA – IST

**SCIENTIFIC COMMITTEE**

ELVIRA FORTUNATO - UNIVERSIDADE NOVA DE LISBOA

JOÃO LOPES DOS SANTOS - UNIVERSIDADE DO PORTO

JOSÉ ANTÓNIO PAIXÃO - UNIVERSIDADE DE COIMBRA

MARGARIDA TELLO DA GAMA - UNIVERSIDADE DE LISBOA - FCUL

MARGARIDA GODINHO - UNIVERSIDADE DE LISBOA - FCUL

NUNO PERES - UNIVERSIDADE DO MINHO

PAULO FREITAS - UNIVERSIDADE DE LISBOA – IST

VAN DER KEES - DIRECTOR CONDENSED MATTER PHYSICS DIVISION, EPS

VÍTOR AMARAL - UNIVERSIDADE DE AVEIRO

JOSÉ LUÍS MARTINS - UNIVERSIDADE DE LISBOA – IST

## OUTLINE

GENERAL INFORMATION .....	6
HOW TO REACH FACULDADE DE CIENCIAS DA UNIVERSIDADE DO PORTO .....	7
SCIENTIFIC PROGRAM .....	9
INVITED LECTURES.....	12
Topological matter: effects of disorder and interactions .....	13
Nonlinear Optics as a probe of Condensed Matter systems .....	14
Circularly Polarized Light Detection using Cellulose Nanocrystals Photonic Dielectrics .....	15
Influence of Matrix Rigidity on Blood Vessel Growth.....	16
Non-equilibrium collective dynamics of colloidal particles .....	17
Advances in spintronic sensor materials and architectures .....	18
Triboelectric nanogenerators: from fundamental concepts to applications in harsh environments ....	19
EPS YOUNG MINDS PROJECT .....	20
ORAL CONTRIBUTIONS .....	22
Chalcogenides the Playground Materials on Condensed Matter Physics: From Quantum Effects to Technological Applications .....	23
Quantum Effects in Electrical Transport Properties of Bismuth Chalcogenides Topological Insulators	24
Temperature-Driven Gapless Topological Insulator .....	25
Non-linear optical response in disordered 2D materials .....	26
Practical band interpolation with a generalised Luttinger-Kohn method .....	27
Theoretical calculations of nonlinear optical responses of 2D materials.....	28
Berry curvature anisotropy and spin current routing in graphene under lateral spin-orbit-coupled superlattice potentials .....	29
Bose-Einstein Condensation of Photons in a Plasma.....	30
Magneto-optical Kerr effect in two-dimensional diluted magnetic transition metal dichalcogenide semiconductors.....	31
Barrier model in muon implantation and application to Lu <sub>2</sub> O <sub>3</sub> .....	32
Narrow Optical Gap Ferroelectric Bi <sub>2</sub> ZnTiO <sub>6</sub> Thin Films Deposited by RF Sputtering.....	33
Structural distortions role on the high-pressure structural transitions and low-temperature magnetic transitions of RFeO <sub>3</sub> .....	34
Hematite nanowires for PEC hydrogen production: the effect of Ti dopant and temperature .....	35
On the conductivity of isolated single wall carbon nanotubes from Ab Initio quantum simulations ....	36
Optimization of electron beam lithography parameters for dense arrays of circular and hexagonally shaped antidots in magnetic thin films.....	37
Resistive Switching of Pt/MgO/M/Ru (M = Ta, Al, Cu, Ag) structures .....	38
Simulation of the temperature profile of BaCaZrTiO <sub>3</sub> thin films during laser annealing.....	39

Gentle Probe AFM: A non-contact method for measuring the viscoelasticity of soft materials.....	40
The effect of diffusion timescales in linker-mediated aggregation .....	41
Enhanced propagation of motile bacteria on surfaces due to forward scattering .....	42
A systematic analysis of cell migration in silicon .....	43
Interaction anisotropy in particle deposition at the edges of drying drops .....	44
Large magnetoelectric coupling observed at room temperature in a chiral lanthanide complex.....	45
Local probe studies and combined ab-initio calculations in $\text{Ca}_3\text{Mn}_2\text{O}_7$ .....	46
Tetragonal Ferroelectric Phase of $\text{GdMnO}_3$ Epitaxial Thin Film Grown onto $\text{SrTiO}_3$ (001).....	47
Multiferroic $\text{CoFe}_2\text{O}_4/\text{LiNbO}_3$ Bilayers.....	48
Acoustically-Powered Microspinners .....	49
Stability of the nematic-isotropic interface of active liquid crystals in a microchannel.....	50
Ordering of Binary Colloidal Crystals by Random Potentials.....	51
Modelling of molecular-scale properties and viscosity of polyisocyanate liquids .....	52
Dynamics of the carbon vacancy in 4H-SiC: a theoretical description .....	53
Ballistic transport in micro-structured bilayer graphene flakes .....	54
Electronic properties of incommensurate van der Waals structures.....	55
Exciton-polaritons in a cylindrical microcavity with an embedded 2D semiconductor layer.....	56
Tuning of Magnetic Activity in Spin-Filter Josephson Junctions Towards Spin-Triplet Transport.....	57
A floating buoy-based triboelectric nanogenerator for maritime applications .....	58
Design of a Microfabrication Protocol Adapting Reactive Ion Etching for Organic Single Crystal-based Photosensors .....	59
Effects of oxygen ion implantation on the structural and electrical properties of $\alpha\text{-MoO}_3$ lamellar crystals .....	60
Ion beam induced current analysis in GaN microwires .....	61
Magnetization change upon illumination: the $\text{Ln}(\text{F}_{20}\text{TPIP})_3$ series .....	62
Impact of atomic disorder on the thermodynamic properties of ferromagnetic $\text{Fe}_2\text{MnSi}$ – a computational study.....	63
Emergence of edge-magnetism in transition metal dichalcogenide nanoribbons.....	64
Magnetic Nanoparticles for Hyperthermia.....	65
Ultrafast Magnetization Dynamics of $[\text{CoFeB}/\text{Pd}]_5/\text{Co}$ Exchange Spring.....	66
Structures.....	66
POSTER COMMUNICATIONS .....	67
P01 - 3D C60 polymers with ordered binary-alloy type structures investigated via DFT .....	68
P02 - Actuation of Magnetoelastic Membranes in Dynamic Magnetic Fields.....	69
P03 - Adsorption of oxygen on metal-semiconductor Zn/ZnO core shell nano-structures.....	70

P04 - Binary Mixture of Locally Coupled Brownian Oscillators.....	71
P05 - Classical and quantum liquids induced by quantum fluctuations .....	72
P06 - Collective dynamics of flexible active particles on substrates: from cells to tissues .....	73
P07 - Comparison between the full non-linear optical response in time and the perturbation theory in graphene .....	74
P08 - Dynamics of Active Polymer Networks.....	75
P9 - Dynamics of epithelial tissues on heterogeneous substrates .....	76
P10 - Electronic Properties of Twisted Bilayer Graphene in the Presence of a Magnetic Field .....	77
P11 - Energy loss by fast-traveling charged particles traversing two-dimensional materials .....	78
P12 - Enhanced localization and protection of topological edge states due to geometric frustration..	79
P13 - Equation of State of Active Colloidal Particles.....	80
P14 - Excitation of Graphene Plasmons by Quantum Emitters .....	81
P15 - Hole localized states in interacting geometrically frustrated systems .....	82
P16 - Magnetic behavior in multi-segmented nanowires of Fe/Cu with different number of layers ....	83
P17 - Magnetic studies of monoclinic $\text{Cu}_4\text{O}(\text{SeO}_3)_3$ , a copper-oxo-selenite derivative .....	84
P18 - Measuring nanoscale interactions with Force Feedback Microscopy.....	81
P19 - Micromagnetic study of the vortex state in sub-micron iron discs .....	82
P20 - Mixed-order symmetry-breaking quantum phase transition far from equilibrium .....	83
P21 - Modeling of Wound Closure in Epithelial Tissue .....	84
P22 - Muon implantation experiments in semiconductor films: characterization of depth resolution.	85
P23 - $\text{Na}_2\text{Ti}_3\text{O}_7$ nanotubes by hydrothermal method.....	86
P24 - Nonlinear optical conductivity of graphene in the independent electron approximation .....	87
P25 - The Kernel Polynomial Approximations of the Thouless Formula .....	88
P26 - Non-linear optical response of hexagonal boron nitride with a magnetic field .....	89
P27 - Non-steady flows in porous media .....	90
P28 - Numerical Simulation of Non-Equilibrium Stationary Current Through Nano-Scale 1D Chains ...	91
P29 - Perturer Angular Correlation Studies On Ferroelectric $\text{Ca}_3\text{Ti}_2\text{O}_7$ .....	93
P30 - Perturbed Angular Correlation Study of $\text{SrMnGe}_2\text{O}_6$ and $\text{CaMnGe}_2\text{O}_6$ .....	94
P31 - Phase Separation of Active Brownian Systems .....	95
P32 - Piezoelectric response tailoring of $\text{K}_{0.5}\text{Na}_{0.5}\text{NbO}_3$ using different sintering methods .....	96
P33 - Probing the structural properties of a solar-cell p-n interface using implanted positive muons .	97
P34 - Self-propelled motion of flexible particles through tortuous channels .....	98
P35 - Simulation of the formation and swelling of polyurethane-based nanogels .....	99
P36 - Spectral and Steady-State Properties of Random Liouvillians.....	100
P37 - Square-Root Topological Insulators: an example using ultracold atoms .....	101

**CMPNC 2019**

P38 - Structural and magnetic properties of Ca and Mn co-substituted multiferroic BiFeO <sub>3</sub> near the MPB region .....	102
P39 - Study of Spin-valve Sensors grown on Polymeric Substrates.....	103
P40 - Study of sub-volume activation in CoFeB/MgO memory devices near spin reorientation transition .....	104
P41 - Terahertz Frequency Comb in Graphene Field-Effect Transistors.....	105
P42 - The shape of liquid bridges.....	106
P43 - Transport through periodically driven systems.....	107
P44 - $\mu$ -Thermoelectric Devices Based on Hybrid Bi <sub>2</sub> Te <sub>3</sub> /PVA Composites .....	108
P45 - Tuning the magnetoelectric coupling in TbMnO <sub>3</sub> by Fe-chemical substitution .....	109
P46 - Broadband third-harmonic generation in multilayer graphene for the characterization of near single-cycle ultrashort light pulses.....	110
P47 - EPR and ab-initio studies of erbium(III) SIMs .....	111
P48 - Synthesis Optimization of Zn-Mn Ferrites for Ferrofluid Applications.....	112

## **GENERAL INFORMATION**

### **WIRELESS**

dfa.wifi.3@fc.up.pt

Password: DfaD2019

### **LUNCH**

Participants can have lunch at FCUP Cantine, next to the Department of Biology. The mean price is 4.50 €. The participants have other choices nearby the Faculty of Sciences.

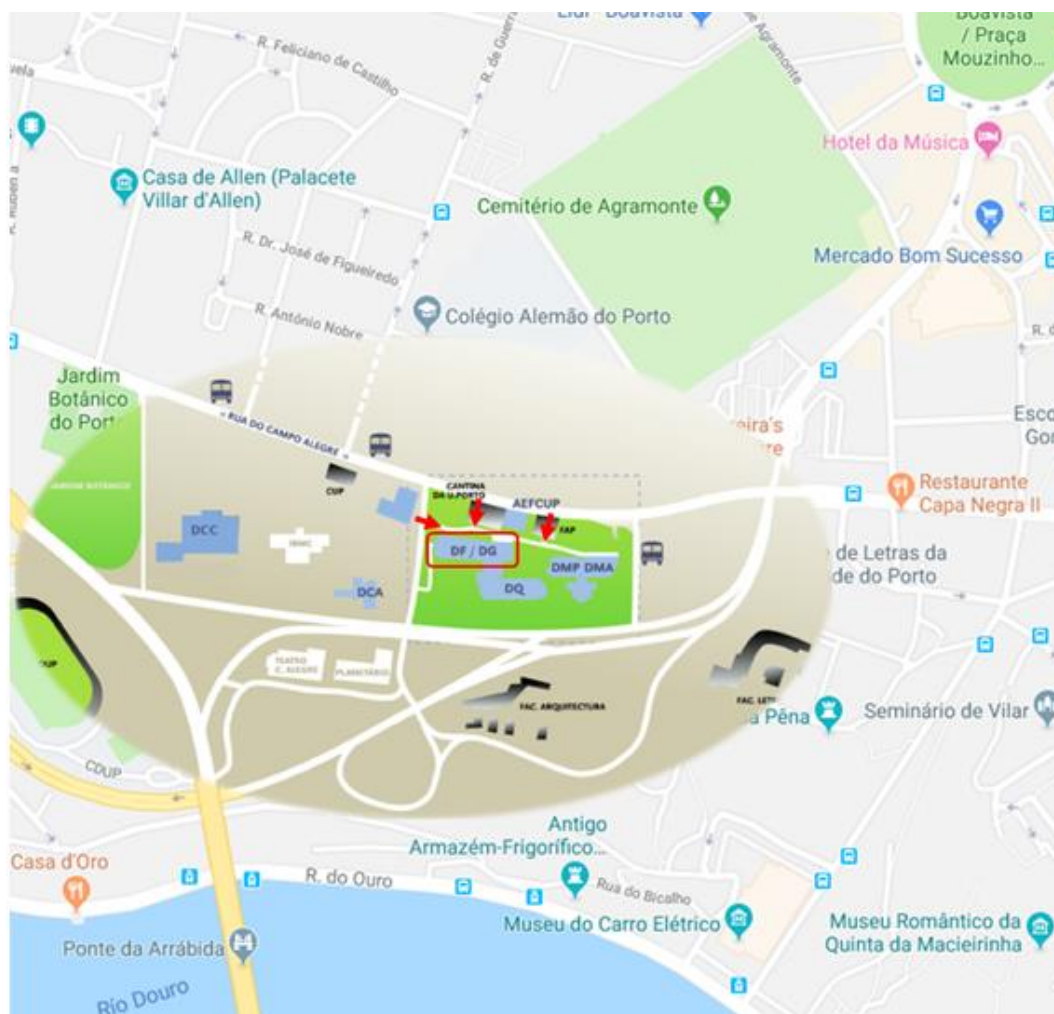
### **PROCEEDINGS**

Peer-reviewed paper will be published in the EPJ Web of Conferences journal (<https://www.epj-conferences.org/>). Authors are invited to submit a 5 pages length papers.

EPJ Web of Conferences is an open access proceedings in Physics and Astronomy and is dedicated to archiving conference proceedings from the whole spectrum of pure and applied physics.



## HOW TO REACH FACULDADE DE CIENCIAS DA UNIVERSIDADE DO PORTO



### Road

Motorways connect Porto to Lisbon (A1), Minho (A3) and Trás-os-Montes (A4), and a major highway connects Porto to Valença (A28).

### Rail

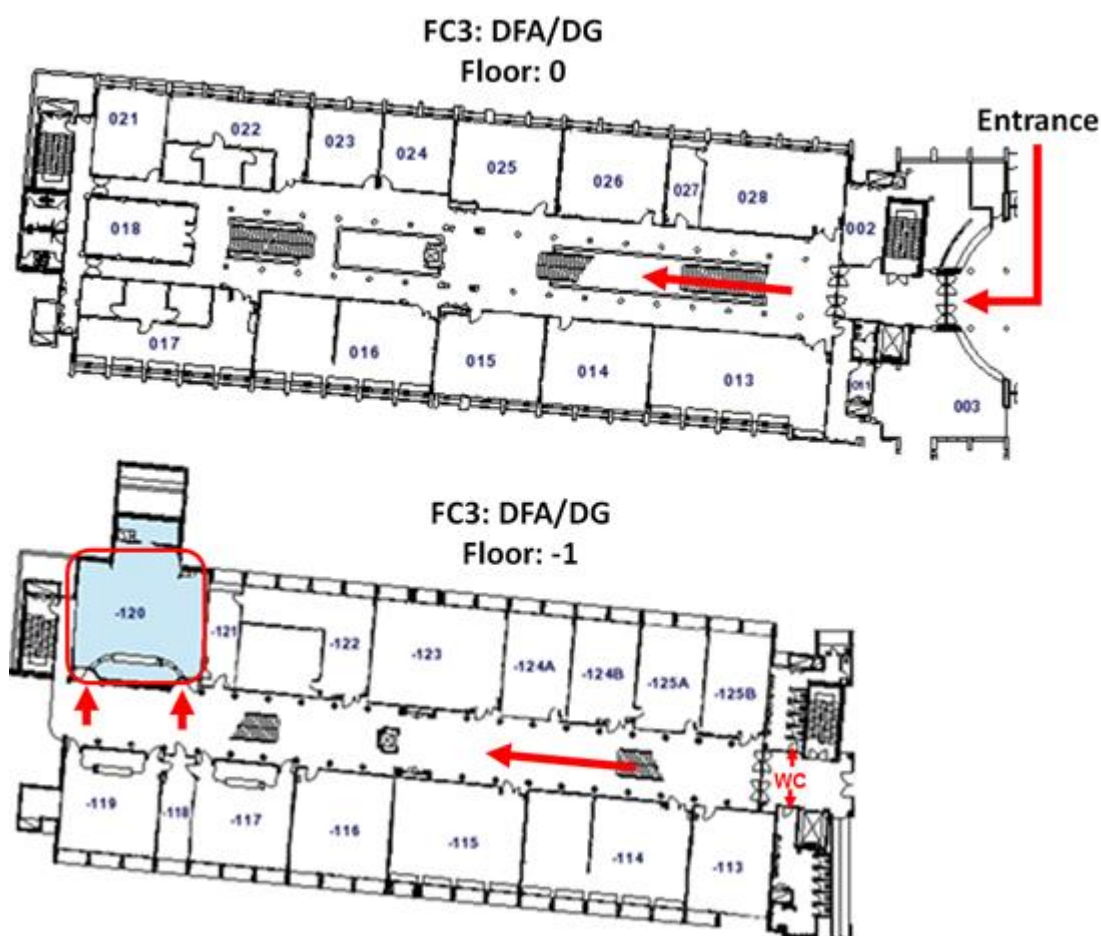
You can travel to Porto by train CP, the Portuguese Railway Company, has regular international links. The city of Porto is served by two main stations: Campanhã Station (for international journeys, but also for journeys to Lisbon, Douro and Minho); and S. Bento Station (for urban and regional connections and connections to Galicia).

### Urban Transport

Within the city limits, public transport services are mainly provided by bus (STCP) and Metro (Metro do Porto).

Board lines 200, 204, 207, 209 and 1M also pass through "Planetário" bus stop, please visit the STCP webpage timetable information.

Find out more about [Transportation in the city of Porto](#).



Inside FCUP, go to **FC3: Department of Physics and Astronomy (DFA)** and Department of Geology (DG).

At the circular entry hall, **turn right**, go through both doors and **descend the stairs** to the -1 floor.

At the -1 floor, go **straight forward**, the conference will take place in the **room -1.20**, the **last one at your right**.

The **Exhibition Hall** will be in the -1.15 and -1.16 rooms, at the same floor.

For **toilet facilities (WC)**, turn backwards after descending the stairs and go through the doors.

## SCIENTIFIC PROGRAM

Wednesday 8 may	
08:00	Registration
09:00	Opening Session
09:30	Topological matter: effects of disorder and interactions Eduardo V Castro
10:15	Chalcogenides the Playground Materials on Condensed Matter Physics: From Quantum Effects to Technological Applications A. L. Pires, Ferreira-Teixeira, E. M. F. Vieira, J. Silva, J.P Araújo, L. Gonçalves, W. R. Branford, L. Cohen, A. M. Pereira
10:30	Quantum Effects in Electrical Transport Properties of Bismuth Chalcogenides Topological Insulators J.A. Paixão, M.S.C. Henriques, C. Micale, E.B. Lopes, V.M.M. Pereira, A.P. Gonçalves
10:45	Temperature-Driven Gapless Topological Insulator Miguel Gonçalves, Pedro Ribeiro, Rubem Mondaini and Eduardo V. Castro
11:00	Coffee Break and Posters
11:30	Non-linear optical response in disordered 2D materials S. M. João, J. M. Viana Parente Lopes
11:45	Practical band interpolation with a generalised Luttinger-Kohn method Carlos L. Reis and José Luís Martins
12:00	Theoretical calculations of nonlinear optical responses of 2D materials G. B. Ventura, D. J. Passos, J. M. Viana Parente Lopes, J. M. B. Lopes dos Santos
12:15	Berry curvature anisotropy and spin current routing in graphene under lateral spin-orbit-coupled superlattice potentials L. M. Martelo and A. Ferreira
12:30	Lunch
14:00	Nonlinear Optics as a probe of Condensed Matter systems Michael Belsley
14:45	Bose-Einstein Condensation of Photons in a Plasma H. Terças
15:00	Magneto-optical Kerr effect in 2D diluted magnetic transition metal dichalcogenide semiconductors G. Catarina, N. M. R. Peres, and J. Fernández-Rossier
15:15	Barrier model in muon implantation and application to $\text{Lu}_2\text{O}_3$ R. C. Vilão, R. B. L. Vieira, H. V. Alberto, J. M. Gil, A. Weidinger, R. L. Lichti, P. W. Mengyan, B. B. Baker, and J. S. Lord
15:30	Narrow optical gap of $\text{Bi}_2\text{ZnTiO}_6$ thin films deposited by RF sSputtering F. G. Figueiras, J. R. A. Fernandes, J. P. B. Silva, D. O. Alikin, E. C. Queirós, C. R. Bernardo, Y. R.-Barcelay, A. Wrzesińska, M. S. Belsley, B. Almeida, P. B. Tavares, A. L. Kholkin, J. Agostinho Moreira, A. Almeida
15:45	Coffee Break and Posters
16:15	Circularly Polarized Light Detection using Cellulose Nanocrystals Photonic Dielectrics L. Pereira
17:00	Structural distortions role on the high-pressure structural transitions and low-temperature magnetic transitions of $\text{RFeO}_3$ R. Vilarinho, M. Guennou, P. Bouvier, M. C. Weber, I. Peral, P. Tavares, G. Garbarino, M. Mezouar, J. Kreisel, A. Almeida and J. Agostinho Moreira
17:15	Hematite nanowires for PEC hydrogen production: the effect of Ti dopant and temperature P. Quitério, A. Apolinário, C. T. Sousa, P. Dias, J. Azevedo, A. M. Mendes, and J. P. Araújo
17:30	On the conductivity of isolated single wall carbon nanotubes from <i>Ab Initio</i> quantum simulations Jaime Silva, Bruce F. Mine, and Fernando Nogueira
17:45	Optimization of electron beam lithography parameters for dense arrays of circular and hexagonally shaped antidots in magnetic thin films Pedro D. R. Araújo, A. V. Silva, S. Cardoso and D. C. Leitao
18:00	Resistive Switching of $\text{Pt/MgO/M/Ru}$ ( $M = \text{Ta, Al, Cu, Ag}$ ) structures C. Dias, H. Lv, S. Cardoso, and J. Ventura
18:15	Simulation of the temperature profile of $\text{BaCaZrTiO}_3$ thin films during laser annealing T. Rebelo and B. G. Almeida
18:30	Posters

Thursday 9 may	
08:30	Registration
09:00	Influence of Matrix Rigidity on Blood Vessel Growth Rui Travasso
09:45	Gentle Probe AFM: A non-contact method for measuring the viscoelasticity of soft materials M. S. Rodrigues
10:00	The effect of diffusion timescales in linker-mediated aggregation J. M. Tavares, G. C. Antunes, C. S. Dias and N. A. M. Araújo
10:15	Enhanced propagation of motile bacteria on surfaces due to forward scattering Vasco C. Braz, Giorgio Volpe and Nuno A.M. Araújo
10:30	A Systematic analysis of cell migration in silicon M. Moreira-Soares, S. Pinto-Cunha, J. R. Bordin, Rui D. M. Travasso.
10:45	Interaction anisotropy in particle deposition at the edges of drying drops C. S. Dias, M. M. Telo da Gama and N. A. M. Araújo
11:00	Coffee Break and Posters
11:30	Large magnetoelectric coupling observed at room temperature in a chiral lanthanide complex M. S. Ivanov, J. Long, V. A. Khomchenko, J.-M. Thibaud, Y. Guari, J. Larionova, and J. A. Paixão
11:45	Local probe studies and combined ab-initio calculations in $\text{Ca}_3\text{Mn}_2\text{O}_7$ P. Rocha-Rodrigues, G. P. Oliveira, S.S. M. Santos, I. P. Miranda, T. Leal, R. Moreira, L. V. C. Assali, H. M. Petrilli, J. G. Correia, J. P. Araújo and A.M. L. Lopes
12:00	Tetragonal Ferroelectric Phase of $\text{GdMnO}_3$ Epitaxial Thin Film Grown onto $\text{SrTiO}_3$ (001) P. Machado, F. G. Figueiras, R. Vilarinho, J. R. A. Fernandes, P. B. Tavares, M. Rosário Soares, S. Cardoso, A. Almeida and J. Agostinho Moreira
12:15	Multiferroic $\text{CoFe}_2\text{O}_4/\text{LiNbO}_3$ Bilayers B.M. Silva, J. Oliveira, J.A. Mendes and B.G. Almeida
12:30	Lunch
14:00	Non-equilibrium collective dynamics of colloidal particles Nuno A. M. Araújo
14:45	Acoustically-Powered Microspinnners M. Tasinkevych, M. Olvera de la Cruz, S. Sabrina, S. Ahmed, A. M. Brooks, T. E. Mallouk, and K. J. M. Bishop
15:00	Stability of the nematic-isotropic interface of active liquid crystals in a microchannel R. C. V. Coelho, N. A. M. Araújo and M. M. Telo da Gama
15:15	Ordering of Binary Colloidal Crystals by Random Potentials André S. Nunes, Sabareesh K. P. Velu, Iryna Kasianiuk, Denys Kasyanyuk, Agnese Callegari, Giorgio Volpe, Margarida M. Telo da Gama, Giovanni Volpe, and Nuno A. M. Araújo
15:30	Modelling of molecular-scale properties and viscosity of polyisocyanate liquids V. Lenzi, P. Driest, D. Dijkstra, M. M. D. Ramos and L. Marques
15:45	Coffee Break and Posters
16:15	Magnetoresistive devices : from magnetic field sensing to novel nanoscale radiofrequency components Ricardo Ferreira
17:00	Dynamics of the carbon vacancy in 4H-SiC: a theoretical description J. Coutinho, V. J. B. Torres, K. Demmouche, and S. Öberg
17:15	Ballistic transport in micro-structured bilayer graphene flakes Hadi Z. Olyafei, Pedro Ribeiro, Eduardo V. Castro
17:30	Electronic properties of incommensurate van der Waals structures B. Amorim, and Eduardo V. Castro
17:45	Exciton-polaritons in a cylindrical microcavity with an embedded 2D semiconductor layer J. N. Gomes, C. Trallero-Giner, N. M. Peres and M. I. Vasilevskiy
18:00	Tuning of Magnetic Activity in Spin-Filter Josephson Junctions Towards Spin-Triplet Transport R. Caruso, D. Massarotti, H. G. Ahmad, A. Miano, A. Pal, V.V. Bolginov, I. V. Vernik, V.V. Ryazanov, O. A. Mukhanov, M. G. Blamire, G. P. Pepe, and F. Tafuri
18:15	Posters and EPS Young Minds Meeting



Friday 10 may	
08:30	Registration
09:00	Advances in spintronic sensor materials and architectures S. Cardoso
09:45	A floating buoy-based triboelectric nanogenerator for maritime applications C. Rodrigues, R. Esteves, C. Duarte, L. Pessoa, A. Pereira and J. Ventura
10:00	Design of a Microfabrication Protocol Adapting Reactive Ion Etching for Organic Single Crystal-based Photosensors J. M. Serra, S. I. Sequeira, I. Domingos, A. P. Oliveira, E. Maçôas, S. Cardoso, H. Alves, D. C. Leitão
10:15	Effects of oxygen ion implantation on the structural and electrical properties of $\alpha$ -MoO <sub>3</sub> lamellar crystals D. R. Pereira, C. Díaz-Guerra, M. Peres, S. Magalhães, J. G. Correia, J. G. Marques, A. G. Silva, E. Alves, K. Lorenz, S. Cardoso, P. P. Freitas
10:30	Ion beam induced current analysis in GaN microwires D. Verheij, M. Peres, S. Cardoso, L.C. Alves, E. Alves, C. Durand, J. Eymery, J. Fernandes, and K. Lorenz
11:45	Coffee Break and Posters
11:15	Triboelectric nanogenerators: from fundamental concepts to applications in harsh environments J. Ventura
12:00	Magnetization change upon illumination: the Ln(F <sub>20</sub> TPIP) <sub>3</sub> series Maria Susano, Jaroslaw Rybusinski, Jacek Szczytko, Peter B Wyatt, Laura C.J. Pereira, Manuela Ramos Silva
12:15	Impact of atomic disorder on the thermodynamic properties of ferromagnetic Fe <sub>2</sub> MnSi – a computational study H. G. Trigo, J. N. Gonçalves, and J. S. Amaral
12:30	Emergence of edge-magnetism in transition metal dichalcogenide nanoribbons F. M. O. Brito, J. M. V. P. Lopes, and E. V. Castro
12:45	Magnetic Nanoparticles for Hyperthermia M. M. Cruz
13:00	Ultrafast Magnetization Dynamics of [CoFeB/Pd] <sub>5</sub> /Co Exchange Spring Structures A. S. Silva, S. P. Sá, S. Bunyaev, G. Kakazei, M. Canhota, M. Miranda, C. Garcia, I. J. Sola, H. Crespo, and D. Navas
13:15	Closing

# INVITED LECTURES

# **TOPOLOGICAL MATTER: EFFECTS OF DISORDER AND INTERACTIONS**

Eduardo V. Castro,<sup>1,\*</sup> Miguel Gonçalves,<sup>2</sup> Rubem Mondaini,<sup>3</sup> and Pedro Ribeiro<sup>2</sup>

<sup>1</sup>CF-UM-UP, DFA-FCUP, Universidade do Porto, 4169-007 Porto, Portugal

<sup>2</sup>CeFEMA, IST, Universidade de Lisboa, Av. Rovisco Pais, 1049-001 Lisboa, Portugal

<sup>3</sup>Beijing Computational Science Research Center, Beijing 100084, China

\*Corresponding Author: [evcastro@fc.up.pt](mailto:evcastro@fc.up.pt)

**Abstract.** The role of disorder, interactions and temperature on topological phases of matter is subtle and often presents dichotomic features. Understanding these effects is however essential to predict the topological properties and their stability in real-world materials. This is particularly relevant for 2D materials, where the low dimensionality typically enhances these effects. As an example of dichotomic behavior, topological phases are suppressed in the presence of strong local interactions [1], while some studies showed that interactions themselves could induce a topological phase on a trivial band [2,3]. The role of disorder is also subtle. For topological insulators with broken time-reversal symmetry, disorder effects localize every eigenstate except two bulk extended states that carry opposite topological numbers [4,5]. The merging of these states, for a sufficiently large disorder strength, is associated with the destruction of the topological phase. Interestingly, a disorder-induced transition into a new topologically nontrivial phase – the topological Anderson insulator – was also shown to be possible [6,7].

To unbiasedly characterize the interplay of all these ingredients we introduce a model system that combines the topological features of the Haldane model with an interaction term of the Falicov-Kimball type. The Haldane-Falicov-Kimball model can be seen as a limiting case of the Hubbard model on an hexagonal lattice, for which one of the spin species is infinitely massive and the other has the hopping matrix elements of the Haldane model. The ability to employ numerically exact methods, renders our model an excellent testbed to unveil the subtle and often contradictory role of interactions and disorder. Moreover, the model can be studied at finite temperatures, where the behavior of topological matter have been much less explored.

By performing a careful numerical and analytic analysis, we obtain the phase diagram on the temperature-interaction plane, displaying a rich set of phases. One of our main results is to show that the thermal fluctuations, that affect the spatial charge ordering, induce a temperature-driven topological phase transition into gapped and gapless topological insulators, present for a wide range of interaction strengths. We also find an insulating charge ordered state with gapless excitations where spectral regions of extended and localized states seem to coexist due to the long range nature of the interaction-induced disorder potential [8].

Recent technological advances in ultracold atoms in optical lattices, in particular, the ability of having fermionic systems with a large mass unbalance and the possibility of realizing topologically non-trivial band structures such as the one of the Haldane model, render this model easily realizable with current experimental setups.

## **References**

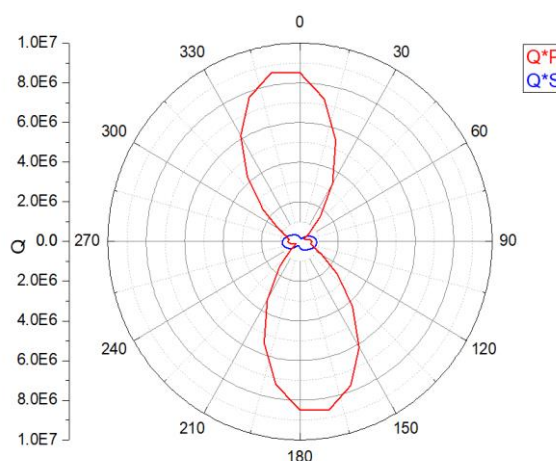
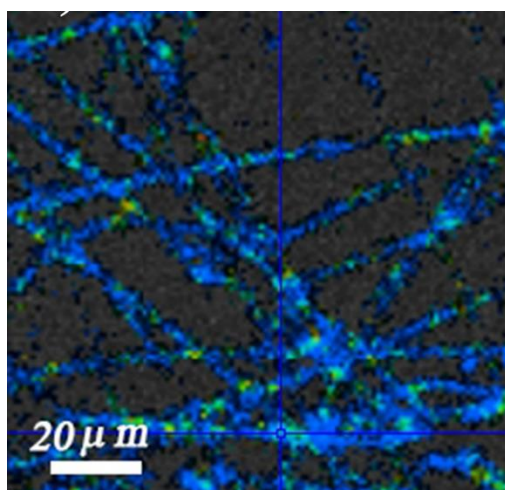
- [1] M.A.N. Araujo, E.V. Castro, and P.D. Sacramento, *Phys. Rev. B*, **87**, 085109 (2013).
- [2] N.A. García-Martínez, A.G. Grushin, T. Neupert, B. Valenzuela, and E.V. Castro, *Phys. Rev. B*, **88**, 245123 (2013).
- [3] S. Rachel, *Rep. Prog. Phys.*, **81**, 116501 (2018).
- [4] E.V. Castro, M.P. López-Sancho, and M.A.H. Vozmediano, *Phys. Rev. B*, **92**, 085410 (2015).
- [5] E.V. Castro, R. de Gail, M.P. López-Sancho, and M.A.H. Vozmediano, *Phys. Rev. B*, **93**, 245414 (2016).
- [6] J. Li, R.-L. Chu, J.K. Jain, and S.-Q. Shen, *Phys. Rev. Lett.*, **102**, 136806 (2009).
- [7] M. Gonçalves, P. Ribeiro, and E.V. Castro, *arXiv:1807.11247* (2018).
- [8] M. Gonçalves, R. Mondaini, P. Ribeiro, and E.V. Castro, *Phys. Rev. Lett.* in press, *arXiv:1808.00978* (2019).

# NONLINEAR OPTICS AS A PROBE OF CONDENSED MATTER SYSTEMS

Michael Belsley

Department of Physics, University of Minho, Braga, Portugal  
belsley@fisica.uminho.pt

Nonlinear optical probes of condensed matter systems can access a wealth of material information with the possibility of monolayer surface sensitivity, micron scale lateral spatial resolution and sub-picosecond temporal discrimination. Furthermore, nonlinear optical responses are strongly influenced by structural symmetries and spatial correlations. These merits have inspired the development of a wide variety of nonlinear optical material characterization techniques. For example, second harmonic generation is now commonly used for label-free imaging of ordered micro-structures in complex biological samples or to delineate ferroelectric domains and semiconductor grain boundaries. This contribution will briefly discuss the underlying physics supporting several of these techniques and illustrate the wide range of potential applications using examples from the recent literature. Topics to be addressed include the assessment of rotational anisotropies, the dynamics of photo-excited carriers [1] and applications used to characterize 2 dimensional materials [2].



Second harmonic image of electrospun nanofibers of para nitroaniline embedded in a Polymethyl methacrylate (PMMA) matrix. This scan contained 128x128 separate acquisition points [3]. On the right is a rotational anisotropy plot of the second harmonic polarization.

## References

- [1] A. J. Goodman and W. A. Tisdale, Physical Review Letters 114, 183902 (2015).
- [2] A. Saynatjoki, et al. Nature Communications 8 893 (2017).
- [3] Hugo Gonçalves et al., J. Phys. D: Appl. Phys 51, 105106 (2018).



**CIRCULARLY POLARIZED LIGHT DETECTION USING CELLULOSE NANOCRYSTALS  
PHOTONIC DIELECTRICS**

P. Grey, S. N. Fernandes, D. Gaspar, R. Martins, E. Fortunato, M. H. Godinho and L. Pereira  
CENIMAT/I3N, Departamento de Ciência dos Materiais, Faculdade de Ciências e Tecnologia, FCT,  
Universidade Nova de Lisboa and CEMOP-UNINOVA  
Campus da Caparica, 2829-516 Caparica (Portugal)  
Corresponding author: [lmnp@fct.unl.pt](mailto:lmnp@fct.unl.pt)

Cellulose nanocrystal (CNC) have been in the spotlight, owing to properties such as iridescence and selective reflection and transmission of CPL, attributed to the inherent chirality of individual CNCs, which self-assemble into left-handed twisted superstructures. Consequently, LCPL is reflected whereas RCPL is transmitted. In this work we report on the integration of bioinspired CNCs films into transistor devices with distinct sensing properties for left- and right-handed circular polarized light (LCPL and RCPL, respectively). The CNC films with a left-handed internal long-range order are infiltrated with alkali ions to yield highly polarizable photonic solid-state electrolytes capable of LCPL reflection and RCPL transmission. They are employed as gate dielectrics in sputtered amorphous indium-galliumzinc- oxide (a-IGZO) semiconductor devices. The obtained depletion mode transistors yield lowvoltage operation ( $< 2$  V), On-Off ratios of up to 7 orders of magnitude, sub-threshold slopes of  $77 \text{ mV dec}^{-1}$  and saturation mobilities of  $8.3 \text{ cm}^2 \text{ V}^{-1} \text{ s}^{-1}$ . Combining the photonic character of the CNC films with the light sensible a-IGZO, the devices are capable of discrimination between LCPL and RCPL signals. This type of devices could find application in photonics, emission, conversion or sensing with CPL but also imaging or spintronics.

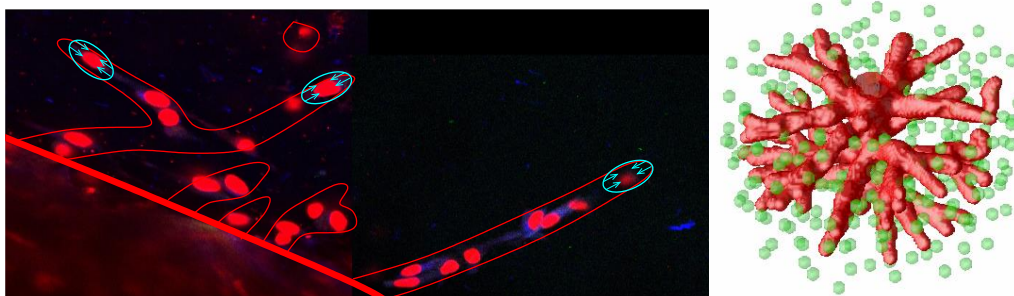
## INFLUENCE OF MATRIX RIGIDITY ON BLOOD VESSEL GROWTH

Rui Travasso,<sup>1,\*</sup> Marcos Gouveia,<sup>1</sup> Maurício Moreira Soares,<sup>1</sup> and João Carvalho<sup>1</sup>

<sup>1</sup>Centro de Física da Universidade de Coimbra (CFisUC), Faculdade de Ciências e Tecnologia, Universidade de Coimbra, Rua Larga, 3004-516, Coimbra, Portugal

\*Corresponding Author: ruit@uc.pt

Biochemical processes regulate extracellular matrix (ECM) remodeling, actin polymerization, membrane deformation and cell-ECM adhesion. These processes permit for cells to exert forces in the ECM, and to migrate and/or to rearrange themselves into complex structures. Blood vessel formation and blood vessel remodeling are processes where biochemical mechanisms are intertwined with vessel mechanics, tissue mechanics, growth factor diffusion, and alteration of matrix mechanical properties and its degradation. In this talk I will show how to construct mathematical models of cell migration and vessel formation by taking into account this mechanical interplay between the cells and their microenvironment. I will draw conclusions regarding the role of ECM rigidity in the formation of complex vascular structures. I will focus on the ability for these models to suggest testable hypothesis and to provide new insights into the mechanisms that drive the dynamics of blood vessel growth.



### References

- [1] Santos-Oliveira, P., Correia, A., Rodrigues, T., Ribeiro-Rodrigues, T.M., Matafome, P., Rodríguez-Manzaneque, J. C., ... Travasso, R. D. (2015). The force at the tip-modelling tension and proliferation in sprouting angiogenesis. *PLoS computational biology*, 11(8), e1004436.
- [2] M. Moreira-Soares, R. Coimbra, L. Rebelo, J. Carvalho, R. D. M. Travasso, Angiogenic factors produced by hypoxic cells drive anastomoses in sprouting angiogenesis – a computational study. (2018). *Scientific Reports*, 8, 8726
- [3] Ramos, J. R., Travasso, R., Carvalho, J. (2018). Capillary network formation from dispersed endothelial cells: Influence of cell traction, cell adhesion, and extracellular matrix rigidity. *Physical Review E*, 97(1), 012408.

## NON-EQUILIBRIUM COLLECTIVE DYNAMICS OF COLLOIDAL PARTICLES

Nuno A. M. Araújo,<sup>1,2\*</sup> Cristóvão S. Dias,<sup>1,2</sup> and Margarida. M. Telo da Gama<sup>1,2</sup>

<sup>1</sup> Departamento de Física, Faculdade de Ciências, Universidade de Lisboa, 1749-016 Lisboa, Portugal

<sup>2</sup> Centro de Física Teórica e Computacional, Universidade de Lisboa, 1749-016 Lisboa, Portugal

\*Corresponding Author: nmaraujo@fc.ul.pt

Colloidal particles are considered ideal building blocks to produce materials with enhanced physical properties. The state-of-the-art techniques for synthesizing these particles provide control over shape, size, and directionality of the interactions. In spite of these advances, there is still a huge gap between the synthesis of individual components and the management of their spontaneous organization towards the desired structures. The main challenge is the control over the dynamics of self-organization. In their kinetic route towards thermodynamically stable structures, colloidal particles self-organize into intermediate structures that are much larger than the individual particles and become the relevant units for the dynamics. To follow the dynamics and identify kinetically trapped structures, one needs to develop new theoretical and numerical tools. In this seminar, we will discuss the self-organization of functionalized colloidal particles with limited valence [1,2,3,4].

#### References

- [1] N. A. M. Araújo, C. S. Dias, M. M. Telo da Gama, *Journal of Physics: Condensed Matter*, 29, 014001 (2017).
- [2] C. S. Dias, N. A. M. Araújo, M. M. Telo da Gama, *Advances in Colloid and Interface Science*, 247, 258 (2017).
- [3] C. S. Dias, J. M. Tavares, N. A. M. Araújo, M. M. Telo da Gama, *Soft Matter*, 14, 2744 (2018).
- [4] T. Geigenfeind, C. S. Dias, M. M. Telo da Gama, D. de las Heras, N. A. M. Araújo, *Soft Matter*, 14, 9411 (2018).

## ADVANCES IN SPINTRONIC SENSOR MATERIALS AND ARCHITECTURES

A. Silva,<sup>1</sup> D. Leitaó,<sup>1,2</sup>, M. Silva<sup>1,2</sup>, P. Ribeiro<sup>1,2</sup>, F. Franco<sup>1,2</sup>, P.P. Freitas<sup>1</sup> and S. Cardoso<sup>1,2</sup><sup>1</sup>INESC-MN, Rua Alves Redol 9, 1000-029 Lisboa, Portugal<sup>2</sup>Instituto Superior Técnico (IST), Univ. de Lisboa, Av. Rovisco Pais, 1000-029 Lisboa, Portugal

\*Corresponding Author: scardoso@inesc-mn.pt

Magnetic field sensors - in particular, magnetoresistive (MR) sensors and spintronic devices - were driven by the technological push from computers and information storage in the early 1990's, and have presently a mature level of implementation in the market. In this talk, the material selection for the spintronic sensors is discussed, focusing on ultrathin ( $\sim 1\text{nm}$ ) amorphous  $\text{AlOx}$  and crystalline  $\text{MgO}$  tunnel barriers, combined with soft ferromagnetic electrodes. The deposition methods are key factors for thin film interface quality control, while tuning the atomic order of the films. The spintronic sensors optimization strategies towards high performing devices are discussed, including magnetic resilience under crossed magnetic fields, thermal stability and noise characteristics. The ultimate field detectable by a MR sensor is conditioned by the noise level, therefore particular interest has been addressed to reaching pTesla detectivities at room temperature, with high impact towards competing technologies as SQUIDS or other hybrid devices, as described in a recent roadmap from the IEEE society [1]. The microfabrication challenges are discussed, supported with the key requirements for some technological applications from non-destructive evaluation [2] to biomedical [3] and robotics applications [4].

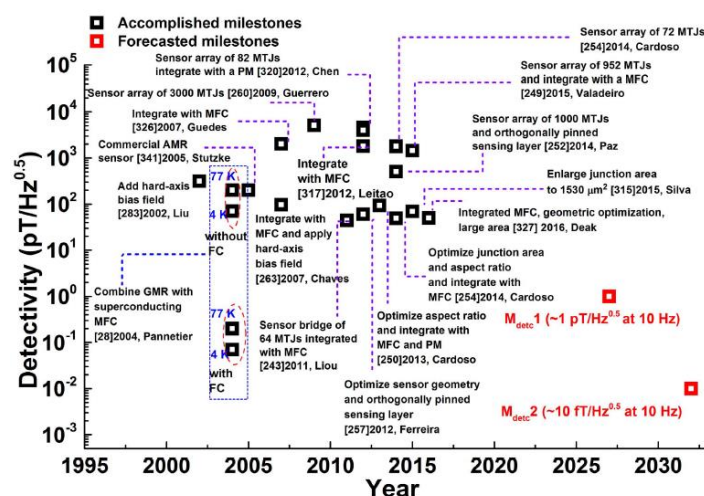


Figure 1. Minimum field detected at room temperature using MR sensors, reported “MR sensor Roadmap”[1].

## References

- [1] Chao Zheng, et.al., “Magnetoresistive Sensor Development Roadmap (Non-Recording Applications)”, IEEE Trans.Magn. 55 (4), pp. 1-30 (2019).
- [2] P.P.Freitas, R.Ferreira and S.Cardoso “Spintronic Sensors”, Proceedings of the IEEE, 104 (10), pp. 1894 - 1918 (2016).
- [3] S.Cardoso, et.al, “Challenges and trends in magnetic sensor integration with microfluidics for biomedical applications”, Journal of Physics D-Applied Physics, 50 (21), 213001 (2017).
- [4] Pedro Ribeiro, et.al., “Bio-inspired ciliary force sensor for robotic platforms” , IEEE Robotics and Automation Letters (RA-L) vol.2 (2), 971-976 (2017).

## TRIBOELECTRIC NANOGENERATORS: FROM FUNDAMENTAL CONCEPTS TO APPLICATIONS IN HARSH ENVIRONMENTS

C. Rodrigues,<sup>1</sup> A. M. Pereira,<sup>1</sup> and J. Ventura<sup>1,\*</sup>

<sup>1</sup>Department of Physics and Astronomy, University of Porto, Rua do Campo Alegre, 687, Porto, Portugal

\*Corresponding author: joventur@fc.up.pt

As the world's economy steadily grows, so does energy consumption, particularly of fossil fuels. This leads to serious environmental and economic problems, as fossil fuels are the major source of greenhouse gases, are non-renewable and limited. Thus, clean and renewable energies, such as hydropower, wind or solar energies are being increasingly applied. An alternative energy form has recently emerged: micro- and nano-energy generation. Micro and nano-generators, able to harvest energy from the environment, have been attracting large interest because they are green, sustainable, cost-efficient and can be easily integrated in common electronic gadgets. A major disruption in the field of mechanical energy harvesting occurred in 2012 when the first triboelectric nanogenerator (TENG) was invented [1]. TENGs are based on the coupling between triboelectric and electrostatic processes that generate a charge distribution at the interface of materials that come into contact. They show very high efficiency (up to 75%), power densities above 500 W/m<sup>2</sup> record voltage outputs above 1200 V, wide material choice, simple design, easy manufacturing and integration. Their applications are almost infinite because of the possibility to use all flexible and dynamic surfaces like cloth or shoes, touchable electronics or even the human body, to produce electricity. They have thus the potential to harvest energy from human activities, rotating tires, ocean waves and tides, water or fluid flow, mechanical vibration, wind, among many others.

Here, we will first discuss the basic phenomena behind triboelectric nanogenerators and their main applications. Then, we will present our efforts on developing triboelectric devices for harsh and remote environments. We will focus on two main applications:

- Novel energy harvesting concepts for extreme conditions (high temperatures up to 150°C and pressures up to 830 bar) for the oil & gas industry;

- Energy harvesting devices able to transform wave and currents energies into useful electrical power for the perpetual deployment of sensing platforms and underwater vehicles in the Ocean.

### References

[1] F. Fan, L. Lin, G. Zhu, W. Wu, R. Zhang, Z. L. Wang, Transparent Triboelectric Nanogenerators and Self-Powered Pressure Sensors Based on Micropatterned Plastic Films, *Nano Letters* 12, 3109 (2012).

# Special Session for Students

## EPS Young Minds Project

The presentation of the Young Minds project is supported by the European Physical Society (EPS), which aims to interconnect young researchers in Europe and to promote science to the broad public through the creation of local sections managed by young scientists - from undergraduates to postdoctoral researchers. It currently has 57 local sections in 30 countries.

The session will feature the talks from the chair of the program, Dr. Roberta Caruso, and members of EPS Young Minds University of Aveiro, currently the only section in Portugal. The talks will give an overview of the project with the relevant information to create a section and the main benefits of the project for a young scientist, and present the typical activities developed by the section of the University of Aveiro.

The session will end with an open discussion addressing the theme "Boost your career through public engagement" and a Q&A session.

*Roberta Caruso is post-doc researcher at Naples University, where she works in the field of low temperature physics, focusing on the characterization of hybrid Josephson junctions and superconducting devices. She became member of the YM project in 2010, founding one of the first sections in Naples, and has become chair of the project in 2018. During this time, she organized and collaborated in a number of projects devoted to outreach, public engagement and professional development.*

*Teresa Coimbra is in the second year of the master's degree in Physics at the University of Aveiro. She became President of the Aveiro section of the YM Project in 2017. Since her entrance in the University of Aveiro in 2014, she has volunteered in various outreach activities organized by the university, directed to younger students and the general public.*

*Sara Mantey is in the first year of the master's degree in Physics Engineering at the University of Aveiro. She accumulates her work as a member of the Aveiro section of the YM Project with the role of treasurer in the Association of the Physics Students of the University of Aveiro.*

# ORAL CONTRIBUTIONS



## CHALCOGENIDES THE PLAYGROUND MATERIALS ON CONDENSED MATTER PHYSICS: FROM QUANTUM EFFECTS TO TECHNOLOGICAL APPLICATIONS

A. L. Pires<sup>1</sup>, S. Ferreira-Teixeira<sup>1</sup>, E. M. F. Vieira<sup>2</sup>, J. Silva<sup>1</sup>, J.P Araújo<sup>1</sup>, L. Gonçalves<sup>2</sup>,  
W. R. Branford<sup>3</sup>, L. Cohen<sup>3</sup>, A. M. Pereira<sup>1</sup>

<sup>1</sup>IFIMUP and IN - Institute of Nanoscience and Nanotechnology, Departamento de Física e Astronomia,  
Faculdade de Ciencias, Universidade do Porto, 4169-007 Porto, Portugal.

<sup>2</sup>Universidade do Minho, CMEMS—UMINHO, Campus Azurem, 4804-533 Guimaraes, Portugal.

<sup>3</sup>Physics Department, Blackett Laboratory, Imperial College London, Prince Consort Road, SW7 2AZ,  
United Kingdom.

Chalcogenides such  $\text{Bi}_2\text{Te}_3$  and  $\text{Sb}_2\text{Te}_3$  have been studied for more than 50 years, with special focus in the area of thermoelectricity since is the most used material for this purpose in its bulk form. Although under studied throughout these years, these materials continue surprising the scientific community by constant new physical phenomena. The peculiar layered structure is one of the main responsible by these effects. It presents a compacted rhombohedral structure belonging to the space group  $R\bar{3}m$ . The lattice can be described as a pseudo-hexagonal unit cell with  $a = 0.438$  nm and  $c = 3.05$  nm. The pseudo-hexagonal unit cell consists of three five-layer-groups with the sequence  $\text{Te1} - \text{Bi (Sb)} - \text{Te2} - \text{Bi} - \text{Te1}$  with weak  $\text{Te1}-\text{Te1}$  Van-der-Walls bondings. At the nanoscale, these materials can be tuned resemble a “*phonon-glass*” while maintaining the “*electron crystal*” thus present increasing for instance the Figure of Merit of the material for thermoelectricity applications. The use of nanoscopic confined structures is probably the best strategy to sharp electronic density of states (dot-/nanowire-like), also offering the possibility to increase phonon scattering at interfaces. On other hand, they also have a crucial impact on the field of topological insulators (TIs), having an insulator bulk and a time reversal protected metallic surface state.

Herein, an overview of the theoretical, experimental and numerical simulations that have been study by our group on chalcogenides with different approaches ranging from different strategies to develop optimal nanostructures (2D and 1D nanomaterials), the use of numerical simulations for the development of technological microdevices and the fabrication of this microdevices using microfabrication. Finally, the presence of weak antilocalization (WAL) at low temperature and low magnetic fields on these materials will be explored unveiling their topological surface state.

### References:

- [1] M. Haras, T. Skotnicki, Nano Energy. 54 (2018) 461–476.
- [2] A. L. Pires, I. F. Cruz, J. Silva, G. N. P. Oliveira, S. Ferreira-Teixeira, A. M. L. Lopes, J. P. Araújo, J. Fonseca, C. Pereira, A. M. Pereira, ACS Appl. Mater. Interfaces. 11 (2019) 8969–8981.
- [3] M. P. Proenca, M. Rosmaninho, P. M. Resende, C. T. Sousa, J. Ventura, J. P. Araújo, L. Fernandes, P. B. Tavares, A. M. Pereira, Mater. Des. 118 (2017) 168–174.
- [4] E. M. F. Vieira, J. Figueira, A. L. Pires, J. Grilo, M. F. Silva, A. M. Pereira, L. M. Goncalves, J. Alloys Compd. 774 (2019) 1102–1116; [5] S. Ferreira-Teixeira, A. M. Pereira, Energy Convers. Manag. 169 (2018) 217–227.

## QUANTUM EFFECTS IN ELECTRICAL TRANSPORT PROPERTIES OF BISMUTH CHALCOGENIDES TOPOLOGICAL INSULATORS

J.A. Paixão<sup>1\*</sup>, M.S.C. Henriques<sup>1</sup>, C. Micale<sup>2</sup>, E.B. Lopes<sup>2</sup>, V.M.M. Pereira<sup>1,3</sup>, A.P. Gonçalves<sup>2</sup>

<sup>1</sup> CFisUC, Departamento de Física, Universidade de Coimbra

<sup>2</sup> C<sup>2</sup>TN, Instituto Superior Técnico, Universidade de Lisboa

<sup>3</sup> Max-Planck Institute, for Chemical Physics of Solids, Dresden

\*Corresponding Author: jap@fis.uc.pt

Topological insulators are celebrated novel materials with a peculiar band structure that features a gap for bulk states but may also host spin-polarised surface conducting states, topologically protected from scattering mechanisms that do not break time-inversion symmetry. A representative family of such materials are bismuth chalcogenides, that have attracted a lot of interest also for they good properties as thermoelectric compounds.

In this work, we present and discuss the results on single-crystals and nanostructured samples of several bismuth chalcogenide compounds including Bi<sub>2</sub>Se<sub>3</sub>, Bi<sub>2</sub>Te<sub>3</sub>, BiSbTe<sub>3</sub> and doped compounds featuring a large range of electric behavior, from semiconducting to metallic-like. Quantum effects such as weak-antilocalisation (WAL) behavior or the presence of Shubnikov–de Haas (SdH) oscillations in the magnetoresistance are clearly observed at low-temperature in the electrical transport properties. The WAL features were analyzed in terms of the Hikami-Larkin-Nagaoka law and the temperature dependence of the coherence length follows closely the expected power law for 2D electronic states [3]. For the most conducting samples, the SdH effect was clearly observed and was analysed within the framework of the Lifshitz-Onsager model. The temperature dependence of the amplitude of the oscillations was found to be in good agreement with the Lifshitz-Kosevich law [4].

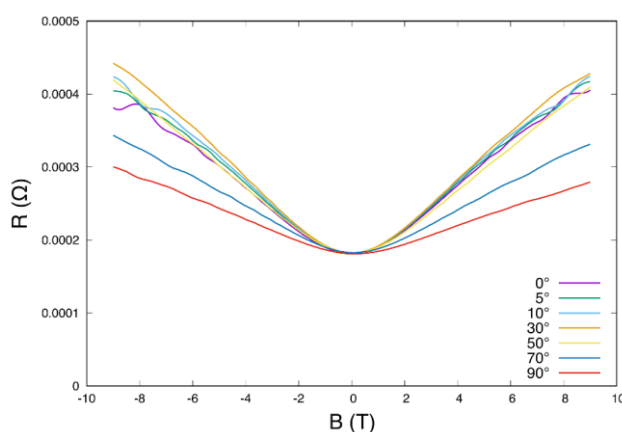


Figure 1. Magnetoresistance of BiSbTe<sub>3</sub> measured at 1.8 K for different angles between the applied magnetic field and the sample surface showing the presence of quantum SdH oscillations.

### References

- [1] Y. Hondo, J. Phys. Soc. Jpn. 82, 102001 (2013).
- [2] D. Park, S. Park, K. Jeong, H-S. Jeong, J.Y. Song, M-H Cho, *Scientific Reports* 6, 19132 (2016).
- [3] V.M.M. Pereira, M.S.C. Henriques, J.A. Paixão, *Physica B* 536, 51.55 (2018).
- [4] I. M. Lifshitz, A. M. Kosevich, *Sov. Phys. JETP* 2, 636 (1955).

# TEMPERATURE-DRIVEN GAPLESS TOPOLOGICAL INSULATOR

Miguel Gonçalves,<sup>1,\*</sup> Pedro Ribeiro,<sup>1,2</sup> Rubem Mondaini<sup>2</sup> and Eduardo V. Castro<sup>1,2,3</sup>

<sup>1</sup>CeFEMA, Instituto Superior Tecnico, Universidade de Lisboa, Av. Rovisco Pais, 1049-001 Lisboa, Portugal

<sup>2</sup>Beijing Computational Science Research Center, Beijing 100084, China

<sup>3</sup>Centro de Física das Universidades do Minho e Porto, Departamento de Física e Astronomia, Faculdade de Ciências, Universidade do Porto, 4169-007 Porto, Portugal

\*Corresponding Author: [miguel.m.goncalves@ist.utl.pt](mailto:miguel.m.goncalves@ist.utl.pt)

Topological, disordered and strongly correlated systems are topics of vast interest in Condensed Matter Physics. Although these systems have been widely studied independently, it is often very difficult to characterize a model that incorporates features of all. An exception is the Haldane-Falicov-Kimball model (HFKM) —a model combining topology, interactions, and spontaneous disorder at finite temperatures. This model combines the topological Haldane model [1] with the Falicov-Kimball model [2] that had important recent developments [3]. Using an unbiased numerical method, we map out the full phase diagram of the HFKM on the interaction-temperature plane [4]. Along with known phases, we unveil an insulating charge ordered state with gapless excitations and a temperature-driven gapless topological insulating phase. Intrinsic—temperature-generated—disorder is the key ingredient explaining the stability of the finite-temperature gapless topological phase. Our findings support the possibility of having temperature-driven topological transitions into gapped and gapless topological insulating phases in mass unbalanced systems with two fermionic species.

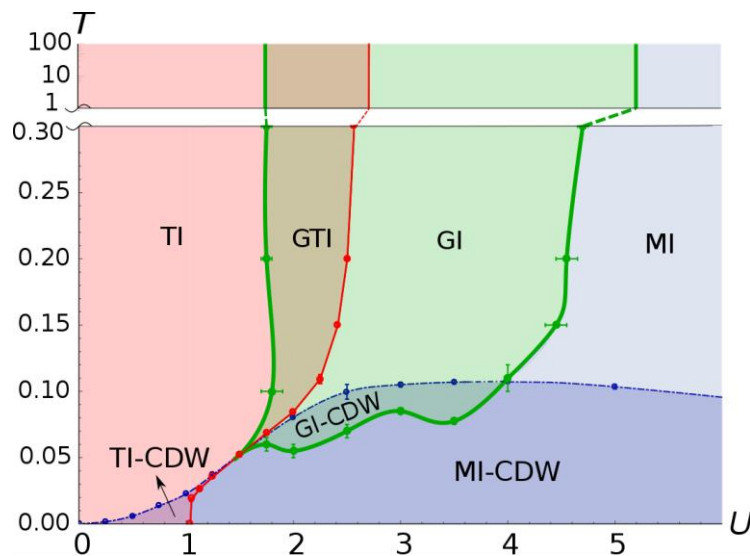


**Figure 1.** Phase diagram of the Haldane-Falicov-Kimball model in the interaction ( $U$ ) - temperature ( $T$ ) plane. Phases at intermediate-to high- $T$ , outside the charge density wave phase (CDW): topological insulator (TI) for small  $U$ , gapless topological insulator (GTI) and gapless insulator (GI) for intermediate  $U$ , and Mott-like insulating phase (MI) for large  $U$ . Phases at low- $T$ , inside the CDW phase: phases with similar features as their high- $T$  counterparts were found and the suffix “-CDW” was added. The thin (red) and dashed-dotted (blue) curves correspond, respectively, to the topological and CDW phase transitions and the thick (green) curve bounds the gapless region of the phase diagram.

## References

- [1] F. D. M. Haldane, Phys. Rev. Lett. 61, 2015 (1988).
- [2] L. M. Falicov and J. C. Kimball, Phys. Rev. Lett. 22, 997 (1969).
- [3] A. E. Antipov, Y. Javanmard, P. Ribeiro, and S. Kirchner, Phys. Rev. Lett. 117, 146601 (2016).
- [4] M. Gonçalves, P. Ribeiro, R. Mondaini, and E. V. Castro, Phys. Rev. Lett. 122, 126601 (2019).

## NON-LINEAR OPTICAL RESPONSE IN DISORDERED 2D MATERIALS

S. M. João,<sup>1,\*</sup> J. M. Viana Parente Lopes<sup>1</sup><sup>1</sup>Centro de Física das Universidades do Minho e Porto, Universidade do Porto, 4169-007, Porto, Portugal

\*Corresponding Author: simao.joao@fc.up.pt

2D materials are a topic of great interest in the realm of nonlinear optics because they possess some of the strongest nonlinear optical responses to light. The bulk of the theoretical work developed in this regard [1] is concerned with translational-invariant systems, where disorder may be added perturbatively. In our work, we extend the work of Passos et al [2] by implementing the velocity gauge methodology within the Keldysh formalism. We develop a general perturbation procedure to deal with non-interacting fermion systems at finite temperature coupled to a time-dependent external field. These expressions gain particular numerical utility when used in the real-space basis, for then we may introduce disorder non-perturbatively and perform the calculations with spectral methods such as the Kernel Polynomial Method (KPM).

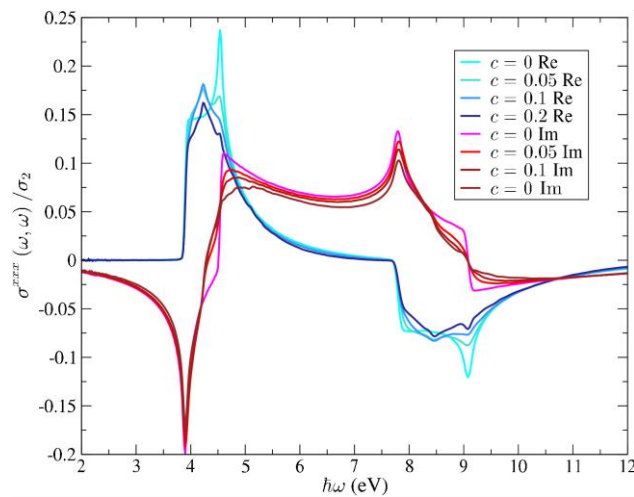


Figure 1. Real and imaginary part of the second-harmonic generation in hexagonal Boron Nitride as a function of the concentration of vacancies in the sample.

Using KITE [3], a quantum transport software developed by ourselves, we explore the effect of disorder in the second-order conductivity, aiming to reproduce mesoscopic samples under realistic conditions. This oral presentation will be concerned about our most recent results with KITE. We will showcase and examine how different models of disorder affect the same system, experimenting with Anderson disorder, impurities and vacancies (Figure 1) in hexagonal Boron-Nitride.

#### Acknowledgments

The authors acknowledge financing of Fundação da Ciência e Tecnologia, of COMPETE 2020 program in FEDER component (European Union), through projects POCI-01-0145-FEDER-02888 and UID/FIS/04650/2013.

#### References

- [1] J. E. Sipe and Ed Ghahramani. 1993. Nonlinear optical response of semiconductors in the independent-particle approximation. *Phys. Rev. B* 48 (Oct 1993), 11705–11722. Issue 16.
- [2] DJ Passos, GB Ventura, JM Viana Parente Lopes, JMB Lopes dos Santos, and NMR Peres. 2018. Non-linear optical responses of crystalline systems: Results from a velocity gauge analysis.
- [3] JV Lopes, SM João, A Ferreira, L Covaci, M Andelkovic, and T Rappoport. 2018. Quantum KITE. Website: <https://quantum-kite.com/>.

## PRACTICAL BAND INTERPOLATION WITH A GENERALISED LUTTINGER-KOHN METHOD

Carlos L. Reis<sup>1,\*</sup> and José Luís Martins,<sup>1,2</sup>

<sup>1</sup>INESC-MN, Rua Alves Redol 9, 1000-029 Lisboa, Portugal

<sup>2</sup>Departamento de Física, Instituto Superior Técnico

\*Corresponding Author: creis@inesc-mn.pt

The electronic band structure, the single particle energy as a function of wave-vector, is a fundamental concept of the physics of crystals. It is used in the interpretation of its electrical and optical properties, and is directly probed by photoemission and inverse photoemission experiments. In electronic structure calculations, the energies and corresponding electron wave-functions are calculated on a discrete number of values of the wave-vector. The computation Density of States (DOS), optical response functions, and transport properties requires a dense sampling of the wave-vectors in reciprocal space. As each calculation is in itself computationally expensive there has been a continuous interest in methods that fit bands close to the calculated points, or extrapolate from those points, or interpolate between the points, from the early work of tight binding band adjustment of Slater and Koster [1] or the k.p extrapolation method [2-4] to the recent development of interpolation schemes using Wannier functions [5].

In the present work we present in the context of one-electron plane-wave pseudopotential calculations a method based on the generalisation of the Luttinger-Kohn [2] functions by Shirley [6] and Pendergast and Louie [7] that interpolates the band structure either along a line given the wave-functions at the extremities, or in an arbitrary k-point inside a tetrahedron given the wave-functions at its corners. It starts by constructing a variational basis with a weighted symmetrical (SVD) orthogonalisation of the Luttinger-Kohn functions derived from the k-points to be interpolated, and subsequent discarding of the less relevant functions. An Hamiltonian is constructed in that local variational basis and diagonalised. At the point to be interpolated, the corresponding wave-functions have unit weight while wave-functions associated with other k-points are attributed a zero weight. Therefore after the symmetric orthogonalisation and discarding procedure only the local wave-functions remain, and the exact eigenvalues at that k-point are trivially recovered, making the procedure an interpolation method.

We present examples of the application of the scheme to density functional calculations of silicon, graphite, copper and C<sub>60</sub>.

### References

- [1] J. C. Slater and G. F. Koster, *Physical Review* 94, 1498 (1954).
- [2] J. Luttinger and W. Kohn, *Physical Review* 97, 869 (1955).
- [3] G. Dresselhaus, A. Kip, and C. Kittel, *Physical Review* 98, 368 (1955).
- [4] E. O. Kane, *Journal of Physics and Chemistry of Solids* 1, 82 (1956).
- [5] N. Marzari, A. A. Mostofi, J. R. Yates, I. Souza, and D. Vanderbilt, *Rev. Mod. Phys.* 84, 1419 (2012).
- [6] E. L. Shirley, *Physical Review B* 54, 16464 (1996).
- [7] D. Pendergast and S. G. Louie, *Physical Review B* 80, 235126 (2009).

## THEORETICAL CALCULATIONS OF NONLINEAR OPTICAL RESPONSES OF 2D MATERIALS

G. B. Ventura,\* D. J. Passos, J. M. Viana Parente Lopes, J. M. B. Lopes dos Santos

Centro de Física das Universidades do Minho e Porto, Universidade do Porto, 4169-007, Porto,  
Portugal

\*Corresponding Author: gbventura@fc.up.pt

One feature of two dimensional (2D) materials is that they possess an exceptional nonlinear optical (NLO) response to light - with susceptibilities (conductivities) that are several orders of magnitude larger than their 3D counterparts [1] – thus making them the ideal subjects for problems in nonlinear optics. Our past works [2,3] have aimed at the understanding and development of tools that provide a theoretical description of these NLO responses in crystalline systems, in both the length and the velocity gauge – two possible choices of representation for an electric field perturbation in a crystal.

The length gauge has been the formalism of choice for over two decades, having been used since the early nineties to calculate NLO coefficients in 3D semiconductors [4]. Though this success is connected with some of the intrinsic advantages of the length gauge, e.g. it enables the use of simplified descriptions of band structures and as such, allows for analytical calculations, it has also to do with the fact that the particularities surrounding the velocity gauge had not been fully understood at the time. Our work on this matter has clarified the importance of sum rules – a set of identities that ensure the equivalence of two formalisms – as well as established the procedure to perform calculations in the velocity gauge. Two striking features of this procedure are that the calculation must, necessarily, involve the full first Brillouin zone (unlike the length gauge); and that the numerical implementations of these calculations are far more efficient than those in its counterpart, the length gauge. This oral presentation thus concerns the main results of our two works and are accompanied by an example of an NLO coefficient – the third harmonic generation of the monolayer of graphene.

### Acknowledgments

The authors acknowledge financing of Fundação da Ciência e Tecnologia, of COMPETE 2020 program in FEDER component (European Union), through projects POCI-01-0145-FEDER-02888 and UID/FIS/04650/2013.

### References

- [1] J. L. Cheng, N. Vermeulen, and J. E. Sipe, *New Journal of Physics*, 16, 053014, (2014).
- [2] G. B. Ventura, D. J. Passos, J. M. B. Lopes dos Santos, J. M. Viana Parente Lopes, and N. M. R. Peres, *Phys. Rev. B*, 96, 035431, (2017).
- [3] D. J. Passos, G. B. Ventura, J. M. V. P. Lopes, J. M. B. L. dos Santos, and N. M. R. Peres, *Phys. Rev. B*, 97, 235446, (2018).
- [4] C. Aversa and J. E. Sipe, *Phys. Rev. B* 52, 14636 (1995).

# BERRY CURVATURE ANISOTROPY AND SPIN CURRENT ROUTING IN GRAPHENE UNDER LATERAL SPIN-ORBIT-COUPLED SUPERLATTICE POTENTIALS

L. M. Martelo<sup>1,2,\*</sup> and A. Ferreira<sup>3</sup>

<sup>1</sup>Departamento de Engenharia Física, Faculdade de Engenharia da Universidade do Porto, Rua Dr. Roberto Frias, 4200-465 Porto, Portugal.

<sup>2</sup>Centro de Física do Porto, Rua do Campo Alegre, 4169-007 Porto, Portugal.

<sup>3</sup>Department of Physics, University of York, York YO10 5DD, United Kingdom.

\*Corresponding author: martelo@fe.up.pt

Spin-orbit coupling has attracted enormous attention due to its central role in topological insulating phases and low-power charge-to-spin conversion with potential applications in next-generation spintronic devices [1]. Recently, atomically thin heterostructures built from graphene and semiconducting dichalcogenides have emerged as strong contenders for fundamental studies of spin-dependent phenomena [2, 3]. Here, we show that lateral spin-orbit-coupled superlattice potentials applied to graphene sheets drastically impact the topological character of 2D Dirac electronic states, leading to the emergence of anisotropic Berry curvature hotspots that can be used to control spin currents. The spatial modulation of the spin-orbit coupling envisaged theoretically in this work could be realised by proximity effect to rippled group-VI dichalcogenide substrates [4]. The spin-Hall angle, which measures the charge to spin current conversion efficiency, is found to change sign with reversal of the lateral gate voltage, allowing all-in-one activation and routing of spin Hall currents with electrostatic control. Our work answers important questions on the effect of spin-orbit patterning in nanostructures, and suggests that tuneable Dirac superlattices will be important components in ultra-low-power spin transistors built from two-dimensional materials.

## References

- [1] A. Soumyanarayanan *et al.* Nature 539, 509 (2016).
- [2] M. Offidani, M. Milletari, R. Raimondi & A. Ferreira. Phys. Rev. Lett. 119, 196801 (2017).
- [3] M. Offidani and A. Ferreira. Phys. Rev. B 98, 245408 (2018).
- [4] Z. Wang ET AL. Phys. Rev. X 6, 041020 (2016).



## BOSE-EINSTEIN CONDENSATION OF PHOTONS IN A PLASMA

H. Terças

Instituto de Plasmas e Fusão Nuclear

Instituto Superior Técnico, Av. Rovisco Pais 1, 1049-001 Lisboa, Portugal

\*Corresponding Author: hugo.tercas@tecnico.ulisboa.pt

Despite the fact of Bose-Einstein statistics being first derived for photons [1], the idea of photon condensation itself has received much criticism and therefore remained elusive for a long time. Two main reasons are at the origin of such reservations: first, photons are massless particles, which makes a vacuum in the lowest energy state (i.e., with infinite wavelength) impossible; second, it is difficult to implement a physical system where the number of photons is kept constant, a feature that is necessary to ensure a second-order phase transition. In this work, we show that the Bose-Einstein condensation of photons in a plasma is possible. We consider four-wave mixing processes of photon and plasmon modes in a isotropic plasma to determine the coupling constant to lowest order. Photon condensation is possible in an unbounded plasma because, in contrast with other optical media, plasmas introduce an effective photon mass. This guarantees the existence of a finite chemical potential and a critical temperature, which is calculated for both transverse photons and plasmons. By considering four-wave mixing processes, we derive the interactions between the photons in the condensate. We also study the elementary excitations (or Bogoliubov modes) of the condensed photon and plasmon gases, and determine the respective dispersion relations. Finally, we discuss the kinetics of photon condensation via inverse Compton scattering between the photons and the electrons in the plasma [2, 3, 4].

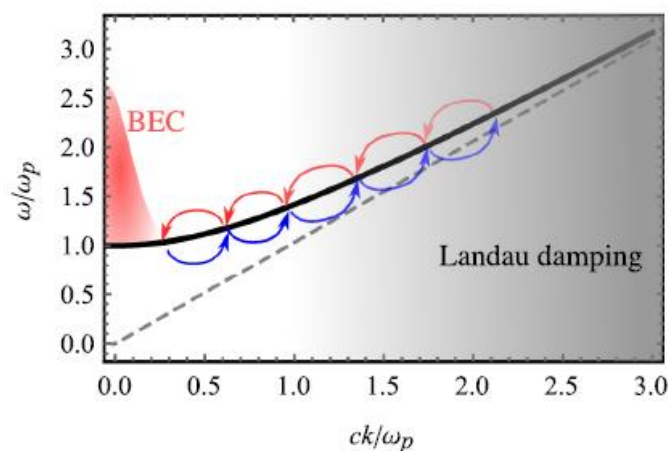


Figure 1. Dispersion relation of photons in a plasma. Compton scattering processes cool down photons at the bottom of the dispersion. Inverse scattering heat the photons up. Condensation is possible when the first process dominates over the last one.

## References

- [1] S. N. Bose, Z. Phys. 26, 178 (1924).
- [2] A. S. Kompaneets, J. Exp. Theoret. Phys. **31**, 876 (1956).
- [3] Y. B. Zel'dovich and E. V. Levich, J. Exp. Theoret. Phys. 28, 1287 (1969).
- [4] J. T. Mendonça and H. Terças, Phys. Rev. A 95, 063611 (2017).



# MAGNETO-OPTICAL KERR EFFECT IN TWO-DIMENSIONAL DILUTED MAGNETIC TRANSITION METAL DICHALCOGENIDE SEMICONDUCTORS

G. Catarina,<sup>1,\*</sup> N. M. R. Peres,<sup>1,2</sup> and J. Fernández-Rossier<sup>1</sup>

<sup>1</sup>QuantaLab, International Iberian Nanotechnology Laboratory, 4715-330, Braga, Portugal

<sup>2</sup>Centro de Física das Universidades do Minho e Porto and Departamento de Física and QuantaLab, Universidade do Minho, Campus de Gualtar, 4710-057, Braga, Portugal

\*Corresponding Author: goncalo.catarina@inl.int

We present a theory to model the Kerr angle for two-dimensional transition metal dichalcogenide semiconductors, such as MoS<sub>2</sub>, doped with a small density of magnetic atoms. The model Hamiltonian describes the band carriers within the effective gapped Dirac theory, accounting for spin-orbit and spin-valley coupling [1]. The magnetic impurities are described within a mean-field virtual crystal approximation, leading to a band-dependent spin splitting of the spectrum [2]. We find that the transverse optical conductivity is non-zero, leading to a finite Kerr rotation, when the exchange-induced splitting in the valence and conduction bands is different. In addition, we conclude that the net Kerr rotation can be seen as a non-cancellation of universal valley-resolved features of a massive Dirac theory (Fig. 1).

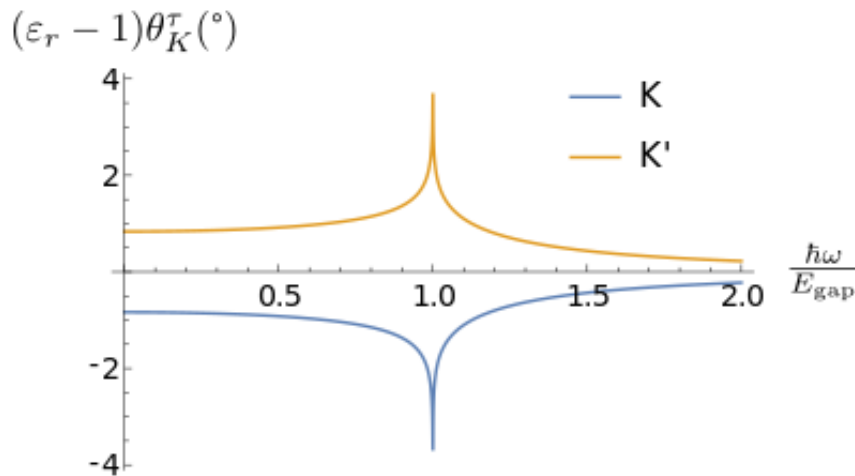


Figure 1. Valley-resolved Kerr rotation,  $\theta_K^\tau$ , as a function of the photon energy  $\hbar\omega$ , for a two-dimensional material described by a massive Dirac theory with gap  $E_{gap}$ , at the charge neutrality point. Polar magneto-optical Kerr effect with normal incidence of light in a monolayer on top of a substrate with relative permittivity  $\epsilon_r > 2$  is assumed. The sum over the two valleys, K and K', leads to a vanishing net Kerr rotation. A combination of both spin-orbit coupling and different exchange-induced splitting in the valence and conduction bands gives rise to four non-degenerate energy gaps in the model, which offset this cancellation.

## References

- [1] D. Xiao, G.-B. Liu, W. Feng, X. Xu, and W. Yao, *Physical Review Letters*, 108, 196802 (2012).
- [2] J. Fernández-Rossier, C. Piermarocchi, P. Chen, A. H. MacDonald, and L. J. Sham, *Physical Review Letters*, 93, 127201 (2004).

BARRIER MODEL IN MUON IMPLANTATION AND APPLICATION TO LU<sub>2</sub>O<sub>3</sub>

R. C. Vilão,<sup>1,\*</sup> R. B. L. Vieira,<sup>2</sup> H. V. Alberto,<sup>1</sup> J. M. Gil,<sup>1</sup> A. Weidinger,<sup>3</sup> R. L. Lichti,<sup>4</sup>  
P. W. Mengyan,<sup>4,5</sup> B. B. Baker,<sup>6</sup> and J. S. Lord<sup>7</sup>.

<sup>1</sup>CFisUC, Department of Physics, University of Coimbra, Portugal

<sup>2</sup>CICECO - Aveiro Institute of Materials, Department of Chemistry, Univ. of Aveiro, Portugal

<sup>3</sup>Helmholtz-Zentrum Berlin für Materialien und Energie, Berlin, Germany

<sup>4</sup>Department of Physics, Texas Tech University, Lubbock, Texas, USA

<sup>5</sup>Department of Physics, Northern Michigan University, Marquette, Michigan, USA

<sup>6</sup>Department of Physics and Engineering, Francis Marion Univ., Florence, South Carolina, USA

<sup>7</sup>ISIS Facility, Rutherford Appleton Laboratory, Chilton, Didcot, United Kingdom

\*Corresponding Author: ruivilao@uc.pt

In implantation experiments, the implanted particle is shot with a certain energy into the material and comes to rest at a site which may not correspond to the final position [1,2]. The rearrangements of the surrounding atoms to accommodate the particle, i.e., the reaction with the host atoms may require some time and lead to delayed formation of the final states. In the case of the implantation of positive muons, this rearrangement process can be followed on a timescale of nanoseconds to microseconds. A delay is expected if an energy barrier inhibits the prompt reaction. We note that the barrier height may change during the rearrangement of the lattice, thus giving rise to a two-dimensional potential profile for the conversion process. The barrier model describes the reaction path of the muon in analogy to the passage over a mountain with a saddle point. The passing over the saddle point corresponds to the lowest energy trajectory. As an example, we discuss the application of the barrier model to solid Lu<sub>2</sub>O<sub>3</sub>.

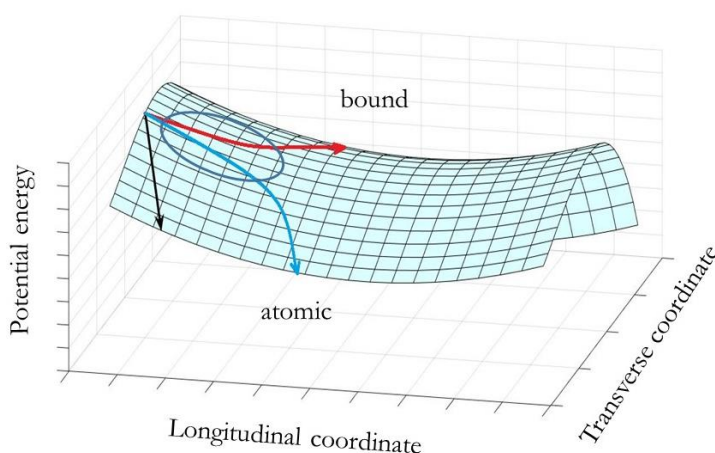


Figure 1. Muonium trajectories (black and colored lines) on a two-dimensional potential landscape during the relaxation of the lattice. Reaction coordinates parallel (longitudinal) and perpendicular (transverse) to the ridge separating the atomic configuration from the bound configuration are indicated. Different potential profiles reflect the changes of the atomic arrangement during the lattice relaxation. The red line shows the path over the barrier (formation of a bound configuration). The black line and the blue line correspond to the prompt and the delayed formation of atom-like muonium, respectively. The encircled region indicates the area of the fairly long-lived (ns to  $\mu$ s) transition state in which the electron is only weakly bound, resulting in a small hyperfine interaction [1].

## References

- [1] R. C. Vilão et al., *Physical Review B*, 96, 195205 (2017).
- [2] R. C. Vilão et al., *Physical Review B*, 98, 115201 (2018).

## NARROW OPTICAL GAP FERROELECTRIC $\text{Bi}_2\text{ZnTiO}_6$ THIN FILMS DEPOSITED BY RF SPUTTERING

F. G. Figueiras<sup>\*a,b</sup>, J. R. A. Fernandes<sup>c</sup>, J. P. B. Silva<sup>a,e</sup>, D. O. Alikin<sup>b,f</sup>, E. C. Queirós<sup>g</sup>, C. R. Bernardo<sup>e</sup>, Y. R.-Barcelay<sup>a,h</sup>, A. Wrzesińska<sup>i</sup>, M. S. Belsley<sup>e</sup>, B. Almeida<sup>e</sup>, P. B. Tavares<sup>g</sup>, A. L. Kholkin<sup>b,f</sup>, J. Agostinho Moreira<sup>a</sup>, A. Almeida<sup>a</sup>

<sup>a</sup> IFIMUP & Physics and Astronomy Department, Sciences Faculty, Porto University. R. Campo Alegre, 687, 4169-007 Porto. Portugal.

<sup>b</sup> CICECO-AIM & Physics Department, Aveiro University, 3810-193 Aveiro, Portugal.

<sup>c</sup> CQVR Physics Department, University of Trás-os-Montes & Alto Douro, 5001-801 Vila Real, Portugal.

<sup>e</sup> Center and Department of Physics, University of Minho, Campus de Gualtar, 4710-057 Braga, Portugal

<sup>f</sup> School of Natural Sciences and Mathematics, Ural Federal University, 620000 Ekaterinburg, Russia.

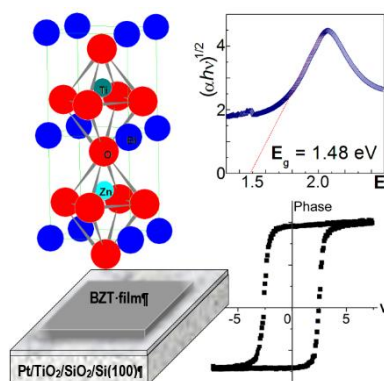
<sup>g</sup> CQVR & Chemistry Department, University of Trás-os-Montes & Alto Douro, 5001-801 Vila Real, Portugal.

<sup>h</sup> Departamento de Física, Instituto de Ciências Exatas, Universidade Federal do Amazonas, CP 69077-000, Manaus, AM, Brasil.

<sup>i</sup> Department of Molecular Physics, Lodz University of Technology, Żeromskiego 116, 90-924, Łódź, Poland.

\* Corresponding author e-mail: [fabio.figueiras@fc.up.pt](mailto:fabio.figueiras@fc.up.pt)

This work reports the deposition of single phase  $\text{Bi}_2\text{ZnTiO}_6$  thin films onto Pt/Si-based substrates using rf-sputtering method and the respective structural, morphological, optical and local ferroelectric characterization. The thin film grows in the polycrystalline form with tetragonal  $P4mm$  symmetry identified by X-ray diffraction [1]. The lack of spatial inversion centre was confirmed by the second harmonic generation. A narrow indirect optical gap of 1.48 eV was measured using optical diffuse reflectance. The ferroelectric domain reversal was further demonstrated through piezo-response force microscopy. This work demonstrates a practical method to fabricate the BZT perovskite phase with outstanding optical and ferroelectric properties, without recurring to high pressure and temperature conditions necessary to synthesize the bulk form.



The Narrow optical gap ( $E_g$ ) ferroelectric (FE) oxides constitute an innovative scientific and technical approach to photovoltaic (PV) and solar energy harvesting devices [1]. In this context, among the widespread research and development of photovoltaic technologies, ferroelectric materials present outstanding benefits over the conventional semiconductor based solar cells. It has been shown theoretically that  $\text{Bi}_2\text{ZnTiO}_6$  (BZT) perovskite can have unique optical and polar properties, such as an indirect band gap of 1.48 eV and saturation polarization up to  $150 \mu\text{C}/\text{cm}^2$ , generated by the large tetragonal distortion ratio  $c/a$  of 1.211. However, bulk BZT requires high pressure and high temperature to be synthesized, which makes its production difficult and expensive [2,3]. Whereas, studies regarding the fabrication of single phase BZT thin films have been scarcely reported so far.

### REFERENCES

- [1] H. An, J.Y. Han, B. Kim, J. Song, S.Y. Jeong, C. Franchini, C.W. Bark, S. Lee, Sci Rep. 2016, 6, 28313, 1-7.
- [2] T. Qi, I. Grinberg, A.M. Rappe, Phys. Rev. B 2011, 83, 224108, 1-6.
- [3] M.R. Suchomel, A.M. Fogg, M. Allix, H. Niu, J.B. Claridge, M.J. Rosseinsky, Chem. Mater. 2006, 18, 4987-4989.

## STRUCTURAL DISTORTIONS ROLE ON THE HIGH-PRESSURE STRUCTURAL TRANSITIONS AND LOW-TEMPERATURE MAGNETIC TRANSITIONS OF RFeO<sub>3</sub>

R. Vilarinho,<sup>1,\*</sup> M. Guennou, P. Bouvier, M. C. Weber, I. Peral, P. Tavares, G. Garbarino, M. Mezouar, J. Kreisel, A. Almeida and J. Agostinho Moreira

<sup>1</sup>IFIMUP, Departamento de Física e Astronomia, Faculdade de Ciências, Universidade do Porto

<sup>2</sup>Luxembourg Institute of Science and Technology, rue du Brill, L-4422 Belvaux, Luxembourg

<sup>3</sup>Université Grenoble-Alpes, CNRS, Institut Néel, 38000 Grenoble, France

<sup>4</sup>European Synchrotron Radiation Facility, 38043 Grenoble, France

\*Corresponding Author: rvsilva@fc.up.pt

Rare-earth orthoferrites (RFeO<sub>3</sub>) have been intensively studied in last years, as they exhibit a variety of interesting physical properties, with a large number of works having addressed the underlying microscopic mechanisms [1]. The R-cation size drives the cooperative rotations of the FeO<sub>6</sub> octahedra, which is known to linearly scale with the octahedra tilt angles [1]. Their physics has been studied with temperature and hydrostatic pressure as external parameters. The RFeO<sub>3</sub> undergo a paramagnetic-antiferromagnetic phase transition at high temperatures ( $T_N \approx 700$  K) [1]. This phase transition is associated with the ordering of the Fe<sup>3+</sup> spin sublattice into the G<sub>x</sub>AyF<sub>z</sub> type. For the cases of R = Pr, Nd, Sm, Tb, Ho, Er, Tm, and Yb, there is a spin reorientation into the F<sub>x</sub>C<sub>y</sub>G<sub>z</sub> structure, in a temperature range strongly dependent on the rare-earth cation [1]. It is currently accepted that the anisotropic interactions between the two antiferromagnetically coupled Fe and R sublattices with opposite net ferromagnetic moment underlies the spin reorientation transition [1].

In order to predict and explain the structural behavior of perovskites under high pressure, several rules have been proposed, based on experimental results, theoretical models and DFT calculations [2-3]. The first attempts to formulate general rules regarding the pressure dependence of the phase sequence in perovskites were based on the ratio between the compressibilities of the AO<sub>12</sub> and BO<sub>6</sub> polyhedra, predicting the octahedral tilts should decrease with increasing pressure [2]. Moreover, this decrease of the octahedral tilting with pressure should yield a structural phase transition into a higher-symmetric structure at some critical pressure [2]. As a matter of fact, these rules are not followed by many of 3:3 perovskites, for example in RFeO<sub>3</sub> a pressure-driven isostructural transition has been found [4].

Our work reports on the evolution of the octahedra distortions of RFeO<sub>3</sub> with applied pressure, by Raman scattering and XRD at the ESRF up to 55 GPa, and with temperature by Raman scattering down to 10 K. We find that the octahedra rotations decrease as pressure increases for R = Nd-Sm, whereas the reverse behavior is observed for R = Tb-Lu [4]. For the compounds where the tilts increase with pressure, the FeO<sub>6</sub> octahedra are compressed at lower rates than for those ones exhibiting opposite pressure tilt dependence. The crossover between the opposite pressure behaviors is discussed in relation to the general rules proposed from different theoretical approaches [4]. From the temperature dependence of the Raman modes, we have ascertained the spin-phonon coupling for NdFeO<sub>3</sub> and TbFeO<sub>3</sub>, well above the spin-reorientation temperature in the case of the latter, interpreted as a manifestation of the interaction between Fe and Tb spins. The linear correlation between the anomalous frequency deviations and magnetization in these compounds is discussed.

### References

- [1] E. Bousquet and A. Cano, *Journal of Physics: Condensed Matter*, 28, 123001 (2016).
- [2] J. Zhao et al., *Acta Crystallographica Section B*, 60, 263-271 (2004).
- [3] H. Xiang et al., *Physical Review B*, 96, 054102 (2017).
- [4] R. Vilarinho et al., *Physical Review B*, 99, 064109 (2019).

## HEMATITE NANOWIRES FOR PEC HYDROGEN PRODUCTION: THE EFFECT OF TI DOPANT AND TEMPERATURE

P. Quitério,<sup>1</sup> A. Apolinário,<sup>1</sup> C. T. Sousa,<sup>1</sup> P. Dias,<sup>2</sup> J. Azevedo,<sup>1,2</sup> A. M. Mendes,<sup>2</sup> and J. P. Araújo<sup>1,\*</sup>

<sup>1</sup>IFIMUP and IN-Institute of Nanoscience and Nanotechnology and Dep. Física e Astronomia, Universidade do Porto, Portugal.

<sup>2</sup>LEPABE, Dep. de Engenharia Química, Faculdade de Engenharia, Universidade do Porto, Portugal.

\*Corresponding Author: jearaujo@fc.up.pt

Sustainable development directives on the energy sector are crucial for the faster decarbonization of our planet. Hydrogen produced directly from renewable resources (sunlight and water) using a photoelectrochemical (PEC) cell has the potential to be a cost-effective route for storing the solar energy [1]. The use of hematite ( $\alpha$ -Fe<sub>2</sub>O<sub>3</sub>) photoanodes for PEC water splitting have attracted considerable attention due to their abundance, excellent long-term stability and suitable band gap (2.2 eV), which allows reaching the theoretical solar-to-hydrogen conversion efficiency of 16.8 % [2]. However,  $\alpha$ -Fe<sub>2</sub>O<sub>3</sub> presents some limitations to the PECs activity, such as poor conductivity and short hole diffusion length, that leads to high electron-hole recombination and significant efficiency losses. Several  $\alpha$ -Fe<sub>2</sub>O<sub>3</sub> nanostructures have been widely investigated to enhance PEC performance, improving the electron transport and charge separation efficiency. In particular, 1D nanostructures such as nanowires (NWs) present high-aspect-ratios providing a more direct pathway for charge transportation up to the charge collector, thus reducing recombination losses [2, 3]. Also, the use of dopants can highly improve the electrical conductivity of  $\alpha$ -Fe<sub>2</sub>O<sub>3</sub>, playing an important role in PEC performance [3, 4].

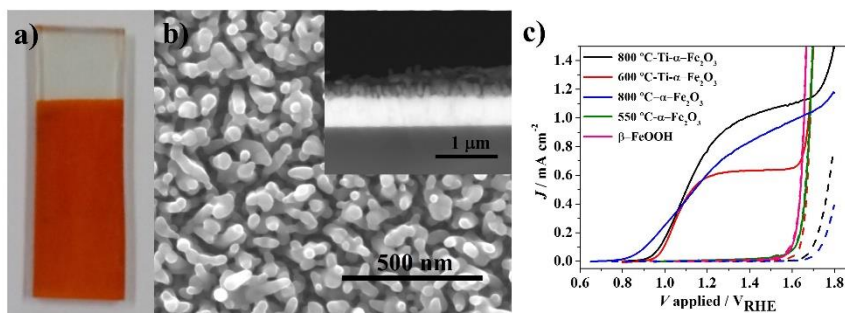


Figure 1. a) Visual aspect of a  $\alpha$ -Fe<sub>2</sub>O<sub>3</sub> photoanode deposited on FTO-glass substrate, b) SEM images showing the  $\alpha$ -Fe<sub>2</sub>O<sub>3</sub> nanowires morphology and c)  $J$ - $V$  curves.

In this work, hematite NWs were prepared by a hydrothermal method and the annealing conditions were varied to optimize the PEC performance: the grown time of  $\beta$ -FeOOH phase (heated at 95 °C, from 4-12 h) [3, 4], and the temperature for formation of the  $\alpha$ -Fe<sub>2</sub>O<sub>3</sub> crystalline phase (ranging from 550-800 °C) - Figure 1. Scanning electron microscopy (SEM) and X-ray diffraction (XRD) techniques were used to analyze the morphology (Figure 1b) and structure of the prepared samples. The PEC performance was evaluated by photocurrent density voltage ( $J$ - $V$ ) curves. The photocurrent showed not only a favorable increment with the use of Ti dopant, but also with annealing temperature (Figure 1c).

### References

- [1] M. Gratzel, *Nature*, 414, 338-344 (2001).
- [2] K. Sivula, F. Le Formal, M. Grätzel, *ChemSusChem*, 4, 432-449 (2011).
- [3] Y. Ling et al., *Nano Letters*, 11, 2119-2125 (2011).
- [4] T. Yang et al., *J. Mater. Chem. A*, 2, 2297 (2014).

# ON THE CONDUCTIVITY OF ISOLATED SINGLE WALL CARBON NANOTUBES FORM AB INITIO QUANTUM SIMULATIONS

Jaime Silva,<sup>1,\*</sup> Bruce F. Mine,<sup>1,2</sup> and Fernando Nogueira<sup>1</sup>

<sup>1</sup>CFisUC, Department of Physics, University of Coimbra, Rua Larga, 3004-516 Coimbra, Portugal

<sup>2</sup>Coimbra Chemistry Centre, Department of Chemistry, Rua Larga, 3004-516 Coimbra, Portugal

\*Corresponding Author: jaime.d.silva@uc.pt

Negative differential conductance (NDC) is a decrease in electrical current when the voltage across certain materials is increased. It is important for oscillators, amplifiers, and fast switching devices. In this work, using real time quantum simulations, we show that this phenomenon occurs in isolated finite armchair single wall carbon nanotubes (SWCNT) without end contacts. For metallic SWCNT, like the armchair SWCNT, NDC due to electron transfer to secondary valleys is not expected to be observed, as a consequence of the two quantum channels at the Fermi energy that are available to conduction. The NDC is due to the finite nature of the SWCNT and the existence of excited states that are blocked, similarly to a Coulomb blockade system, thus preventing any further current flow. We also show that the SWCNT conductivity depends on its length and that the current flowing on the SWCNT behaves like a Bloch oscillation that is disrupted in the presence of a molecule, decreasing the conductivity, providing a rationalisation for the behaviour of SWCNT organic gas sensors.

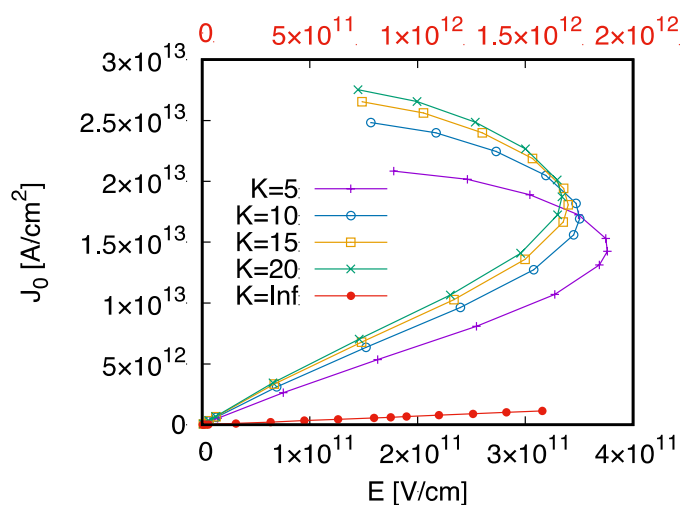


Figure 1. Current density for SWCNT with different lengths. The red horizontal scale corresponds to the infinite SWCNT.



# OPTIMIZATION OF ELECTRON BEAM LITHOGRAPHY PARAMETERS FOR DENSE ARRAYS OF CIRCULAR AND HEXAGONALLY SHAPED ANTIDOTS IN MAGNETIC THIN FILMS

Pedro D. R. Araujo,<sup>1,2\*</sup> A. V. Silva,<sup>1,2</sup> S. Cardoso<sup>1,2</sup> and D. C. Leitao<sup>1,2</sup>

<sup>1</sup>INESC-MN and IN, Rua Alves Redol 9, 1000-029 Lisboa, Portugal

<sup>2</sup>Instituto Superior Técnico, Universidade de Lisboa, Av. Rovisco Pais, 1000-029 Lisboa, Portugal

\*Corresponding Author: pedro.d.r.araujo@ist.utl.pt

Local modification of the magnetic properties of thin films can be achieved by introducing defects at the nanoscale that act as pinning centers for the magnetic domain walls. Key physical magnetic properties can be modified such as coercive field or local anisotropy [1] which can be tailored by controlling the defect properties: shape, lattice, density and size [2]. In this work we optimized the patterning of dense nanostructures into the layers of a spin valve structure deposited by ion beam deposition. Electron beam lithography dose parameter was optimized to define the structures in positive resist with a RAITH 150 system (acceleration voltage 10kV, 10 $\mu$ m aperture). The resist had a thickness  $t_{\text{resist}} = 108 \pm 4$  nm when coated with a spin speed of 3 krpm followed by a bake at 160°C for 4 minutes. Holes with diameter (D) ranging from 100 nm up to 500 nm were targeted with different wall-to-wall spacings. Three modes of exposure were used: area, line and dot modes. This allowed to optimize and minimize the exposure time while enhancing feature definition. Structures were considered well defined when presenting a size within 5% maximum deviation to the nominal value. Optimizations in dot exposure mode were done for different wall-to-wall spacings for the smaller holes to evaluate the proximity effects – figure 1.A. Patterned features started to present higher values of D when the nominal spacing was reduced to 200 nm. Several different lattices were optimized: quadrangular, rectangular and triangular. Magnetic confinement sites with hexagonal shape were achieved up to a minimum wall width of around 110 nm for different diagonal lengths – figure 1.B. The pattern was transferred to the underlying magnetic films by ion milling. Atomic force microscopy scans were used to verify shadowing effects due to the aspect ratio feature size/resist thickness. A maximum deviation of 1 nm of the targeted value was estimated for the smallest holes fabricated -  $t_{\text{resist}}/D \approx 1$ . The impact on the coercive field in structures with exchange bias (NiFe/MnIr) will be addressed. The ability to nano define such arrays goes beyond hardening effects in magnetic thin films and can be extended to applications in other fields such as photonics or magnonics.

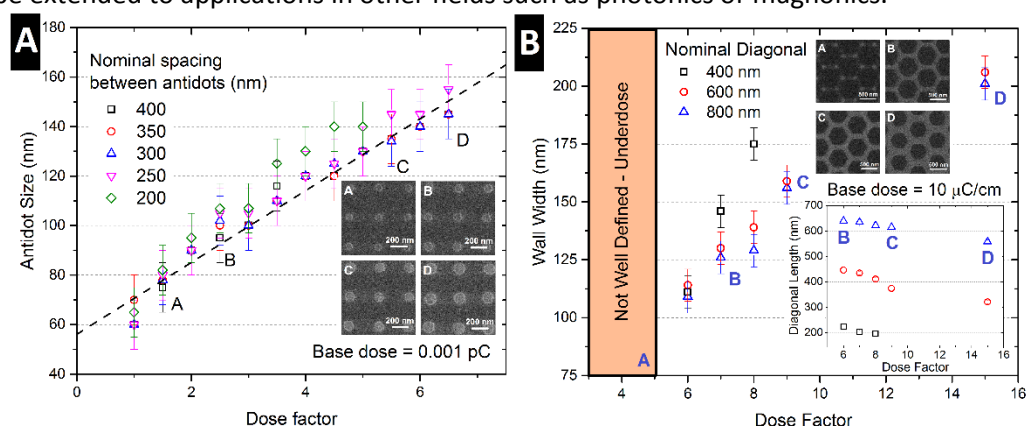


Figure 1. A – Dose optimization for differently spaced hole arrays targeting holes up to 150 nm diameter in dot exposure mode. B – Dose optimization for the magnetic confinement sites in line exposure mode. The error bars correspond to 10 nm.

## References

- [1] D. Tripathy *et al.*, *Applied Physics Letters* 93.2, 022502 (2008).
- [2] C. T. Sousa *et al.*, *Applied Physics Reviews* 1.3, 031102 (2014).

## RESISTIVE SWITCHING OF PT/MGO/M/RU (M = TA, AL, CU, AG) STRUCTURES

C. Dias,<sup>1,\*</sup> H. Lv,<sup>2</sup> S. Cardoso,<sup>2</sup> and J. Ventura<sup>1</sup><sup>1</sup>IFIMUP-IN and Department of Physics and Astronomy, Faculty of Sciences, Porto, Portugal<sup>2</sup>INESC-MN and IN - Institute of Nanoscience and Nanotechnology, Lisboa, Portugal

\*Corresponding Author: c.dias@fc.up.pt

The downscaling of conventional non-volatile memories is reaching its fundamental limit and there is thus a tremendous demand for novel scalable approaches. Among the most interesting technologies for novel memories are metal-insulator-metal (MIM) memristive devices [1,2] that exhibit non-volatile resistive switching [2,3] between low (LRS; ON) and high resistive states (HRS; OFF). Resistive switching comprises Set (OFF to ON) and Reset (ON to OFF) processes that can be operated under two modes: unipolar and bipolar. Resistive switching is being studied for a large range of applications such as memory (resistive random access memories; ReRAMs), logic, neuromorphic or sensing.

We obtained resistive switching in Pt (150) / MgO (30) / M (20) / Ru (5) (nm) structures, for different types of metals as top electrode, namely Ta, Al, Cu and Ag. The resistive switching behavior can then be explained by the formation and rupture of oxygen vacancies filaments inside MgO from the M towards the Pt electrode in the case of Ta, Al and Cu. For these cases, the resistive switching is unipolar, since Set and Reset can occur at either voltage polarity. For Ag as top electrode, the resistive switching is bipolar, with Set and Reset happening only at opposite polarities, and the conductive filaments being composed of silver ions. A good separation between the two resistance states was kept over time for all electrodes. Furthermore, taking into account the natural variability of the operation parameters, statistical studies were performed.

Knowing the influence of the top electrode on the resistive switching behavior and parameters, our results open the prospect to improve switching performance in other resistive switching systems. Furthermore, the insulator/metal dynamics can be chosen according to the type of application.

## References

- [1] L. Chua, *IEEE Trans. Circuit Theory*, 18, 507-51 (1971).
- [2] D. B. Strukov et al., *Nature*, 453, 80-83 (2008).
- [3] R. Waser, M. Aono, *Nat. Mater.*, 6, 833-840 (2007).



## SIMULATION OF THE TEMPERATURE PROFILE OF BACAZRTIO3 THIN FILMS DURING LASER ANNEALING

T. Rebelo,<sup>1,\*</sup> B. G. Almeida<sup>1</sup>

<sup>1</sup>Centre of Physics/Department of Physics, University of Minho, Gualtar Campus, Braga, Portugal

\*Corresponding Author: rebelo.tiago@gmail.com

Multiferroic piezoelectric-magnetostrictive composites have been attracting much attention, since they allow exploring coupled electric/magnetic responses. In this respect, composite nanostructures made of  $\text{Ba}_{0.85}\text{Ca}_{0.15}\text{Ti}_{0.9}\text{Zr}_{0.1}\text{O}_3$  (BCZT, ferroelectric) thin films on metglas substrates (ferromagnetic), the BCZT has to be deposited at low temperatures (400 °C), so as to not damage the substrate (crystallization temperature ~450 °C). However, thin films deposited at low temperatures exhibit a disordered structure, with a high density of crystallographic defects and low crystallinity. In such cases the films may be annealed after deposition, but in the BCZT/metglas case this can't be done in a conventional oven since it would degrade the substrate. An alternative is performing a pulsed laser annealing, minimizing the heated region and the degradation of the metglas. As such, the simulation of the annealing process is useful to understand how the annealing parameters (energy and fluence of the laser, pulse duration, etc) influence the optimization of the crystallinity of the film (temperature vs depth in the film, phase changes in the film, etc).

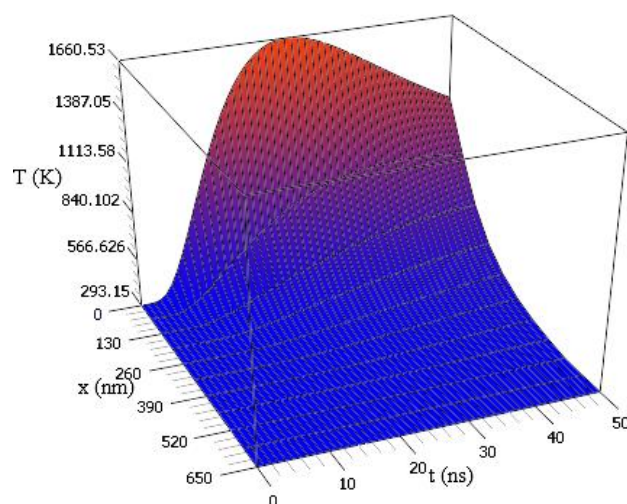


Figure 1. Temperature profile of the sample during one laser pulse.

In this work the variation of the temperature with the depth relative to the film's surface and on annealing time was studied (Figure 1). The sample was composed by a BCZT thin film prepared by laser ablation on a Metglas 2826MB. A 248 nm KrF pulsed laser was used for both the ablation and the annealing. The geometry of the film/incident laser is such that the 1D heat diffusion equation is appropriate. A finite difference method was used, considering the dependence of the laser intensity on time and the sample's heat conductivity and specific heat dependence on temperature, as well as its reflectivity. The effect of the diffusivity of the BCZT on the temperature distribution, instead of separated heat conductivity and specific heat, was also studied.

No phase changes were detected in both the BCZT and metglas for the values of laser fluence studied (40, 50 and 80  $\text{mJ}/\text{cm}^2$ ). - however, for 80  $\text{mJ}/\text{cm}^2$  the maximum temperature reached approached the BCZT's fusion temperature. Additionally, it was found that the film's heat conductivity decreases with increasing fluence, which may indicate that lower fluences allow a better distribution of the laser's energy through the crystal lattice. Consequently the crystallinity improves for low fluences, as compared to higher fluences. It was further observed that between consecutive pulses the film's temperature stabilizes at room temperature.

## GENTLE PROBE AFM: A NON-CONTACT METHOD FOR MEASURING THE VISCOELASTICITY OF SOFT MATERIALS

M. S. Rodrigues

University of Lisboa, Faculty of Sciences, BioISI - Biosystems & Integrative Sciences Institute, Lisboa,  
Portugal

e-mail: msrodrigues@fc.ul.pt

Viscoelastic properties of cells have been increasingly associated to important processes such as cell division, mechanotransduction, metastasis or locomotion. However, many of the measuring methodologies employed so far suffer from various weaknesses that hinder a quantitative determination of these properties with a high degree of accuracy. For instance, common methodologies such as the atomic force microscope (AFM) often require mechanical contact between a nanosized-tip and the sample which, besides the obvious side effects of applying huge pressures on living beings, often masks the viscoelastic response of cells under adhesive interactions between probe and specimen. Furthermore, the use of atomic force microscopes requires accurate calibration of both cantilever stiffness and sensitivity of optical beam deflection measuring system often employed in this instruments. The accurate and independent measurement of these quantities has been the target of numerous studies and is still the object of a significant debate in the AFM community. In this sense, the separation of sample and probe deflections remains a crucial problem in this kind of measurement. Finally spectroscopic measurements of sample compliance is needed to separate their viscous and elastic response. These are highly complex to do in conventional microscopes, especially when one wants to avoid possible artifacts introduced by the frequency response of the probes used, which arise when one measures sample compliance at frequencies linked to the AFM cantilever eigenmodes. These difficulties, among others, are thought to be at the origin of order-of-magnitude differences in the results of several studies of the same or similar organisms.

We measured the viscoelastic properties of Cystic Fibrosis Bronchial Epithelial cells by oscillating a common AFM cantilever with a colloidal probe in a non contact regime, from several hundreds of nm to the onset of contact. In this way we produce a hydrodynamic excitation [1] of the specimen and its response is in turn monitored by measuring the AFM cantilever dynamical behavior. The dynamic response of the AFM tip undergoes a transition from a pure inelastic (at long range) to a viscoelastic (at short range) regime. The distance at which this transition occurs depends on the sample compliance, fluid viscosity and frequency of oscillation. A clear advantage of this method is that it is possible to obtain the sample elasticity even if the cantilever spring constant is not known.

This experiment is complemented by subsequently performing conventional indentation experiments with the same probe, but using a Force Feedback methodology [2] to clearly separate sample and cantilever deformation.

### References

- [1] S Leroy, E Charlaix, *Journal of Fluid Mechanics*, 674, 389-407 (2011).
- [2] M S Rodrigues et al., *App. Phys. Lett.* 101, 203105 (2012).

## THE EFFECT OF DIFFUSION TIMESCALES IN LINKER-MEDIATED AGGREGATION

J. M. Tavares<sup>1,2\*</sup>, G. C. Antunes<sup>3</sup>, C. S. Dias<sup>1,4</sup> and N. A. M. Araújo<sup>1,4</sup>

<sup>1</sup> Centro de Física Teórica e Computacional, Universidade de Lisboa, 1749-016 Lisbon, Portugal.

<sup>2</sup> Instituto Superior de Engenharia de Lisboa, Lisbon, Portugal.

<sup>3</sup> Max Planck Institute for Intelligent Systems, Stuttgart, Germany

<sup>4</sup> Departamento de Física, Faculdade de Ciências, Universidade de Lisboa, 1749-016 Lisbon, Portugal.

\*Corresponding Author: jmtavares@fc.ul.pt

The classical Smoluchowski equation has analytical solutions for constant, additive and multiplicative kernels but, in all these cases, a single rate constant (or time scale) for aggregation is assumed. Inspired by processes in bioengineered systems - where the components have very different diffusion constants - we study the irreversible aggregation of  $f$ -functional (slow) particles mediated by bifunctional (fast) monomers or linkers. We generalize Smoluchowski equation to include two time scales and solve it for two types of kernels. We obtain - as a function of  $f$ , of the ratio  $\varphi$  between the concentrations of linkers and particles, and of the ratio  $\alpha$  between the two time scales - analytical expressions for the cluster size distribution, for the percolation threshold and for some scaling relations between different bond probabilities. Numerical calculations reveal that the percolation time varies strongly with both  $\alpha$  and  $\varphi$ , and that for each  $\varphi$  there is an  $\alpha$  that minimizes it.

The analytical results are compared with those of simulations obtained with molecular dynamics for a 2D system and with kinetic Monte Carlo for a 3D system.

## ENHANCED PROPAGATION OF MOTILE BACTERIA ON SURFACES DUE TO FORWARD SCATTERING

Vasco C. Braz,<sup>1,2\*</sup> Giorgio Volpe<sup>3</sup> and Nuno A.M. Araújo<sup>1,2</sup>

<sup>1</sup>Faculdade de Ciências, Universidade de Lisboa, 1749-016 Lisbon, Portugal.

<sup>2</sup>Centro de Física Teórica e Computacional, Universidade de Lisboa, 1749-016 Lisbon, Portugal.

<sup>3</sup>Department of Chemistry, University College London, 20 Gordon Street, London WC1H 0AJ, United Kingdom.

\*Corresponding Author: [vascobraz@alunos.fc.ul.pt](mailto:vascobraz@alunos.fc.ul.pt)

How motile bacteria move near a surface is a problem of fundamental biophysical interest and is key to the emergence of several phenomena of biological, ecological and medical relevance, including biofilm formation. Solid boundaries can strongly influence a cell's propulsion mechanism, thus leading many flagellated bacteria to describe long circular trajectories stably entrapped by the surface. Experimental studies on near-surface bacterial motility have, however, neglected the fact that real environments have typical microstructures varying on the scale of the cells' motion. Here, we combine experiments and numerical simulations to show that randomly distributed micro-obstacles influence the propagation of bacteria on a surface in a non-monotonic way. Instead of hindering it, an optimal, relatively low obstacle density can significantly enhance cells' propagation on surfaces due to individual forward scattering events. This finding provides new insight on the emerging dynamics of chiral active matter in complex environments and inspires novel routes to control microbial ecology in natural habitats.

### References

[1] *Enhanced propagation of motile bacteria on surfaces due to forward scattering*, S. Makarchuk, V. C. Braz, N. A.M. Araújo, L. Ciric, G. Volpe (Preprint), [arxiv.org/abs/1901.08682](https://arxiv.org/abs/1901.08682) (2019).

**A SYSTEMATIC ANALYSIS OF CELL MIGRATION IN SILICON**

M. Moreira-Soares<sup>1</sup>, S. Pinto-Cunha<sup>1</sup>, J .R. Bordin<sup>2</sup>, Rui D. M. Travasso<sup>1</sup>

<sup>1</sup> CFisUC, Departamento de Física da Universidade de Coimbra, Coimbra, Portugal

<sup>2</sup> Departamento de Física da Universidade Federal de Pelotas, UFPel, Pelotas, Brazil

e-mail: mmsoares@uc.pt

Migration is one of the most fundamental cellular functions and plays a key role in life and also in several diseases. Despite its importance and the effort employed by the scientific community in the study of the underlying mechanisms associated to migration there are still many unanswered questions. A prominent biological phenomenon associated to cell movement is metastasis: the process carried when a malignant cell

detaches itself from the primary tumor colony and migrate through the extracellular matrix (invasion) in the attempt to reach the blood circulation (intravasation). Further, while in the vessels the cancer cell can reach distant organs or tissues (extravasation) and may start a secondary colony (colonisation). We applied a computational approach to investigate the role of mechanical constraints imposed by the extracellular matrix in regulating cell migration and shape using a phase-field model. We measure the migrating velocity and characterise cell shape as a function of the density of fibres in the extracellular matrix and the adhesion.

**INTERACTION ANISOTROPY IN PARTICLE DEPOSITION AT THE EDGES OF DRYING DROPS**C. S. Dias<sup>1,2\*</sup>, M. M. Telo da Gama<sup>1,2</sup>, and N. A. M. Araújo<sup>1,2</sup><sup>1</sup> Departamento de Física, Faculdade de Ciências, Universidade de Lisboa, 1749-016 Lisbon, Portugal.<sup>2</sup> Centro de Física Teórica e Computacional, Universidade de Lisboa, 1749-016 Lisbon, Portugal.

\*Corresponding Author: csdias@fc.ul.pt

The deposition process at the edge of evaporating colloidal drops varies with the shape of suspended particles. Experiments with prolate ellipsoidal particles suggest that the spatiotemporal properties of the deposit depend strongly on particle aspect ratio. As the aspect ratio increases, the particles form less densely-packed deposits and the statistical behavior of the deposit interface crosses over from the Kardar-Parisi-Zhang (KPZ) universality class to another universality class which was suggested to be consistent with the KPZ plus quenched disorder. Here, we numerically study the effect of particle interaction anisotropy on deposit growth. In essence, we model the ellipsoids, at the interface, as disk-like particles with two types of interaction patches that correspond to specific features at the poles and equator of the ellipsoid. The numerical results corroborate experimental observations and further suggest that the deposition transition can stem from interparticle interaction anisotropy. Possible extensions of our model to other systems are also discussed.

**References**

- [1] C. S. Dias et al., *EPL*, 107, 56002 (2014)
- [2] C. S. Dias et al., *Soft. Matter*, 14, 2744 (2018)

## LARGE MAGNETOELECTRIC COUPLING OBSERVED AT ROOM TEMPERATURE IN A CHIRAL LANTHANIDE COMPLEX

M. S. Ivanov<sup>1,\*</sup>, J. Long<sup>2</sup>, V. A. Khomchenko<sup>1</sup>, J.-M. Thibaud<sup>2</sup>, Y. Guari<sup>2</sup>, J. Larionova<sup>2</sup>, and J. A. Paixão<sup>1</sup>

<sup>1</sup>CFisUC, Department of Physics, University of Coimbra, 3004-516 Coimbra, Portugal

<sup>2</sup>Institut Charles Gerhardt Montpellier, Université de Montpellier, 34095 Montpellier, France

\*Corresponding Author: maxim.ivanov@uc.pt

Multiferroics are long known as multifunctional materials that demonstrate at least two ferroic orders for example ferromagnetism and ferroelectricity [1] and may provide a basis for developing high-density data storage, spintronics or low consumption devices [2, 3]. In natural materials, there are no examples of such association and designing of these systems is not straightforward owing to the phenomenological origin of both ferroic properties. On the other hand, magneto-electrical materials such as ferroelectric paramagnets are a more common class of materials that could also provide an interplay between magnetic and electrical properties [4]. In current work, taking advantage of the flexibility of molecular chemistry, we describe an example of multiferroic sample consisting of molecular paramagnetic and ferroelectric materials based on a chiral lanthanide complex that also exhibits a Near Infra-Red luminescence. Our molecular approach to design multifunctional multiferroics with strong coupling between the magnetic and ferroelectric features relies on the association of lanthanide ions with a chiral diamagnetic zinc or nickel complexes in order to favor the crystallization in one of the ten polar point groups compatible with ferroelectricity. We provide experimental evidence of room-temperature magneto-switching of the ferroelectric domains at the nanometric scale in such multifunctional molecular ferroelectrics.

The proof of concept of electrical polarization switchability at room temperature using a low magnetic field confirms that molecular materials can be competitive with pure inorganic materials, opening new horizons in the design of multiferroics and magneto-electrical systems.

### References

- [1] S.W. Cheong, M. Mostovoy, *Nat. Mater.* 6, 13-20, (2007)
- [2] J.F. Scott, *Nat. Mater.* 6, 256-257, (2007)
- [3] P. Mandal et al. *Nature* 525, 363-366, (2015)
- [4] W. Eerenstein, N.D. Mathur & J.F. Scott, *Nature* 442, 759-765, (2006)



P. Rocha-Rodrigues,<sup>1,\*</sup> G. P. Oliveira,<sup>1</sup> S.S. M. Santos,<sup>1</sup> I. P. Miranda,<sup>2</sup> T. Leal,<sup>1</sup> R. Moreira,<sup>1</sup> L. V. C. Assali,<sup>2</sup> H. M. Petrilli,<sup>2</sup> J. G. Correia<sup>3</sup>, J. P. Araújo<sup>1</sup> and A.M. L. Lopes<sup>1</sup>

<sup>1</sup>IFIMUP, Departamento de Física e Astronomia da Faculdade de Ciências da Universidade do Porto,  
4169-007 Porto,

<sup>2</sup>Instituto de Física, Universidade de São Paulo, São Paulo, Brasil,

<sup>3</sup>Centro de Física Nuclear da Universidade de Lisboa, 1749-016 Lisboa, Portugal

\*Corresponding Author: pedro.da.r.rodrigues@gmail.com

Naturally layered perovskites (NLP) such as the Ruddlesden-Popper phases ( $\text{Ca}_{n+1}\text{Mn}_n\text{O}_{3n+1}$ ) have appeared as a fascinating route to achieve nonexpensive room temperature multiferroic materials [1]. In these NLP, specifically in the  $A2_1am$  structural phase of  $\text{Ca}_3\text{Mn}_2\text{O}_7$ , distortions of the lattice such  $\text{MnO}_6$  octahedron rotation and tilting modes couple to polar cation dislocation modes, inducing a ferroelectric polarization in a mechanism known as hybrid improper ferroelectricity. The novel idea behind this prototypical multiferroic is that the ferromagnetic and ferroelectric orders can be coupled through the same lattice instability, providing an indirect but very strong magneto-electric coupling.[1]  $\text{Ca}_3\text{Mn}_2\text{O}_7$  is also known to undergo a 1<sup>st</sup> order structural phase transition, from the polar  $A2_1am$  to the non-polar  $Acaa$  space group symmetry, near room temperature conditions. In the later space group,  $\text{Ca}_3\text{Mn}_2\text{O}_7$  exhibit an unusual uniaxial negative thermal expansion, which has also been proven to be highly correlated with the type of condensed  $\text{MnO}_6$  octahedral distortions [2].

Perturbed Angular Correlation  $\gamma$ - $\gamma$  (PAC) hyperfine technique offers a unique opportunity to probe with high sensitivity, and at a local scale, the structural transitions that  $\text{Ca}_3\text{Mn}_2\text{O}_7$  undergoes. At ISOLDE-CERN, by using radioactive probes, PAC measurements were performed in a wide range of temperatures, from 1200K to 11K. Complementary ab-initio electronic structure calculations in the framework of the Density Functional Theory (DFT) were also implemented to understand and show how the measured Hyperfine quantities, such as the Electrical Field Gradient, at the probing sites, are valuable tools to probe the distinct  $\text{MnO}_6$  octahedron distortion modes that underlie the  $\text{Ca}_3\text{Mn}_2\text{O}_7$  structural transitions and functional properties.

## References

- [1] N.A. Benedek, C.J. Fennie, Physical Review Letters, 106, 3 (2011).
- [2] M.S. Senn, A. Bombardi, C.A. Murray, C. Vecchini, A. Scherillo, X. Luo, S.W. Cheong, Physical Review Letters, 114, 23 (2015).

# TETRAGONAL FERROELECTRIC PHASE OF GDMNO<sub>3</sub> EPITAXIAL THIN FILM GROWN ONTO SRTIO<sub>3</sub> (001)

P. Machado<sup>1</sup>, F. G. Figueiras<sup>1,2,\*</sup>, R. Vilarinho<sup>1</sup>, J. R. A. Fernandes<sup>3,4</sup>, P. B. Tavares<sup>5</sup>, M. Rosário Soares<sup>6</sup>, S. Cardoso<sup>7</sup>, J. Agostinho Moreira<sup>1</sup>, A. Almeida<sup>1</sup>

<sup>1</sup> IFIMUP-IN & Physics & Astronomy Department, Sciences Faculty, University of Porto. R. Campo Alegre, 687, 4169-007 Porto. Portugal.

<sup>2</sup> CICECO & Physics Department, University of Aveiro, 3810-193 Aveiro, Portugal.

<sup>3</sup> INESC-TEC & Physics & Astronomy Department, Sciences Faculty, University of Porto. R. Campo Alegre, 687, 4169-007 Porto. Portugal.

<sup>4</sup> CQVR & Physics Department, University of Trás-os-Montes e Alto-Douro, Ap.º 1013, 5001-801 Vila Real, Portugal

<sup>5</sup> CQVR & Chemistry Department, University of Trás-os-Montes e Alto-Douro, Ap.º 1013, 5001-801 Vila Real, Portugal

<sup>6</sup> CICECO & LCA, University of Aveiro, 3810-193 Aveiro, Portugal.

<sup>7</sup> INESC-MN, Rua Alves Redol, 9, 1000-029 Lisboa, Portugal.

\* Corresponding author e-mail: pedro.machado@fc.up.pt

High quality GdMnO<sub>3</sub> thin films were deposited on SrTiO<sub>3</sub> (001)-oriented substrates by RF magnetron sputtering. The structure, microstructure and polar properties were investigated in detail. The films grown up to a 35 nm thickness exhibit an epitaxial tetragonal symmetry, where the basal lattice parameters are imposed by the cubic structure of the substrate, contrarily to the expected orthorhombic bulk symmetry. The slower growth rate imposed by the RF-sputtering method, in comparison to other synthesis processes, yields a remarkable increase of the thickness threshold, below which GdMnO<sub>3</sub> epitaxial tetragonal films can be grown. Furthermore, the emergence of a noteworthy spontaneous electric polarization below ~31 K points to the stabilization of an improper ferroelectric phase at low temperatures, which is not observed in bulk GdMnO<sub>3</sub>.

MULTIFERROIC  $\text{CoFe}_2\text{O}_4/\text{LiNbO}_3$  BILAYERSB.M. Silva,<sup>1,\*</sup> J. Oliveira,<sup>2</sup> J.A. Mendes and B.G. Almeida<sup>1</sup><sup>1</sup>CF-UM-UP, Dep. Física, Univ. Minho, Campus de Gualtar, 4710-057 Braga, Portugal

\*Corresponding Author: mdasilvabrana@gmail.com

Nanostructured multiferroic thin films constructed by combining magnetostrictive and piezoelectric materials have attracted recently much scientific and technological interest. In addition to possessing ferroelectricity and ferromagnetism in each individual phase, they are shown to exhibit a stress mediated coupling between their magnetic and electric properties, the so called magnetoelectric effect. This coupling between their magnetic and electric degrees of freedom may then give rise to new physical phenomena and applications. In this context, improvement of the strain transfer between the phases in multiferroic composites can be achieved in nanostructures, due to the ability to combine the materials at the atomic level. Additionally, the exploration of new materials and systems involving multiple functionalities in the same structure (electric, magnetic and optical) broaden the prospects of potential applications. In this regard, lithium niobate ( $\text{LiNbO}_3$ ) is a ferroelectric material ( $T_C = 1230^\circ\text{C}$ ) widely used in electro-optical devices. Due to its high piezoelectric, pyroelectric, electro-optical, birefringent, photorefractive and photoelastic properties, lithium niobate presents a rich variety of favourable properties towards applications. On the other hand, cobalt ferrite presents a high magnetocrystalline anisotropy and magnetostriction, making it suitable for application in magnetoelectric composite thin films. Here, bilayer composite thin films, composed by a  $\text{LiNbO}_3$  layer deposited over a  $\text{CoFe}_2\text{O}_4$  film have been prepared by laser ablation on platinum covered  $\text{Si}(001)$  substrates, with a KrF excimer laser ( $\lambda = 248\text{ nm}$ ). Their structural, microstructural and dielectric properties were characterized. The X-ray diffraction measurements show that the films are polycrystalline, presenting the  $\text{LiNbO}_3$  rhombohedral ferroelectric phase and the  $\text{CoFe}_2\text{O}_4$  cubic spinel structure. The SEM micrographs show dense films, with cobalt ferrite and lithium niobate layer thicknesses in the range 100-200 nm and 400-800nm, respectively. Their dielectric properties were characterized by impedance spectroscopy, for temperatures 15-200°C and in the frequency range 10 Hz – 3 MHz. Using appropriate models for the behaviour of the polarization (Cole-Cole, Havriliak-Negami), as well as including a conductivity contribution, the electrical permittivity (real and imaginary components) was modelled and fitted (figure 1), in order to obtain the relaxation times and activation energies. As such, the influence of the synthesis conditions on the dielectric properties of the films and, in particular, their evolution with individual layer thicknesses, will be discussed and presented.

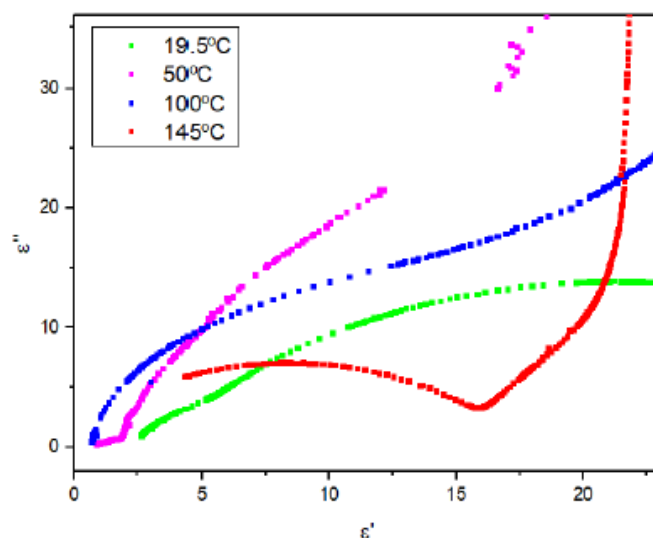


Figure 1. Imaginary component of electrical permittivity as a function of real component.

## ACOUSTICALLY-POWERED MICROSPINNERS

M. Tasinkevych<sup>1,\*</sup>, M. Olvera de la Cruz<sup>2</sup>, S. Sabrina<sup>3</sup>, S. Ahmed<sup>3</sup>, A. M. Brooks<sup>3</sup>, T. E. Mallouk<sup>3</sup>, and K. J. M. Bishop<sup>4</sup>

<sup>1</sup>Centro de Física Teórica e Computacional, Departamento de Física, Faculdade de Ciências, Universidade de Lisboa, Campo Grande P-1749-016, Lisboa, Portugal.

<sup>2</sup>Department of Materials Science and Engineering, Northwestern University, Evanston, Illinois 60208, USA.

<sup>3</sup>Department of Chemical Engineering, The Pennsylvania State University, University Park, Pennsylvania 16802, USA.

<sup>4</sup>Department of Chemical Engineering, Columbia University, New York, NY 10027, USA.

\*Corresponding Author: mtasinkevych@fc.ul.pt

The propulsion of micro-particles using ultrasound is an attractive strategy for the remote manipulation of colloidal matter using biocompatible energy inputs. However, the physical mechanisms underlying acoustic propulsion are poorly understood, and our ability to transduce acoustic energy into different types of particle motions remains limited. Here, we show that the three-dimensional shape of a colloidal particle can be rationally engineered to direct desired particle motions powered by ultrasound. We demonstrate experimentally that gold microplates with twisted star shape ( $C_{nh}$  symmetry) trapped at the nodal plane of a uniform acoustic field at megahertz frequencies can rotate about their symmetry axis, with the direction and rate of rotation dictated by the particle shape. In particular, we investigate the rotational motion as a function of the particle size, chiral asymmetry, and degree of rotational symmetry  $n$ . Particles of the opposite chirality rotate in opposite directions; achiral particles do not rotate. Interestingly, the direction of rotation also depends on the degree of rotational symmetry of the particles. For example, 3-fold symmetric particles rotate in the opposite direction as 4-fold ones. These observations are explained by a propulsion mechanism based on asymmetric acoustic streaming, whereby the presence of a particle in the primary oscillatory fluid flow gives rise to secondary (in Reynolds) steady fluid flows. We perform numerical analysis based on boundary elements method to describe the hydrodynamic flows surrounding acoustically-activated spinners and to calculate how the resulting angular velocity depends on the particle shape. Surprisingly, numerical calculations predict the reversal of the direction of the particle rotation upon increasing of the frequency of the driving acoustic field. The threshold value of the frequency is sensitive to the particle shape. Our results suggest how particle shape can be used to design colloids capable of increasingly complex motions powered by ultrasound. This may be useful for creation of colloidal machines – that is, dynamic assemblies of colloidal components that perform useful functions.



Figure 1. Microscopic image showing a pair of counter-rotating spinners with the lateral size  $\sim 10\mu\text{m}$ , adapted from [1].

#### Reference

[1] S. Sabrina et al., *ACS Nano* 12, 2939 (2018)

# STABILITY OF THE NEMATIC-ISOTROPIC INTERFACE OF ACTIVE LIQUID CRYSTALS IN A MICROCHANNEL

R. C. V. Coelho,<sup>1,\*</sup> N. A. M. Araújo<sup>1</sup> and M. M. Telo da Gama<sup>1</sup>

<sup>1</sup> Centro de Física Teórica e Computacional, Faculdade de Ciências, Universidade de Lisboa, P-1749-016 Lisboa, Portugal

\*Corresponding Author: rvc Coelho@fc.ul.pt

In Nature there are systems formed by many elongated units or particles capable of transforming the energy of the environment in directed motion. Examples are dense suspensions of bacteria, mixtures of microtubule-kinesin and shoals of fish. Such systems, when composed of a dense population of these particles, exhibit a collective behavior that can be described by the hydrodynamic equations of active liquid crystals. As with passive liquid crystals, the active ones can be in the nematic phase (where particles align along a preferred direction) or in the isotropic one (disordered). We present results of the numerical simulations of interfaces between the nematic and isotropic phases of active liquid crystals. As will be shown, the interfacial behavior in microchannels depends sensitively on the activity: propagation at constant velocities as for passive liquid crystals subjected to a shift in the coexistence temperature; instabilities and subsequent Poiseuille-like velocity profiles; dancing states, where rotating defects are formed in a regular lattice; or a chaotic regime (active turbulence). We examine the conditions under which the interface is stable and show that stable active interfaces may occur for shift in the coexistence temperature and small activities. When the activity is higher than a certain value, the interface rapidly disappears and the known states for active nematics are recovered.

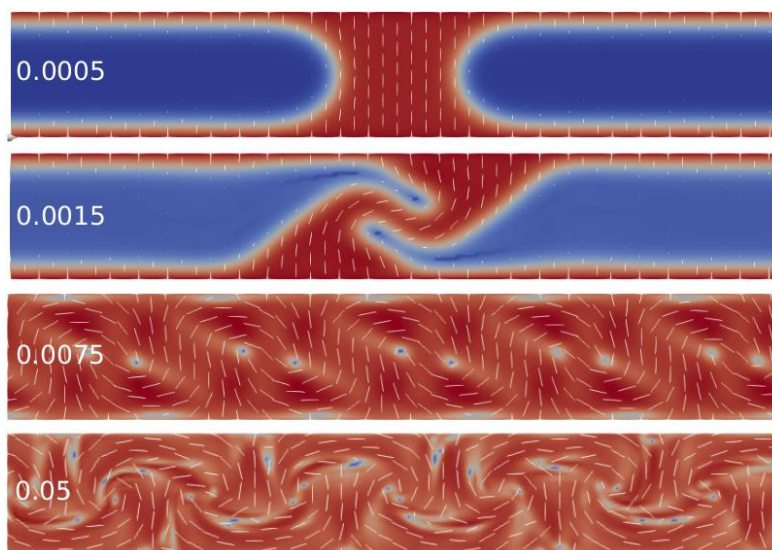


Figure 1. Active interface for different activities. The colors represent the scalar order parameter, the white lines stand for the directors and the activity is given in the corresponding image in simulation units. From top to bottom, the states of the interface are: stable interface, dancing state with one pair of defects, dancing state with 5 pairs of defects and active turbulence.

## ORDERING OF BINARY COLLOIDAL CRYSTALS BY RANDOM POTENTIALS

André S. Nunes,<sup>1</sup> Sabareesh K. P. Velu,<sup>2</sup> Iryna Kasianiuk,<sup>3</sup> Denys Kasyanyuk,<sup>3</sup> Agnese Callegari,<sup>3</sup> Giorgio Volpe,<sup>4</sup> Margarida M. Telo da Gama,<sup>1</sup> Giovanni Volpe,<sup>2,5</sup> and Nuno A. M. Araújo<sup>1,\*</sup>

<sup>1</sup>Centro de Física Teórica e Computacional and Departamento de Física, Faculdade de Ciências, Universidade de Lisboa, P-1749-016 Lisboa, Portugal.

<sup>2</sup>Department of Physics, Bilkent University, Cankaya, 06800 Ankara, Turkey.

<sup>3</sup>Department of Physics, Bilkent University and UNAM, Cankaya, 06800 Ankara, Turkey.

<sup>4</sup>Department of Chemistry, University College London, 20 Gordon Street, London WC1H 0AJ, United Kingdom.

<sup>5</sup>Department of Physics, University of Gothenburg, 41296 Gothenburg, Sweden.

\*Corresponding Author: nmaraujo@fc.ul.pt

Structural defects are ubiquitous in condensed matter, and not always a nuisance. For example, they underlie phenomena such as Anderson localization and hyperuniformity, and they are now being exploited to engineer novel materials. Here, we show experimentally that the density of structural defects in a 2D binary colloidal crystal can be engineered with a random potential. We generate the random potential using an optical speckle pattern, whose induced forces act strongly on one species of particles (strong particles) and weakly on the other (weak particles). Thus, the strong particles are more attracted to the randomly distributed local minima of the optical potential, leaving a trail of defects in the crystalline structure of the colloidal crystal. While, as expected, the crystalline ordering initially decreases with increasing fraction of strong particles, the crystalline order is surprisingly recovered for sufficiently large fractions. We confirm our experimental results with particle-based simulations, which permit us to elucidate how this non-monotonic behavior results from the competition between the particle-potential and particle-particle interactions.

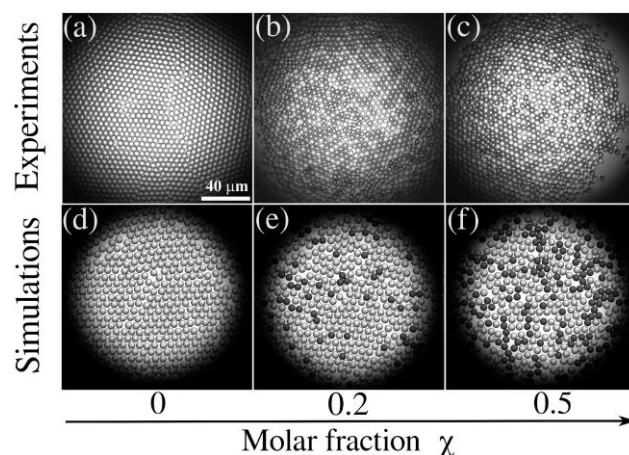


Figure 1. Snapshots of the final configurations in experiments (a-c) and simulations (d-f) of a mixture of colloidal particles in the presence of a random potential (speckle). The weak (silica) particles are light gray, and the strong (polystyrene) particles are dark gray. The global order is controlled by the molar fraction of strong particles ( $\chi$ ).

## Reference

[1] A. S. Nunes, S. K. Velu, I. Kasianiuk, D. Kasyanyuk, A. Callegari, G. Volpe, M. M. T. da Gama, G. Volpe, and N. A. Araújo, arXiv preprint arXiv:1903.01579 (2019)



## MODELLING OF MOLECULAR-SCALE PROPERTIES AND VISCOSITY OF POLYISOCYANATE LIQUIDS

V. Lenzi<sup>1,\*</sup>, P. Driest<sup>2,3</sup>, D. Dijkstra<sup>2</sup>, M. M. D. Ramos<sup>1</sup> and L. Marques<sup>1</sup>

<sup>1</sup>CFUM/UP, Campus de Gualtar, Braga, Portugal.

<sup>2</sup>Covestro AG, CAS Global R&D, Leverkusen, Germany.

<sup>3</sup>Technical Medical Centre, Department of Science and Technology, Univ. Twente, Enschede, the Netherlands.

\*Corresponding Author: veniero.lenzi@fisica.uminho.pt

Isocyanates are nowadays amidst the most used and important chemical families, as fundamental precursors of polyurethane materials. To meet the contemporary demands of advanced functionalities and application-tailored properties, a control of the micro- and nanostructure of the final material is desired, hence a deep understanding of the material's components at the molecular level is required. Surprisingly, isocyanates were scarcely studied from a fundamental level, and many of their properties are still poorly understood.

In this work, the authors present the result of combined computational and experimental studies on aliphatic polyisocyanates, aiming at investigating the connection between their viscosity and their molecular-level interactions and structure. Ultrapure samples were prepared by vacuum distillation techniques and their viscosity was measured[1]. *Ab initio* and density functional theory methods were used to study the intermolecular interactions in isocyanates[2]. A specific force field[3] has been developed and validated upon experimental data to perform molecular dynamics simulations on (poly)isocyanate liquids, and used to obtain free energy estimates and information on the local structure. Three possible interactions were identified in polyisocyanates, depending upon the involvement of isocyanate groups and/or isocyanurate rings. Ring-based interactions revealed themselves as rather strong (ca -13 kcal/mol) and dominated by dispersion. Isocyanate-isocyanurate interactions, although weaker (6-8 kcal/mol), showed a marked tendency for cooperation, allowing for the strongest interaction energies found in such systems. The interaction scheme proposed was fully capable to explain the experimentally observed viscosity trends, i.e. the high viscosities measured for functional isocyanurates compared to the lower ones for non-functional isocyanurates and isocyanate monomers.

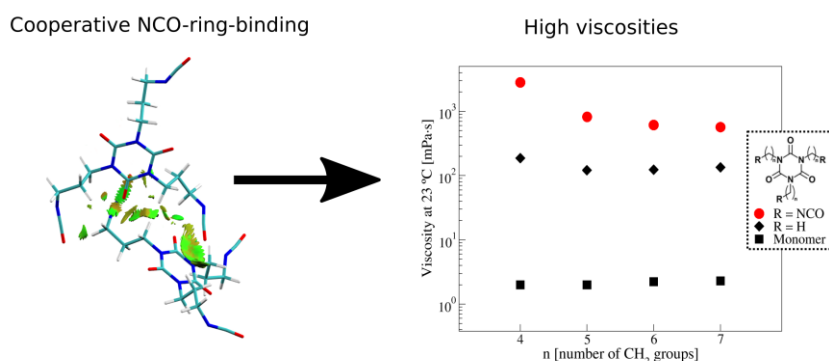


Figure 1. On the left, a representation of a functional isocyanate dimer showing multiple NCO-Ring interactions. Coloured surfaces are the result of an NCI analysis on the electron density. On the right, measured viscosities on ultrapure samples for a series of diisocyanate monomers, non-functional and functional isocyanate trimers.

### References

- [1] P. Driest, et al.(2017), Polymer for Advanced Technologies, 28:1299-1304. DOI:10.1002/pat.3891
- [2] V. Lenzi, et al. (2019), Journal of Molecular Liquids, 280:25-33. DOI:10.1016/j.molliq.2019.01.165
- [3] V. Lenzi, et al. (2019), Molecular Simulation, 45(3):207-214. DOI:10.1080/08927022.2018.1554902



## DYNAMICS OF THE CARBON VACANCY IN 4H-SiC: A THEORETICAL DESCRIPTION

J. Coutinho,<sup>1,\*</sup> V. J. B. Torres,<sup>1</sup> K. Demmouche,<sup>2</sup> and S. Öberg<sup>3</sup><sup>1</sup>Department of Physics and I3N, University of Aveiro, 3810-193 Aveiro, Portugal<sup>2</sup>Department, CUBBAT, Institut des Sciences, B.P. 284, 46000 Ain Temouchent, Algeria<sup>3</sup>Department of Engineering Sciences and Mathematics, Luleå University of Technology, SE-97187 Luleå, Sweden

\*Corresponding Author: jose.coutinho@ua.pt

Due to its wide bandgap, high chemical and thermal stability, as well as radiation and electrical hardness, silicon carbide (SiC) is becoming the material *de facto* for high-voltage and high-power applications. Among the several polytypes, the 4H stacked material has been the most used by the industry, which is offering already a wide range of products, from Schottky-barrier diodes to insulated-gate bipolar transistors with breakdown voltage of 1200-1700 V. It is known that the carbon vacancies in 4H-SiC are major carrier recombination centers and a cause for device failure. It is reasonably accepted that the carbon vacancy ( $V_C$ ) gives rise to  $Z_{1/2}$  and  $EH_{6/7}$  deep-level transients corresponding to traps at  $E_C-(0.5-0.6)$  eV and  $E_C-(1.5-1.7)$  eV [1,2], which were assigned to pairs of acceptor  $[(-/-)$  and  $(-/0)]$  and donor  $[(0/+)$  and  $(+/++)]$  levels, respectively.

Earlier electron paramagnetic resonance (EPR) experiments combined with first-principles calculations [3,4], have provided us with a rather detailed picture of the electronic structure of the vacancy, particularly regarding the static (ion-clamped) properties. However, several questions are still unanswered. For instance, the Jahn-Teller (JT) theorem states that any nonlinear atomic arrangement with an open-shell degenerate electronic ground state will undergo a spontaneous geometrical distortion, essentially removing the degeneracy to lower the overall energy. Yet, the undistorted (trigonal)  $V_C^+$  is a  $a_1^+$  singlet, meaning that the JT-effect cannot be invoked to account for the observed monoclinic symmetry of the E15 and E16 signals [3,4]. Other puzzles are some marked differences between  $V_C$  in the pseudo-cubic and hexagonal sites, which show dissimilar distortions, annealing behavior, and level ordering (the donor transitions seem to have a negative- $U$  ordering, depending on the crystallographic site). From density functional calculations employing semi-local and non-local treatments to the exchange-correlation potential, we show that a pseudo-Jahn-Teller (PJT) effect can explain the observed distortions of the singlet states. Unlike the JT effect, the PJT involves a vibronic coupling between ground and excited states, and this is actually the only possible source of instability of high-symmetry configurations in non-degenerate states. Using the nudged elastic band method to inspect the potential energy surface of  $V_C$  (in its five charge states) between equivalent (P)JT-distorted ground states, we arrived at a detailed configuration coordinate diagram for the defect. We further show that the PJT effect, combined with distinct crystal-field splitting amplitudes for the cubic and hexagonal sites, are able to explain the above differences.

## References

- [1] C. G. Hemmingsson, N. T. Son, A. Ellison, J. Zhang, and E. Janzén, *Phys. Rev. B* 58, R10119 (1998).
- [2] I. D. Booker, E. Janzén, N. T. Son, J. Hassan, P. Stenberg, et al., *J. Appl. Phys.* 119, 235703 (2016).
- [3] M. Bockstedte, M. Heid, and O. Pankratov, *Phys. Rev. B* 67, 193102 (2003).
- [4] T. Umeda, J. Isoya, N. Morishita, T. Ohshima, T. Kamiya, A. Gali, P. Deák, N. T. Son, and E. Janzén, *Phys. Rev. B* 70, 235212 (2004).
- [5] J. Coutinho, V. J. B. Torres, K. Demmouche and S. Öberg, *Phys. Rev. B* 96, 174105 (2017).

# BALLISTIC TRANSPORT IN MICRO-STRUCTURED BILAYER GRAPHENE FLAKES

Hadi Z. Olyafei <sup>1\*</sup>, Pedro Ribeiro <sup>1,2</sup>, Eduardo V. Castro <sup>1,2,3</sup>

<sup>1</sup>CeFEMA, Instituto Superior Técnico, Universidade de Lisboa, Av. Rovisco Pais, 1049-001 Lisboa, Portugal

<sup>2</sup>Beijing Computational Science Research Center, Beijing 100084, China and

<sup>3</sup>Centro de Física das Universidades do Minho e Porto,  
Departamento de Física e Astronomia, Faculdade de Ciências,  
Universidade do Porto, 4169-007 Porto, Portugal

\*Corresponding Author: hadi.olyaei@tecnico.ulisboa.pt

The transmission across a graphene bilayer region is calculated for two different types of connections to monolayer leads. We compute the conductance in the presence of a domain wall in the gate bias and show that, in this case, geometries with different types of connection to monolayer leads behave similarly. The two configurations are found to behave similarly when no gate voltage is applied. For a finite gate voltage, both develop a conductance gap characteristic of a biased bilayer, but only one shows a pronounced conductance step at the gap edge. A gate voltage domain wall applied to the bilayer region renders the conductance of the two configurations similar. For a microstructure consisting of equally spaced domain walls, we find a high sensitivity to the domain size. This is attributed to the presence of topologically protected in-gap states localized at domain walls, which hybridize as the domain size becomes of the order of their confining scale. Our results show that transmission through a bilayer region can be manipulated by a gate voltage in ways not previously anticipated.

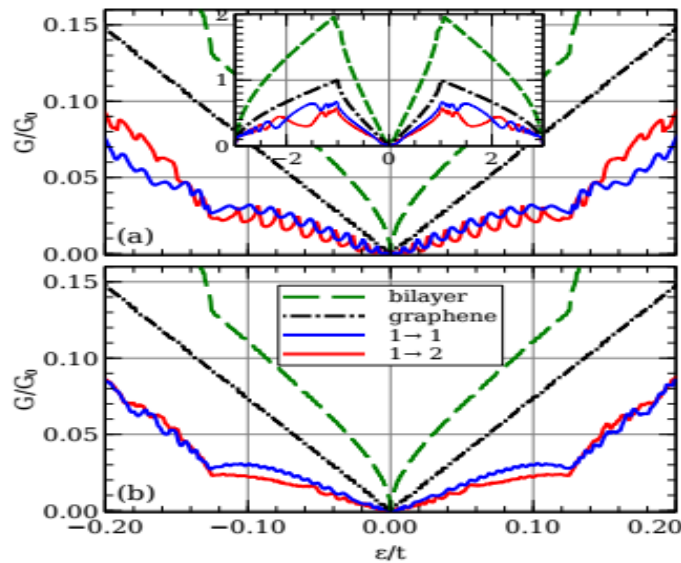


Figure 1. Plot of conductance-Data as a function of energy.

## References

- [1] J. Nilsson, A. H. Castro Neto, F. Guinea, and N. M. R. Peres, Phys. Rev. B 76, 165416 (2007).
- [2] F. Giannazzo, I. Deretzis, A. La Magna, F. Roccaforte, and R. Yakimova, Physical Review B 86, 235422 (2012).
- [3] M. Büttiker, Y. Imry, R. Landauer, and S. Pinhas, Physical Review B 31, 6207 (1985).

## ELECTRONIC PROPERTIES OF INCOMMENSURATE VAN DER WAALS STRUCTURES

B. Amorim,<sup>1,2\*</sup> Eduardo V. Castro<sup>3</sup><sup>1</sup>CeFEMA, Instituto Superior Técnico, Universidade de Lisboa, Av. Rovisco Pais, 1049-001 Lisboa, Portugal<sup>2</sup>Centro de Física das Universidades do Minho e Porto, Universidade do Minho, Campus de Gualtar, 4710-057, Braga, Portugal<sup>3</sup>Centro de Física das Universidades do Minho e Porto, Departamento de Física e Astronomia, Faculdade de Ciências, Universidade do Porto, 4169-007 Porto, Portugal

\*Corresponding Author: amorim.bac@gmail.com

Multilayered van der Waals structures, formed by stacked two-dimensional materials, have emerged in recent years as new platforms for the study of fundamental condensed matter and the development of electronic/optical devices [1]. These structures, due the mismatch/misalignment between different layers, often lack periodicity, which makes their modeling very challenging.

The goal of this work [2] is to develop an efficient method to model the electronic properties of such systems.

Building on previous work for bilayers, we develop a tight-binding based, momentum space formalism capable of describing incommensurate multilayered van der Waals structures for arbitrary lattice mismatch and/or misalignment between different layers. We demonstrate how the developed formalism can be used to model angle-resolved photoemission spectroscopy measurements, and scanning tunneling spectroscopy which can probe the local and total density of states. The general method is then applied to model angle-resolved photoemission spectroscopy in twisted bilayer structures and comparison to experimental data is made. The general method is also used to study incommensurate twisted trilayer graphene structures, where it is found that the coupling between the three layers can significantly affect the low energy spectral properties, in a way which cannot be simply attributed to the pairwise hybridization between the layers [3].

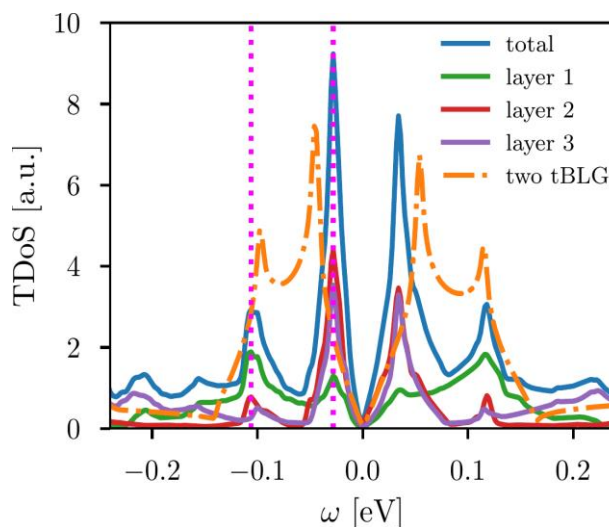


Figure 1. Modeled low energy total, and layer resolved, density of states of a twisted trilayer graphene structure with twist angles:  $-0.71^\circ$ ,  $2.1^\circ$  and  $0^\circ$ . For comparison, the averaged total density of states for two twisted bilayer graphene structures is also shown. It is clear that hybridization between the three layers plays an important role.

## References

- [1] A. K. Geim and I. V. Grigorieva, *Nature*, 499, 419–425 (2013).
- [2] B. Amorim, Eduardo V. Castro, *arXiv preprint*, arXiv:1807.11909 (2018).

[3] W.-J. Zuo, J.-B. Qiao, D.-L. Ma, L.-J. Yin, G. Sun, J.-Y. Zhang, L.-Y. Guan, and L. He, *Phys. Rev. B*, 97, 035440 (2018).

## EXCITON-POLARITONS IN A CYLINDRICAL MICROCAVITY WITH AN EMBEDDED 2D SEMICONDUCTOR LAYER

J. N. Gomes<sup>1,\*</sup>, C. Trallero-Giner,<sup>2,3</sup> N. M. Peres<sup>1,4</sup> and M. I. Vasilevskiy<sup>1,4</sup>

<sup>1</sup>Centro de Física, Universidade do Minho, Campus de Gualtar, Braga 4710-057, Portugal.

<sup>2</sup>Facultad de Física, Universidad de La Habana, Vedado 10400, La Habana, Cuba.

<sup>3</sup>CLAF - Centro Latino-Americano de Física, Av. Venceslau Braz, 71, Fundos, 22290-140, Rio de Janeiro, Brasil.

<sup>4</sup>International Iberian Nanotechnology Laboratory, Braga, Portugal.

\*Corresponding Author: nunobg93@hotmail.com

We describe exciton-polariton modes formed by the interaction between excitons in a nearly two-dimensional (2D) layer of a transition metal dichalcogenide (TMD) embedded in a cylindrical microcavity and the microcavity photons. For this, an expression for the excitonic susceptibility of a 2D semiconductor disk placed in the symmetry plane perpendicular to the axis of the microcavity is derived using the second order perturbation theory. Using it, classical electrodynamics provides dispersion relations for the polariton modes, while the quantum-mechanical treatment of a simplified model yields the Hopfield coefficients<sup>[1]</sup> that measure the degree of exciton-photon mixing in the coupled modes. The density of states (DOS) and its projection onto the photonic subspace are calculated taking monolayer MoS<sub>2</sub> embedded in a silica cylinder as an example. The calculated results demonstrate a strong enhancement of the total and local DOS (Purcell effect<sup>[2]</sup>) caused by the presence of the 2D layer. The effect is stronger than in a planar cavity that has been considered before<sup>[3]</sup>.

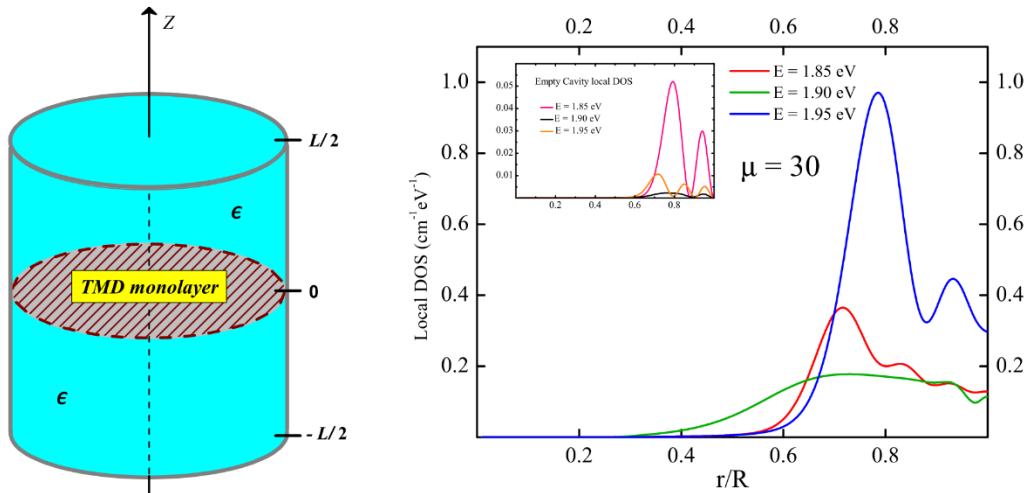


Figure 1. Left: Sketch of the considered system consisting of an ideal cylindrical cavity with a TMD layer inserted in the symmetry plane. Right: Local photon-projected DOS of exciton-polariton states with angular momentum number of 30 near the TMD monolayer, calculated for three different values of energy. Inset shows the local DOS calculated for empty cavity (without TMD layer) Cavity radius  $R=3\mu\text{m}$ , refractive index of the cavity material  $\sqrt{\epsilon} = 1.5$ .

### References

- [1] J. J. Hopfield, *Phys. Rev.* 112, 1555 (1958)
- [2] E. M. Purcell, *Phys. Rev.* 69, 681 (1946)
- [3] M. I. Vasilevskiy et al., *Phys. Rev. B* 92, 245435 (2015)

## TUNING OF MAGNETIC ACTIVITY IN SPIN-FILTER JOSEPHSON JUNCTIONS TOWARDS SPIN-TRIPLET TRANSPORT

R. Caruso,<sup>1,2,3\*</sup> D. Massarotti,<sup>4,2</sup> H. G. Ahmad,<sup>1,2</sup> A. Miano,<sup>1,2</sup> A. Pal,<sup>5</sup> V.V. Bolginov,<sup>6,7</sup> I. V. Vernik,<sup>3,8</sup> V.V. Ryazanov,<sup>6</sup> O. A. Mukhanov,<sup>3,8</sup> M. G. Blamire,<sup>5</sup> G. P. Pepe,<sup>1,2</sup> and F. Tafuri<sup>1,2</sup>

<sup>1</sup>Department of Physics, University of Naples Federico II, Complesso Universitario Monte S. Angelo, I-80126 Naples, Italy.

<sup>2</sup>CNR-SPIN, c/o complesso di Monte S. Angelo, via Cinthia, I-80126 Napoli, Italy.

<sup>3</sup>SeeQC-eu S.r.l., via dei Due Macelli 66, I-00187 Roma, Italy.

<sup>4</sup>Department of Electrical Engineering and Information Technologies, University of Naples Federico II, via Claudio, I-80125 Naples, Italy.

<sup>5</sup>Department of Materials Science and Metallurgy, University of Cambridge, 27 Charles Babbage Road, Cambridge CB3 0FS, United Kingdom.

<sup>6</sup>Institute of Solid State Physics (ISSP RAS), Chernogolovka, Moscow Region 142432, Russia.

<sup>7</sup>Skobeltsyn Institute of Nuclear Physics, Moscow State University, Moscow 119991, Russia.

<sup>8</sup>Hypres, Inc. 175 Clearbrook Road, 10523 Elmsford, New York, USA.

\*Corresponding Author: caruso@fisica.unina.it

The interaction between superconductivity and magnetism has generated great interest in the last decades, and the use of hybrid superconductor/ferromagnet devices is sought to be a viable approach to face the challenges of high performance and quantum computation.

Here we present two experiments carried out in our laboratories at University of Naples aimed at the study of two types of ferromagnetic Josephson junctions, both characterized by lower dissipation and higher quality factors when compared to standard ferromagnetic junctions. These properties make this class of devices excellent candidates for the realization of superconducting qubits with intrinsic critical current tunability and low sensitivity to external noise and of integrated quantum-classical circuits with low-noise, energy-efficient readout and control.

The first type is NbN-GdN-NbN junctions, characterized by the strong suppression of one of the two spin channels, due to the insulating nature of the ferromagnetic GdN. We characterized these junctions down to 20 mK for spin-filter efficiency values ranging from 30% to 98%, revealing the presence of an unconventional  $I_c(T)$  relation pointing at the presence of triplet components in the supercurrent. These non-dissipative spin polarized currents can be of great interest for applications in the emerging field of superconducting spintronics and for the realization of a superconducting qubit with intrinsic critical current tunability and thus low quasiparticle noise.

The second type of junctions is Nb-Al/AIOx-(Nb)-PdFe-Nb junctions, that have been reported to be suitable as basic memory cells for energy efficient magnetic RAMs. In such devices, the logical states are identified by two critical current values, and the switching between them is controlled using magnetic field pulses. We have demonstrated how the separation between critical current levels can be enhanced using an external RF field, using a specific set of parameters the enhancement can be as high as 80%. These junctions are fully compatible with existing RSFQ technology, so they can be used as the storage element of an integrated classical-quantum circuit where the control is performed via RSFQ pulses and the quantum bit is realized with a ferromagnetic junctions.

### References

- [1] R. Caruso et al. *Phys. Rev. Lett.*, 122, 047002, (2019).
- [2] R. Caruso et al. *J. Appl. Phys.*, 123, 133901, (2018).

## A FLOATING BUOY-BASED TRIBOELECTRIC NANOGENERATOR FOR MARITIME APPLICATIONS

C. Rodrigues,<sup>1,\*</sup> R. Esteves,<sup>2</sup> C. Duarte<sup>2</sup>, L. Pessoa<sup>2</sup>, A. Pereira<sup>1</sup> and J. Ventura<sup>1</sup>

<sup>1</sup>IFIMUP and Department of Physics and Astronomy, Faculty of Sciences, University of Porto, Portugal

<sup>2</sup>INESC TEC and Department of Electrical and Computer Engineering, Faculty of Engineering of University of Porto, Porto, Portugal

\*Corresponding Author: catia.rodrigues@fc.up.pt

In line with the vital role of the Oceans regarding climate action, environment, and raw materials, there is a need to monitor a set of physical parameters of the ocean and track migrations and changes in the behaviors of species. The use of autonomous underwater vehicles (AUVs) capable of transporting a multitude of sensors, and covering wide areas in remote oceanic locations, constitutes an affordable option to collect the essential data to enable economically viable large-scale ocean monitoring. However, AUV use is mainly limited by the duration of the energy source charge. There is thus a need for an energy solution that can support the operation of AUVs within remote oceanic or coastal locations for long periods of time to ensure the continuous monitoring of environmental and human activities in remote oceanic locations [1,2]. As a solution, triboelectric nanogenerators (TEGs) appeared just in 2012 as a powerful mean to generate electrical power from ever present environmental or mechanical motions. TENGs are based on the coupling of the triboelectric effect with electrostatic induction [3,4] and are characterized by high output power densities, low weight, cost-effective materials and highly adaptable designs for different applications [3,4]. Through the repeated contact between triboelectric materials, static charges are created on their surface (with opposite tribo-polarities) due to triboelectrification [5]. The subsequent separation of the triboelectric layers then induces the redistribution of the electrostatic potential, driving the flow of electrons through an external load. Here, we developed a floating buoy-based triboelectric nanogenerator to harvest mechanical energy in maritime applications. The prototype is composed by a hollow sphere having inside a multiple flexible tribo-pairs and small metallic spheres with free movement, as show in Fig. 1. When the prototype is used within an ocean scenario, with the water dynamics, energy is generated by the frequent contact of the metallic spheres with the flexible tribo-pairs. The prototype also includes a gyroscopic electronic sensor platform with local logging capability.



Figure 1. Photography of the floating buoy-based triboelectric nanogenerator.

### References

- [1] R. B. Wynn, V. A. Huvenne, T. P. L. Bas, B. J. Murton, D. P. Connelly, B. J. Bett, H. A. Ruhl, K. J. Morris, J. Peakall, D. R. Parsons, E. J. Sumner, S. E. Darby, R. M. Dorrell, and J. E. Hunt, *Marine Geology*, 352, 451–468 (2014).
- [2] G. Marani, S. K. Choi, and J. Yuh, *Ocean Engineering*, 36, 15–23 (2009).
- [3] Z. L. Wang. *Nano Energy*, 58, 669–672 (2019).
- [4] C. Rodrigues, C. Alves, J. Puga, A. Pereira, J. Ventura, *Nano Energy*, 30, 379–386 (2016).
- [5] M. Seol, S. Kim, Y. Cho, K. E. Byun, H. Kim, J. Kim, S. K. Kim, S. W. Kim, H. J. Shin, S. Park. *Advanced Materials*, 30, 1801210 (2018).



## DESIGN OF A MICROFABRICATION PROTOCOL ADAPTING REACTIVE ION ETCHING FOR ORGANIC SINGLE CRYSTAL-BASED PHOTODEVICES

J. M. Serra<sup>\*1</sup>, S. I. Sequeira<sup>1,2</sup>, I. Domingos<sup>3</sup>, A. P. Oliveira<sup>3</sup>, E. Maçôas<sup>2</sup>, S. Cardoso<sup>1,2</sup>, H. Alves<sup>2,3</sup>, D. C. Leitão<sup>1,2</sup>

1 – INESC Microsystems and Nanotechnologies, Lisbon, Portugal – [www.inesc-mn.pt](http://www.inesc-mn.pt)

2 – Instituto Superior Técnico, Universidade de Lisboa, Lisbon, Portugal

3 – UA-CICECO – Aveiro Institute of Materials, University of Aveiro, Aveiro, Portugal

\*Corresponding Author: [joampsserra@tecnico.ulisboa.pt](mailto:joampsserra@tecnico.ulisboa.pt)

Organic single crystals (OSCs) have attracted great interest in integrated photonic devices due to their light absorption properties in the visible range [1], providing an alternative material for photosensors with applications such as visible light communication [2]. Large scale fabrication of fully integrated photonic devices demands new strategies to include OSC patterning in the semiconductor fabrication line. However, most conventional fabrication techniques typically used in integrated circuit production are incompatible with organic crystals, causing the crystals to be damaged [3]. In this work we define an innovative fabrication protocol to allow the use of standard cleanroom techniques (optical lithography and Reactive Ion Etching (RIE)) for OSC patterning. Such a strategy paves the way for the microfabrication of integrated OSC microdevices [1]. OSCs present exciton conduction, where the electric current is a result of excitons (excited electron-hole pairs in the crystal) diffusing through the lattice. This is the origin of photoconductivity in OSCs: a photon will excite a charge carrier, generating an exciton, which can be collected to obtain an electric current.

In previous works, rubrene single crystals grown by physical vapor transport were directly laminated on glass and subsequently connected to macroscopic contacts with carbon ink [4]. To enable chip integration of the devices, we begin the process by laminating the rubrene OSCs over pre-patterned Au contacts (Fig. 1a). A PVA/PMMA protection layer is spin-coated to protect the crystals from reactive species, followed by optical lithography to define the device geometry. RIE conditions were optimized for different gas combinations, with an etch rate of  $1.63 \pm 0.87 \text{ Å/s}$ . The etching process end point control is performed visually. As rubrene crystals fluoresce when optically excited under a 468 nm wavelength, confocal fluorescence microscopy was used to verify the complete etch of the organic single crystals. The patterned devices are then characterized for their opto-electronic behavior. Fig 1b. shows a confocal fluorescence microscope image of a patterned crystal, with Fig 1c. showing the fluorescence spectrum in the delimited regions. Full patterning of the rubrene single crystals was successfully achieved by this protocol, proving it as a viable step towards fully integrated OSC microfabricated devices. Most recent results on photocurrent measurements and the impact of the microfabrication process on the device performance will be discussed.

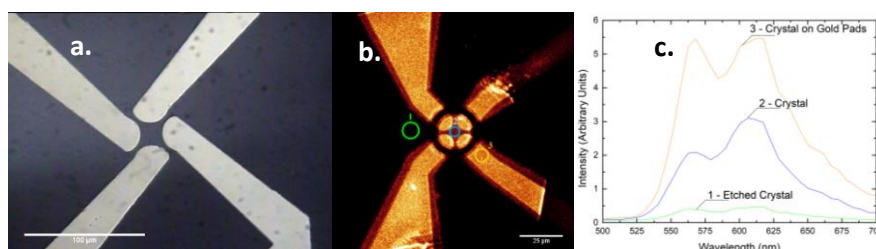


Figure 1. (a) Laminated crystal on top of microfabricated Au contacts, before crystal patterning. (b) Confocal fluorescence microscope image of patterned organic single crystal. (c) Fluorescence spectra acquired in the regions defined in Fig. 1b.

### References

- [1] H. H. Fang et al., *Laser & Photonics Reviews*, 7:281-288, (2013).
- [2] M. Figueiredo, et al., *IEEE Consum. Electron. Mag.*, 6:28-37 (2017).
- [3] R. Li et al., *Accounts of Chemical Research*, 43:529-540 (2010).
- [4] R. M. Pinto et al., *Journal of Materials Chemistry C*, 2: 3639-3644 (2014).



## EFFECTS OF OXYGEN ION IMPLANTATION ON THE STRUCTURAL AND ELECTRICAL PROPERTIES OF $\alpha$ -MOO<sub>3</sub> LAMELLAR CRYSTALS

D. R. Pereira<sup>1,2,\*</sup>, C. Díaz-Guerra<sup>4</sup>, M. Peres<sup>2</sup>, S. Magalhães<sup>2</sup>, J. G. Correia<sup>3</sup>, J. G. Marques<sup>3</sup>, A. G. Silva<sup>5</sup>, E. Alves<sup>2</sup>, K. Lorenz<sup>1,2</sup>, S. Cardoso<sup>1</sup>, P. P. Freitas<sup>1,6</sup>

<sup>1</sup>Instituto de Engenharia de Sistemas de Computadores-Microsystems and Nanotechnology (INESC-MN), Lisboa, Portugal.

<sup>2</sup>IPFN, Instituto Superior Técnico, Universidade de Lisboa, Portugal.

<sup>3</sup>C2TN, Instituto Superior Técnico (IST), Universidade de Lisboa, Portugal.

<sup>4</sup>Departamento de Física de Materiales, Facultad de Ciencias Físicas, Universidad Complutense de Madrid, Madrid, Spain.

<sup>5</sup>Cefitec, Departamento de Física, Faculdade de Ciências e Tecnologia, Universidade Nova de Lisboa, Campus da Caparica, 2829-516, Caparica, Portugal.

<sup>6</sup>INL - International Iberian Nanotechnology Laboratory, Braga, Portugal.

\*Corresponding Author: [danielapereira@ctn.tecnico.ulisboa.pt](mailto:danielapereira@ctn.tecnico.ulisboa.pt)

Molybdenum oxide (MoO<sub>3</sub>) is a wide band gap semiconductor, with interesting structural properties for several applications such as biosensors, gas sensors, solar cells and lithium ion batteries. Changes in the oxidation state of MoO<sub>3</sub>, for example by the creation of oxygen vacancies, can lead to different behaviors, which can range from semiconductor to metallic. The possibility of tuning the electrical properties by controlling the concentration of defects, is a useful and valuable tool for design and optimization of new devices. In this work, we use oxygen ion implantation to modify the electrical and structural properties of orthorhombic MoO<sub>3</sub> lamellar crystals [1]. A controllable and significant increase of the electrical conductivity, over several orders of magnitude, is observed after implantation at high fluences. By analyzing the high resolution X-ray diffraction (HRXRD) and the micro-Raman spectroscopy measurements, the modifications were attributed to the formation of extended defects, amorphous regions, and new phases more conductive than the  $\alpha$ -MoO<sub>3</sub> orthorhombic phase.

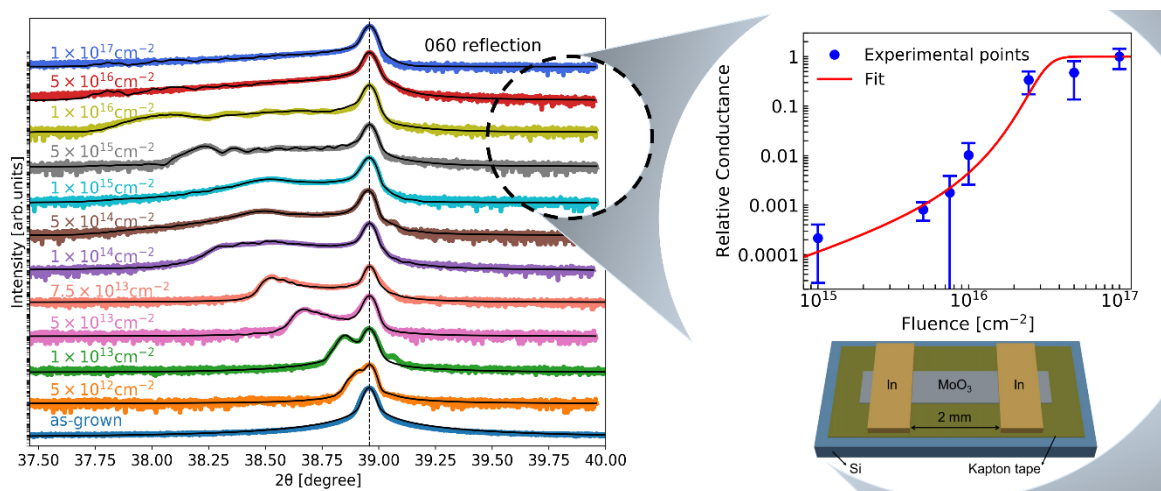


Figure 1. HRXRD 2θ-θ scans around the 060 reflection performed in an as-grown sample and as-implanted samples of MoO<sub>3</sub> implanted with different fluences (left); Evolution of the relative conductance with increasing fluence (top right); Schematic illustration of the geometry of a device used for electrical characterization (bottom right).

### Reference

[1] D. R. Pereira et al., *Acta Materialia*, 169,15-27 (2019).

## ION BEAM INDUCED CURRENT ANALYSIS IN GAN MICROWIRES

D. Verheij,<sup>1,2,\*</sup> M. Peres,<sup>2</sup> S. Cardoso,<sup>1</sup> L.C. Alves,<sup>3</sup> E. Alves,<sup>2</sup> C. Durand,<sup>4</sup> J. Eymery,<sup>5</sup> J. Fernandes,<sup>6</sup> and K. Lorenz<sup>1,2</sup>

<sup>1</sup> Instituto de Engenharia de Sistemas e Computadores - Microsistemas e Nanotecnologia (INESC-MN), Rua Alves Redol 9, 1000-029 Lisboa, Portugal

<sup>2</sup> IPFN, Instituto Superior Técnico (IST), Campus Tecnológico e Nuclear, Estrada Nacional 10, 2695-066 Bobadela LRS, Portugal

<sup>3</sup> C2TN, Instituto Superior Técnico (IST), Campus Tecnológico e Nuclear, Estrada Nacional 10, 2695-066 Bobadela LRS, Portugal

<sup>4</sup> CEA INAC-Pheliqs-NPS, Université Grenoble Alpes, Grenoble, France

<sup>5</sup> CEA INAC-MEM-NRS, Université Grenoble Alpes, Grenoble, France

<sup>6</sup> Instituto de Engenharia de Sistemas e Computadores – Investigação e Desenvolvimento (INESC-ID), Rua Alves Redol 9, 1000-029, Lisboa, Portugal

\*Corresponding Author: dirkjanverheij@ctn.tecnico.ulisboa.pt

GaN is a wide bandgap semiconductor which is expected to withstand high radiation doses [1]. Consequently, it is considered a promising material for new generation particle detectors in radiation related applications. Nonetheless, due to high dislocation densities, sensors based on thin film technology suffer from significant leakage currents. GaN nano and microwires, on the other hand, can be grown with high crystalline quality, even on lattice mismatched substrates, and may be a good alternative [2]. To assess their potential as radiation sensors, unintentionally n-doped and core-shell p-n junction microwires were contacted at their extremities and their electrical response was analysed when irradiating the samples with a 2 MeV proton beam with fluences above  $4 \times 10^{16}$  protons/cm<sup>2</sup>. Both the n-type and p-n junction microwires show good capabilities to detect the protons, nonetheless, due to the high dark current related to high doping concentrations introduced during the growth of the microwires, the ratio between both is low for the n-type samples. A small persistent ionocurrent is also measured after turning the proton beam off. The pn-junction microwires show faster response times and the ratio between the ion beam induced current and the dark current reaches values up to  $10^3$ . To analyse the regions responsible for the detection of protons position dependent measurements were also performed which are allowed since the spot size of the proton beam is smaller than the length of the microwire. In the case of the n-doped microwires we saw that detection was more efficient in the area between the two contacts while the areas close to the p-contact were more sensitive in the case of the p-n junction microwire. Despite the successful detection, a high damage was created by the proton beam. Albeit issues regarding reproducibility and stability, the results confirm that GaN microwires are possible candidates for next generation radiation sensors.

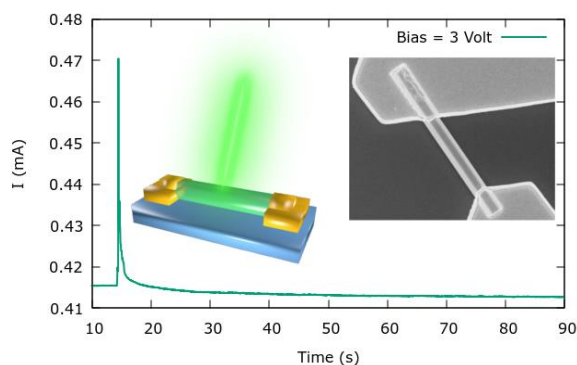


Figure 1. Transient measurement of the ion beam induced current in an n-type microwire during a short pulse of a 2 MeV proton beam. A SEM image of the sample is shown in the right corner.

## References

- [1] S.J. Pearton, R. Deist, F. Ren, L. Liu, A.Y. Polyakov, J. Kim, *Journal of Vacuum Science and Technology A*, 31, 050801 (2013).
- [2] R. Koester, J.S. Hwang, C. Durand, D. Le Si Dang, J. Eymery, *Nanotechnology*, 21, 015602 (2010).

MAGNETIZATION CHANGE UPON ILLUMINATION: THE  $\text{Ln}(\text{F}_{20}\text{TPIP})_3$  SERIES

Maria Susano,<sup>1\*</sup> Jaroslaw Rybusinski,<sup>2</sup> Jacek Szcztyko,<sup>2</sup> Peter B Wyatt,<sup>3</sup> Laura C.J. Pereira,<sup>4</sup> Manuela Ramos Silva<sup>1</sup>

<sup>1</sup>CFisUC, Department of Physics, University of Coimbra, P-3004-516 Coimbra, Portugal

<sup>2</sup>Faculty of Physics, University of Warsaw, Pasteura 5, 02-093 Warsaw, Poland

<sup>3</sup>Materials Res. Inst., Queen Mary Univ. of London, Mile End Road, London E1 4NS, UK <sup>4</sup>Solid State Group, IST/CTN, UTL, Estrada Nacional 10, 2695-066 Bobadela LRS, Portugal

\*Corresponding Author: maria.susano@gmail.com

A series of  $\text{Ln}(\text{F}_{20}\text{TPIP})_3$  compounds, where  $\text{F}_{20}\text{TPIP}$  stands for tris(tetrakis(pentafluorophenyl)imidodiphosphinato), were synthesized according to the procedure described in [1]. Both  $\text{Er}(\text{F}_{20}\text{TPIP})_3$  [2] and  $\text{Gd}(\text{F}_{20}\text{TPIP})_3$  display Single-Ion Magnetic (SIM) behavior. Although AC susceptibility measurements indicate the presence of significantly fast quantum tunneling magnetization at zero field, as evidenced by the absence of coercivity at very low temperatures, the application of a static field slows down the relaxation and an energy barrier for the moment reversal could be identified.

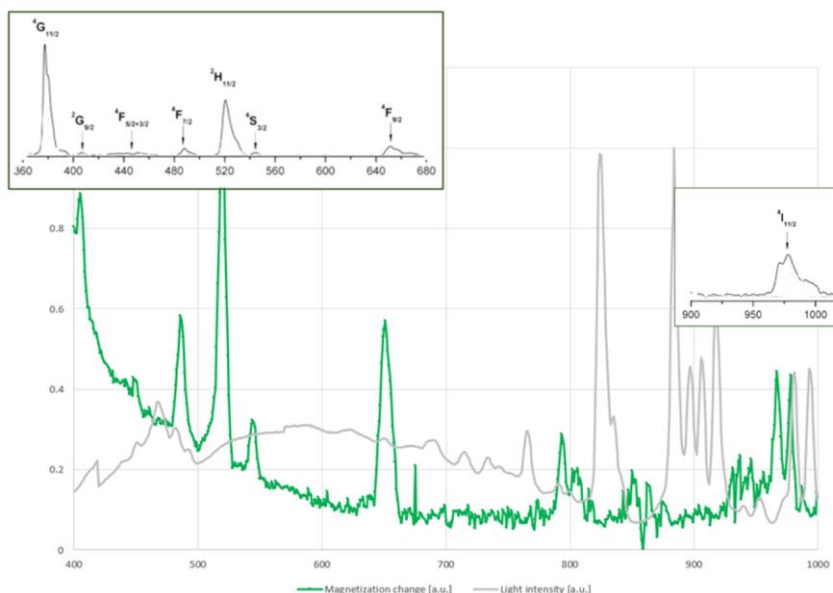


Figure 1. Plot of magnetization change in function of the illumination wavelength for  $\text{Er}(\text{F}_{20}\text{TPIP})_3$ . The inserts show the absorption of the solid sample for matching wavelengths.

For  $\text{Er}(\text{F}_{20}\text{TPIP})_3$ , the magnetization displayed from room to low temperature is determined by the population of the  $J=15/2$  sub-levels (originated by the electric field of the coordination ligands). Once submitted to illumination, either by an indirect effect through the surrounding organic ligand or directly through lanthanide light absorption, an excited state with  $J=13/2$  (or even higher in energy) is populated [3]. A sudden change in magnetization is therefore expected and that is what is observed in the figure above (Figure 1), where the difference between dark and light magnetization is plotted in function of excitation wavelength. Results for other  $\text{Ln}(\text{F}_{20}\text{TPIP})_3$  will be presented and discussed.

## References

- [1] Wyatt *et al.*, J. Phys. Chem. C 117 23970, (2013).
- [2] Pereira *et al.*, Mat. Chem. Phys. 160, 429-434, (2015).
- [3] Wyatt *et al.*, Nature Materials 13, 382-386, (2014).

## IMPACT OF ATOMIC DISORDER ON THE THERMODYNAMIC PROPERTIES OF FERROMAGNETIC $\text{Fe}_2\text{MnSi}$ – A COMPUTATIONAL STUDY

H. G. Trigo,<sup>1,\*</sup> J. N. Gonçalves,<sup>1</sup> and J. S. Amaral<sup>1</sup>

<sup>1</sup>Departamento de Física e CICECO, Universidade de Aveiro, Portugal

\*Corresponding Author: [hugogt@ua.pt](mailto:hugogt@ua.pt)

Heusler alloys are intermetallic compounds which exhibit many technologically relevant properties, including semi-metallic behavior, and strong magneto volume coupling [1]. The richness in the properties of this family of alloys lies in the wide range of possible doping compositions of magnetic and non-magnetic ions. In terms of applications in magnetic refrigeration, Heusler alloys (such as  $\text{NiMnInCo}$ ) can show a giant magnetocaloric effect [2], which shows how tuning the thermodynamic properties of these alloys can lead to the discovery of new high-performance refrigerants.  $\text{Fe}_2\text{MnSi}$  is a well-known ferromagnetic alloy, typically referred to as having a  $L2_1$  structure. Still, in earlier works, a small degree ( $\sim 12\%$ ) of  $\text{DO}_3$  disorder was observed via neutron scattering experiments [3]. This disorder corresponds to an exchange of atomic positions between Fe (A,C position) and Mn (B position). Recently, it was shown through a combined Density Functional Theory (DFT) and Monte-Carlo (MC) approach this 12% amount of  $\text{DO}_3$  disorder would lead to a remarkable increase of Curie temperature ( $T_C$ ) from 160 K of the pure system to 200 K of the disordered one [4].

In this work, we explore in more detail the impact of  $\text{DO}_3$  disorder in the  $\text{Fe}_2\text{MnSi}$  alloy, also employing a combined DFT and MC approach. We assess the dependency of  $T_C$  over a wider disorder range, including the use of two different lattices, one a super lattice where atomic positions are species are taken into account, and another, approximated lattice where average magnetic interaction values are considered. The quantitative agreement between simulated values of both  $T_C$  and magnetization dependence on field and temperature of both these lattices opens the way to explore the thermodynamic properties of other Heusler alloys (e. g.  $\text{Co}_2\text{FeSi}$ ,  $\text{Fe}_2\text{MnGe}$ , ...), including the effects of atomic disorder.

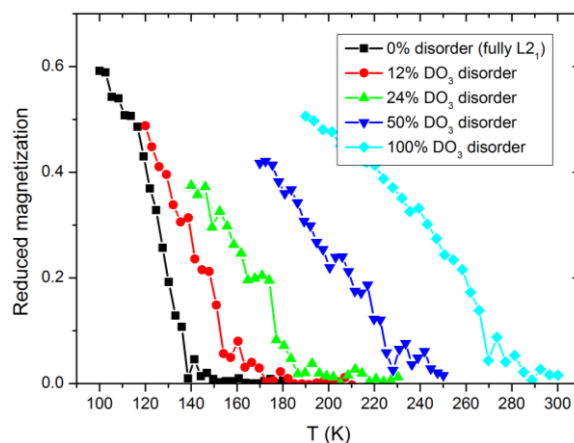


Figure 1. Reduced magnetization as a function of temperature for several  $\text{DO}_3$  disorder values in  $\text{Fe}_2\text{MnSi}$ .

### References

- [1] Reis, M. S. et al. Experimental realisation of off-stoichiometric Fe-Mn-Si full Heusler alloy with hexagonal crystal structure by pulsed laser deposition, *Materials & Design*, 143, 268-273 (2018).
- [2] Pérez-Landazábal, J. I. et al. Giant direct and inverse magnetocaloric effect linked to the same forward martensitic transformation, *Nature, Scientific Reports* 7, 13328 (2017).
- [3] K.A. R. Ziebeck & P. J. Webster: The antiferromagnetic and ferromagnetic properties of  $\text{Fe}_2\text{MnSi}$ , *Philosophical Magazine*, 34:6, 973-982 (1976).
- [4] Lezaic, M. et al. Complex magnetic behavior and high spin polarization in  $\text{Fe}_{3-x}\text{Mn}_x\text{Si}$  alloys, *Physical Review, B* 83, 094434 (2011).

## EMERGENCE OF EDGE-MAGNETISM IN TRANSITION METAL DICHALCOGENIDE NANORIBBONS

F. M. O. Brito,<sup>1,\*</sup> J. M. V. P. Lopes,<sup>1</sup> and E. V. Castro<sup>1</sup>

<sup>1</sup>Centro de Física das Universidade do Minho e Porto, Departamento de Física, Faculdade de Ciências da Universidade do Porto, Rua do Campo Alegre, s/n, 4169-007 Porto, Portugal

\*Corresponding Author: francisco.brito@fc.up.pt

We focus on emerging edge-magnetism in zigzag-edged transition metal dichalcogenide (TMD) nanoribbons. Building on a symmetry-based 3-band tight-binding (TB) model, found to capture edge state-related properties of the system [1], we include electron-electron interactions via an intra-orbital Hubbard term. Using this minimal model and a numerical treatment, we probe the system for edge-magnetic order. The Determinant Quantum Monte Carlo (DQMC) algorithm that we use suffers from the well known sign problem [2] for this model. Thus, it can only be used for electron densities higher than in the charge neutral case. For those, we find edge-antiferromagnetism. The results of Fig. 1 (below) were obtained with DQMC with a Hubbard interaction of around 3 eV and with an electron density about 10% higher than that corresponding to charge neutrality (1 electron per M-atom). The temperature is set to 23 meV. The results agree with the mean field ones and show evidence of antiferromagnetic ordering. This behaviour is fundamentally different from that obtained for the bulk, hole-doped monolayer, where there is a transition to a ferromagnetic phase [3].

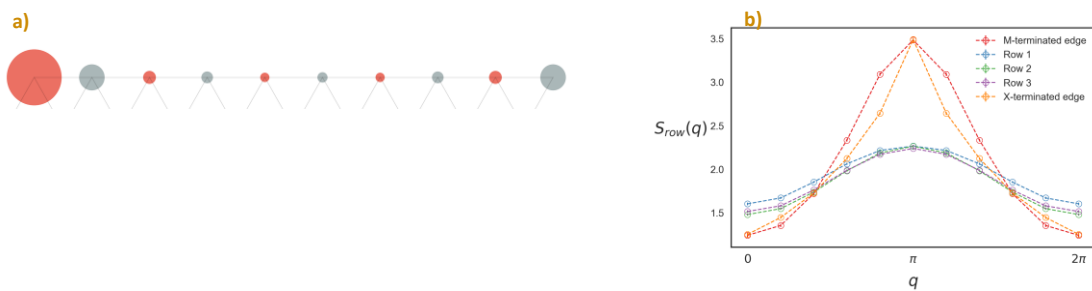


Figure 1: a) Spin-spin correlations relative to the leftmost site on the chalcogen-terminated edge of MoS<sub>2</sub> (Molybdenum Disulfide) nanoribbon (the color red represents a positive correlation, while blue represents a negative correlation). b) Structure factor obtained with DQMC for each of the rows of the ribbon. The peaks at  $\pi$  on the edges represent a tendency towards antiferromagnetic ordering.  $q$  is in units of the lattice constant.

We find edge-magnetism in TMD nanoribbons for realistic values of the Hubbard interaction of around 3 eV. The DQMC algorithm can only be used for electron densities above that corresponding to charge neutrality due to the fermion-sign problem. Decreasing the electron density, we treat the problem approximately and find evidence of a transition towards edge-ferromagnetism at the charge neutral point.

### References

- [1] G.-B. Liu, W.-Y. Shan, Y. Yao, W. Yao, and D. Xiao, *Phys. Rev. B*, **88**, 085433 (2013).
- [2] M. Troyer, U.-J. Wiese, *Phys. Rev. Lett.*, **94**, 170201 (2005).
- [3] J. E. H. Braz, B. Amorim, E. V. Castro *Phys. Rev. B*, **98**, 161406 (2018).

## MAGNETIC NANOPARTICLES FOR HYPERTHERMIA

M. M. Cruz <sup>1,\*</sup>

<sup>1</sup>University of Lisboa, Faculty of Sciences, BioISI - Biosystems & Integrative Sciences Institute/ Physics Department, Lisboa, Portugal

\*Corresponding Author: mmcruz@ciencias.ulisboa.pt

In the last years, magnetic nanoparticles have been investigated for different medical applications, namely for cancer treatment by magnetic hyperthermia, since the nano-size allows their integration in cells and heating can be achieved by a driving alternate magnetic field. The heating ability of the nanoparticles is generally parametrized by their specific loss power (SLP). Although several materials have been explored, magnetite is still considered the best candidate for the nanoparticle composition due to its biocompatibility and high saturation magnetization. Two main problems persist nowadays that limit the efficacy of the hyperthermia technique: the ability to locate the magnetic nanoparticles in the tumour cells and the “small” heating efficiency of the nanoparticles.

In BioISI/FCUL research is carried out on the optimization of the heating efficiency of magnetite nanoparticles. It is considered that the best SLP value will be obtained when the magnetic relaxation of the nanoparticles is close to the frequency of the alternate magnetic field. This implies small and monodisperse nanoparticles and the tailoring of their magnetic anisotropy that controls the Néel relaxation frequency. Also, methods of synthesis involving the use of undesirable reagents such as surfactants and organic solvents should be avoided, and good stable suspensions are required.

In this work, we present results for magnetite NPs with a mean size around 10 nm, obtained by green synthesis methods, including structural and magnetic characterization as well as induction heating studies under alternating magnetic fields for stable suspensions of these nanoparticles.

**Acknowledgements:** Work supported by [UID/MULTI/04046/2019](#) Research Unit grant from FCT, Portugal (to BioISI) and project PTDC/NAN-MAT/28785/2017.



## ULTRAFAST MAGNETIZATION DYNAMICS OF [COFeB/PD]<sub>5</sub>/CO EXCHANGE SPRING STRUCTURES

A. S. Silva,<sup>1,\*</sup> S. P. Sá,<sup>1</sup> S. Bunyayev,<sup>1</sup> G. Kakazei,<sup>1</sup> M. Canhota,<sup>1</sup> M. Miranda,<sup>1</sup> C. Garcia,<sup>2</sup> I. J. Sola,<sup>3</sup> H. Crespo,<sup>1</sup> and D. Navas,<sup>1,\*</sup>

<sup>1</sup>Department of Physics and Astronomy, IFIMUP-IN, Faculdade de Ciências, Universidade do Porto, Porto, Portugal.

<sup>2</sup>Department of Physics, Technical University Federico Santa María, 2390123 Valparaíso, Chile.

<sup>3</sup>Grupo de Investigación en Aplicaciones del Láser y Fotónica, Departamento de Física.

Aplicada, University of Salamanca, E-37008 Salamanca, Spain.

\*Corresponding Author: anasilva@fc.up.pt; dnavas@fc.up.pt

Multilayer thin films with perpendicular magnetic anisotropy (PMA) are of great interest for technological applications such as in recording media and in spin-torque transfer (STT) magnetic random access memory (MRAM) [1]. Combining PMA layers with in-plane ferromagnetic (FM) layers may cause exchange spring (ES) behavior, increasing their potential applications [2]. In this work, we studied [CoFeB/Pd]<sub>5</sub>/Co exchange spring structures by comparing timeresolved magneto-optical Kerr effect (TR-MOKE) measurements with ferromagnetic resonance analysis (VNA-FMR). TR-MOKE measurements show a sudden drop within the first picosecond and a fast recovery (remagnetization) within a few picoseconds. This is followed by a clear oscillation or precession during a slower magnetization recovery. From the analysis of the precession behavior, we determined both the ferromagnetic resonance frequency  $\omega_{\text{FMR}}$  and the effective Gilbert damping parameter  $\alpha_{\text{eff}}$ . Both parameters have been compared with the results obtained from the VNA-FMR measurements. Finally, the ultrafast demagnetization and the fast remagnetization processes within the initial picoseconds has been analyzed using an external applied field of 2615 Oe and a time delay ranging from – 0.6 to 4.4 ps. Under these experimental conditions, measurements of the laser-induced demagnetization revealed a minimum at  $t \approx 320$  fs for the [CoFeB/Pd]<sub>5</sub>/Pd/Co(7Å) sample.

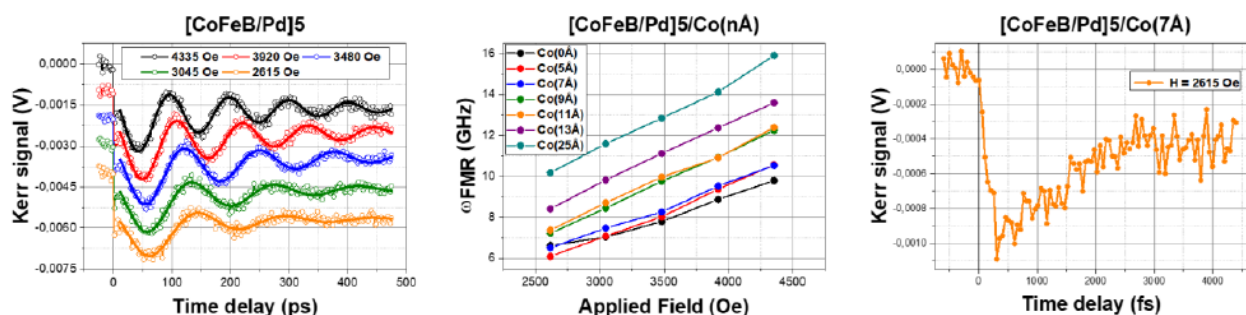


Figure 1. TR-MOKE measurements at a pump laser fluence of 1.0 mJ/cm<sup>2</sup> on the [CoFeB/Pd]<sub>5</sub> multilayer thin film and with different applied external magnetic fields (open symbols). The solid lines are the theoretical fittings. (b) Field dependence of the resonance frequency of the exchange spring systems. (c) Experimental demagnetization data of the [CoFeB/Pd]<sub>5</sub>/Pd/Co(7Å) exchange spring system.

### References

- [1] A. F. Franco, C. Gonzalez-Fuentes, J. Åkerman and C. Garcia, Phys. Rev. B 95, 144417 (2017).
- [2] A. F. Franco, C. Gonzalez-Fuentes, R. Morales, C. A. Ross, R. Dumas, J. Åkerman and C. Garcia, Phys. Rev. B 94, 064431 (2016).
- [3] C.S. Gonçalves, A. S. Silva, D. Navas, M. Miranda, F. Silva, P. Oliveira, H. Crespo and D.S. Schmool, Sci. Rep. 6, 22872 (2016).



# POSTER COMMUNICATIONS

## P01 - 3D C60 POLYMERS WITH ORDERED BINARY-ALLOY TYPE STRUCTURES INVESTIGATED VIA DFT

J. Laranjeira<sup>a\*</sup>, L. Marques<sup>a</sup>, N. M. Fortunato<sup>a</sup>, M. Melle-Franco<sup>b</sup>, K. Strutyński<sup>b</sup> and M. Barroso<sup>c</sup>

<sup>a</sup> Departamento de Física and CICECO, Universidade de Aveiro, 3810 Aveiro, Portugal.

<sup>b</sup> Departamento de Química and CICECO, Universidade de Aveiro, 3810 Aveiro, Portugal.

<sup>c</sup> Departamento de Física and I3N, Universidade de Aveiro, 3810 Aveiro, Portugal.

\*Corresponding Author: jorgelaranjeira@ua.pt

Three-dimensional (3D) C60 polymerized structures with each molecule adopting one of the two standard orientations, have been studied via density functional theory methods (DFT). Well-known ordered binary-alloy (AB) structures - AuCuI, Au<sub>3</sub>Cu, CuPt, "A<sub>2</sub>B<sub>2</sub>" - , have been used as prototypes, in which one standard orientation corresponds to atom A and the other orientation corresponds to atom B. In all the studied structures there is no bond between molecules with the same orientation but between molecules with different orientation there is the formation of a 56/56 2+2 cycloaddition polymeric bond. It, thus, corresponds to an orientational antiferromagnetic interaction and the system can be mapped onto Ising fcc antiferromagnet. The bonding type, 56/56 2+2 cycloaddition, is different from the 66/66 2+2 cycloaddition characteristic of the low-dimensional, 1D and 2D, C60 polymers, as it is formed between intramolecular single bonds of neighboring molecules and not between intramolecular double bonds.

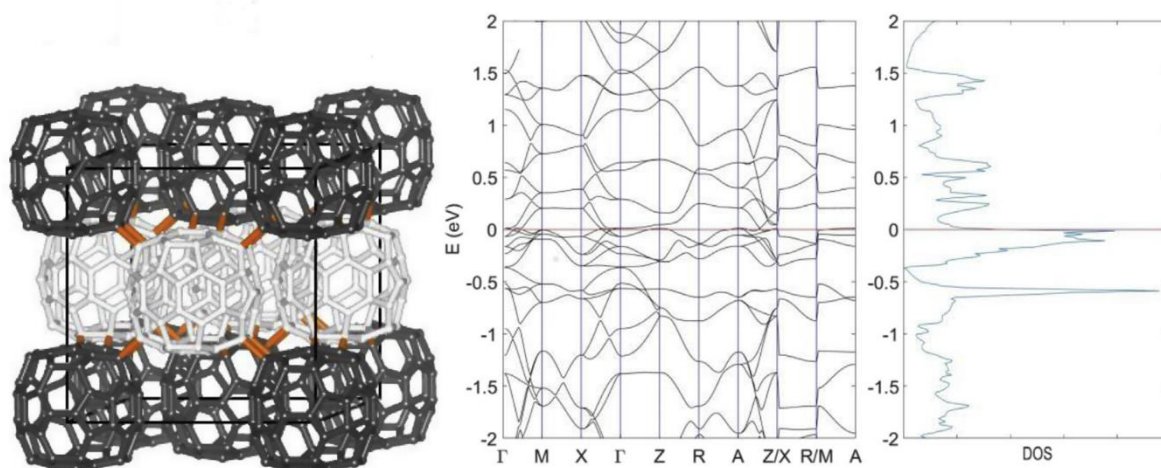


Figure 2 crystal structure, electronic band structure and density of states of the AuCuI-type C60 polymer structure.

These 3D polymer structures are candidates to be obtained experimentally at high pressure once the observed frustration could be relieved [1]. Their structural, elastic and electronic properties were calculated at room pressure and at 9.5 GPa and all of them show a metallic behavior [2].

### References

- [1] J. Laranjeira, L. Marques, M. Mezouar, M. Melle-Franco, K. Strutyński, Phys. Stat. Sol. RRL, 11, 1700343 (2017).
- [2] J. Laranjeira, L. Marques, N. Fortunato, M. Melle-Franco, K. Strutyński, M. Barroso, Carbon, 137, 511-518 (2018).

## P02 - ACTUATION OF MAGNETOELASTIC MEMBRANES IN DYNAMIC MAGNETIC FIELDS

M. Tasinkevych<sup>1,\*</sup>, M. Olivera de la Cruz<sup>2</sup>, C. A. Brisbois<sup>2</sup>, and P. Vázquez-Montejo<sup>3</sup>

<sup>1</sup>Centro de Física Teórica e Computacional, Departamento de Física, Faculdade de Ciências, Universidade de Lisboa, Campo Grande P-1749-016, Lisboa, Portugal

<sup>2</sup>Department of Materials Science and Engineering, Northwestern University, Evanston, Illinois 60208, USA

<sup>3</sup>Facultad de Matemáticas, Universidad Autónoma de Yucatán, Mérida, Yucatán, 97110, México

\*Corresponding Author: mtasinkevych@fc.ul.pt

Superparamagnetic nanoparticles are readily manipulated by external magnetic fields, which control the strength and direction of their magnetic dipole moments. Incorporating superparamagnetic nanoparticles into elastic media allows for the precise control of actuating materials through the competition between induced magnetic interactions and elastic bending.

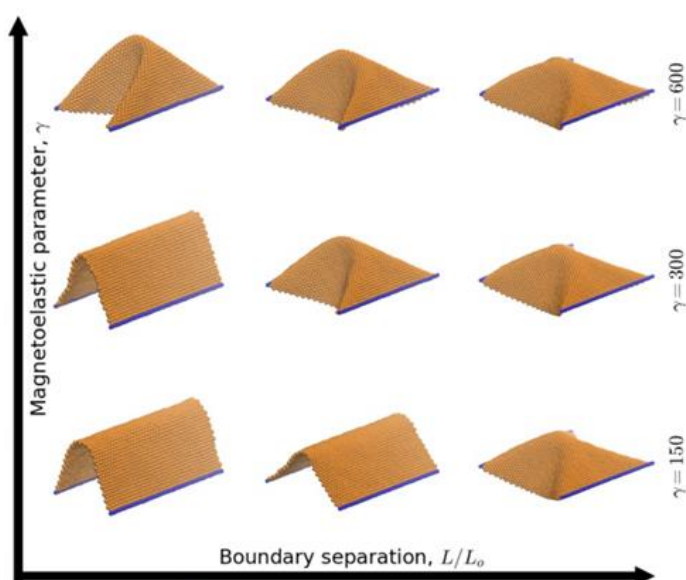


Figure 1. Snapshots of membrane configurations at different boundary separation, and at different strength of the magnetic field, parametrized by the magnetoelastic parameter  $\gamma$ . Adapted from ref. [1].

We combine here continuum mechanics approach and molecular dynamics simulations to study the behavior of magnetoelastic membranes subject to time dependent magnetic fields. We show how induced magnetic interactions affect the buckling and the configuration of the membranes in rapidly precessing magnetic fields. The field, in competition with the bending and stretching of the membrane, transmits forces and torques that drives the membrane to expand, contract, or twist. We identify critical field values that induce spontaneous symmetry breaking as well as field regimes where multiple membrane configurations may be observed. At low precession frequencies, dynamic periodic motion is induced in the membrane. Our insights into buckling mechanisms provide the bases to develop soft, autonomous robotic systems that can be used at micro- and macroscopic length scales.

### Reference

[1] C. A. Brisbois et al., *Proc. Natl. Acad. Sci. USA* 116, 2500 (2019).

### P03 - ADSORPTION OF OXYGEN ON METAL-SEMICONDUCTOR ZN/ZNO CORE SHELL NANO-STRUCTURES

A. Castro<sup>2\*</sup>, S. Calderon V.<sup>1</sup>, L. Marques<sup>2</sup>

<sup>1</sup>INL - International Iberian Nanotechnology Laboratory, Av. Mestre José Veiga s/n, 4715-330 Braga, Portugal

<sup>2</sup>University of Minho, Centre/Department of Physics, Campus of Gualtar, 4710-057 Braga, Portugal.

\*Corresponding Author: antoniojose.castro@gmail.com

Zn/ZnO nanostructures have been studied extensively due to their potential use in many applications, such as oxygen scavenger for food packaging applications [1]. Both ZnO and Zn crystallise in a hexagonal structure, as such ZnO tends to grow epitaxially on the surface of Zn via oxidation process [2]. However, the mechanisms governing Zn oxidation are still not fully understood, which is essential for a controlled oxidation in many technological applications. In this work, Ab initio DFT calculations were performed to help elucidate the mechanisms underlying the epitaxial growth of a ZnO layer on a Zn substrate. The calculations focus on the adsorption of oxygen on top of the ZnO (0001) surface and estimation of Mott potential for Zn/ZnO interface. The improved knowledge on the oxidation behaviour will help to design strategies to control the oxidation process of the metal-semiconductor core-shell structures.

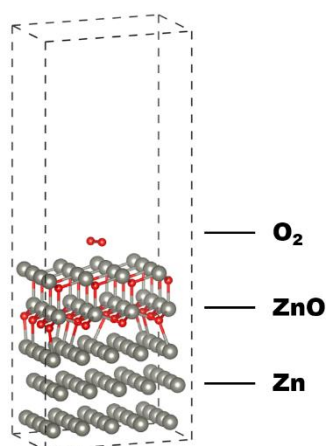


Figure 3. Zn/ZnO core-shell system with adsorbed O<sub>2</sub> molecule used on DFT calculations. Zn and O atoms are depicted as grey and red spheres respectively.

#### References

- [1] S. Calderon et al., *Nanoscale*, 9(16), 5254–5262 (2017).
- [2] Z.Wang et al., *Journal of Experimental Nanoscience*, 11(5), 383–394 (2016).

## P04 - BINARY MIXTURE OF LOCALLY COUPLED BROWNIAN OSCILLATORS

G.S. Paulo,<sup>1,2\*</sup> M. Tasinkevych,<sup>1,2</sup><sup>1</sup>Departamento de Física, Faculdade de Ciências, Universidade de Lisboa, 1749-016 Lisboa, Portugal.<sup>2</sup>Centro de Física Teórica e Computacional, Universidade de Lisboa, 1749-016 Lisboa, Portugal.

\*Corresponding Author: fc48275@alunos.fc.ul.pt

Synchronization has been a phenomena studied for a long time and it is present in many natural and artificial systems and in some of these systems it is the key phenomena to study [1,2]. We can see synchronization in biological systems, in fireflies or in our circadian cycle, in social systems, people clapping their hands at the same time, and even in artificial systems, where clocks synchronize because they are connected. The goal of this study is to understand the synchronization behavior of a binary mixture of oscillators, where similar oscillators synchronize and distinct ones desynchronize.

We perform molecular dynamics simulation (by using open source LAMMPS[3] library) of a modified Kuramoto model in order to address this problem. Our system consists of a binary mixture of 2 types of particle that interact positively (align their phases) between particles of the same type and that interact negatively (counter align their phases) when the particles are of different type. We simulate a “dense” phase, packing fraction  $\sim 0.49$ , and a “dilute” phase, packing fraction  $\sim 0.24$ , to see if the density of the system influences the synchronization

We find that the both sub-systems can synchronize for some values of the desynchronizing coupling strength, and that the presence of this “negative” interaction between unlike particles can even enhance the synchronization speed of both sub-systems. Surprisingly, the results also suggest that the existence of the negative interaction alone can synchronize non-interacting (in a synchronization sense) particles.

To conclude, binary mixtures of synchronizing/desynchronizing phase field oscillators are able to synchronize because the system as a whole gets locked in a state where the similar particles are synchronized, with the  $\pi/2$  phase shift between the two sub-systems. We speculate, that in order to suppress the synchronization a more complex interactions among the oscillators must be introduced. This research is currently in progress.

## References

- [1] D. Levis, I. Pagonabarraga, *Phys. Rev. X*, 7, 011028 (2017)
- [2] V. H. P. Louzada, N. A. M. Araújo, *Scientific Reports*, 2, Article number: 658 (2012)
- [3] S. Plimpton, *J Comp Phys*, 117, 1-19 (1995).

**P05 - CLASSICAL AND QUANTUM LIQUIDS INDUCED BY QUANTUM FLUCTUATIONS**

Miguel M. Oliveira,<sup>1,\*</sup> Pedro Ribeiro,<sup>1</sup> and Stefan Kirchner<sup>2</sup>

<sup>1</sup>CeFEMA, Instituto Superior Técnico, Universidade de Lisboa, Av. Rovisco Pais, 1049-001 Lisboa, Portugal.

<sup>2</sup>Zhejiang Institute of Modern Physics, Zhejiang University, Hangzhou, Zhejiang 310027, China.

Zhejiang Province Key Laboratory of Quantum Technology and Devices, Zhejiang University, Hangzhou 310027, China.

\*miguel.m.oliveira@tecnico.ulisboa.pt

Geometrically frustrated interactions may render classical ground-states macroscopically degenerate. The connection between classical and quantum liquids and how the degeneracy is affected by quantum fluctuations is, however, not completely understood.

We study a simple model of coupled quantum and classical degrees of freedom, the so-called Falicov-Kimball model, on a triangular lattice and away from half-filling. For weak interactions the phase diagram features a charge disordered state down to zero temperature. We provide compelling evidence that this phase is a liquid and show that it is divided by a crossover line that terminates in a quantum critical point.

Our results offer a new vantage point to address how quantum liquids can emerge from their classical counterparts.

**Reference**

[1] M. M. Oliveira, P. Ribeiro, S. Kirchner, arXiv:1810.10582, 2018

## P06 - COLLECTIVE DYNAMICS OF FLEXIBLE ACTIVE PARTICLES ON SUBSTRATES: FROM CELLS TO TISSUES

H. P. M. Melo,<sup>1,2\*</sup> A. S. Nunes,<sup>1,2</sup> D. E. P. Pinto,<sup>1,2</sup> and N. A. M. Araújo<sup>1,2</sup>

<sup>1</sup> Centro de Física Teórica e Computacional, Faculdade de Ciências, Universidade de Lisboa, P-1749-016 Lisboa, Portugal.

<sup>2</sup> Departamento de Física, Faculdade de Ciências, Universidade de Lisboa, P-1749-016 Lisboa, Portugal.

\* Corresponding Author: hpmelo@fc.ul.pt

Understanding how cells goes from a scattered distribution to a mechanically robust tissue on the substrate poses technological and theoretical challenges in studies of morphogenesis, wound healing, and cancer [1,2]. Several of these theoretical challenges are deeply related to longstanding problems in soft condensed matter such as adsorption and wetting, nonequilibrium dynamics, and the mechanics of flexible objects and membranes. We developed a model to study the dynamics of adhesion, motility and proliferation of cells on substrates. We aim to understand how the collective dynamics of cells leads to the complex spatial patterns shown in experiments and the particular role of each mechanism in the overall dynamics [2,3,4]. To compare our model with experiments we used image processing algorithms to determine the nuclei position of cells and thus we measured a number of statistical properties like the pair correlation function, distribution of area of Voronoi cells and number of neighbors. By controlling each one of the mechanisms individually (adhesion, motility and proliferation), we are able to reproduce the spatial heterogeneous distribution of cells in substrates, which may lead to a better understanding of tissues growth.

### References

- [1] S. Kaliman et al, *Frontiers in Physiology*, 7, 551 (2016)
- [2] M. R. Carvalho et al, *Nanomedicine*, 12, 581 (2017)
- [3] S. A. Gudipaty et al, *Nature*, 543, 118 (2017)
- [4] H. Jeon et al, *Nature Materials*, 14, 918 (2015)



## P07 - COMPARISON BETWEEN THE FULL NON-LINEAR OPTICAL RESPONSE IN TIME AND THE PERTURBATION THEORY IN GRAPHENE

S. M. João<sup>1</sup>, G. B. Ventura<sup>1</sup> and J. M. Viana Parente Lopes<sup>1\*</sup>

<sup>1</sup>Centro de Física das Universidades do Minho e do Porto, CF-UM-UP, Departamento de Física e Astronomia, Faculdade de Ciências da Universidade do Porto, Rua do Campo Alegre, s/n, 4169-007 Porto, Portugal

\*Corresponding Author: jlopes@fc.up.pt

Recently, we presented a coherent procedure to include the electromagnetic perturbation in a crystal in the velocity gauge [1]. For two-dimensional materials, this corresponds to the inclusion of a time dependent Peierls phase, yielding a uniform time dependent vector potential in the crystal plane. This approach avoids the divergences that plagued the linear and non-linear calculations for several years and explicitly gives the sum rules at all orders of perturbation theory that connect the velocity and length gauge [2].

The full nonlinear optical response of graphene is obtained by the time integration of the optical Bloch equations within the relaxation time approximation [3]. By using the velocity gauge representation, one can reduce this problem to the numerical integration of an ordinary differential equation - where each  $\mathbf{k}$ -point of the reciprocal space is treated independently - as opposed to the length gauge, where the Bloch equations are coupled partial differential equations in both  $\mathbf{k}$  and time [4].

In this work, we compare the results from perturbation theory with those of the full nonperturbative response of graphene. Since we are not restricted to the Dirac Hamiltonian [5], and are working with the full first Brillouin zone, we are able to explore a broad range of frequencies. We are particularly interested in exploring the limits of the perturbation theory and its deviation from the exact response as a function of the applied field. We analyze the saturation effects for strong fields due the Pauli blocking of the graphene bands [6].

### References

- [1] D. J. Passos, G. B. Ventura, J. M. Viana Parente Lopes, J. M. B. Lopes dos Santos, and N. M. R. Peres, *Nonlinear optical responses of crystalline systems: Results from a velocity gauge analysis*, Phys. Rev. **B 97**, 235446, 2018.
- [2] Ventura, G. B., D. J. Passos, J. M. B. Lopes dos Santos, J. M. Viana Parente Lopes, and N. M. R. Peres, *Gauge Covariances and Nonlinear Optical Responses*, Phys. Rev. **B 96**, no. 3, 2017.
- [3] Boyd, R. W., *Nonlinear Optics*, 3rd ed. (Elsevier Science Publishing Co. Inc., London, 2008)
- [4] J. L. Cheng, N. Vermeulen, and J. E. Sipe, *Numerical study of the optical nonlinearity of doped and gapped graphene: From weak to strong field excitation*, Phys. Rev. **B 92**, 235307, 2015.
- [5] Ishikawa, K. L., *Nonlinear optical response of graphene in the time domain*, Phys. Rev. **B 82**, 201402R, 2010
- [6] Marini, A., J. D. Cox, and F. J. García de Abajo, *Theory of Graphene Saturable Absorption*, Phys. Rev. **B 95**, no. 12, 2017.

## P08 - DYNAMICS OF ACTIVE POLYMER NETWORKS

F. R. Cerdeira,<sup>1,2\*</sup> P. M. Patrício,<sup>2,3</sup> and N. A. M. Araújo<sup>1,2</sup><sup>1</sup> Departamento de Física, Faculdade de Ciências, Universidade de Lisboa, 1749-016 Lisboa, Portugal.<sup>2</sup> Centro de Física Teórica e Computacional, Faculdade de Ciências, Universidade de Lisboa, 1749-016 Lisboa, Portugal.<sup>3</sup> ISEL - Instituto Superior de Engenharia de Lisboa, Instituto Politécnico de Lisboa, 1959-007, Lisboa, Portugal.

\*Corresponding Author: fc45311@alunos.fc.ul.pt

The cytoskeleton is a dynamic network of interconnected filaments inside the cell that is relevant for its intracellular transport, shape, motility, and interaction with external environment. Due to the finite stiffness of the filaments and low volume fraction, these networks yield a complex mechanical behavior, contrasting often with their now better understood synthetic counterparts [1]. Experimental studies suggest a strong nonlinear increase in the elastic moduli, and an additional, and quite unusual, negative normal stress, as a response to an increasing strain levels exerted on the network [2-4]. A reversible strain softening has also been observed as well as network failures after high levels of compression. These phenomena might be explained by the unbinding of crosslinkers as the stress is exerted, and subsequent binding after its relaxation, due to the active nature of the network [2-7].

We aim to describe the cytoskeleton as an active polymer network, whose links can be added and removed dynamically. For that, we developed a statistical model that, despite simple, grasps the relevant physics. We represent each polymer as a chain of beads, subject to drag and random thermal forces, connected by harmonic springs. We observe that under a shear flow, the intrinsic viscosity increases linearly with temperature, the drag coefficient of the individual beads, and the number of beads squared. To shed light on the inter-polymer interaction, we investigate the evolution of bead aggregates, their aggregation and fragmentation rates, that depend on the intensity of the binding potential and the thermostat temperature.

### References

- [1] C. P. Broedersz, F. C. MacKintosh, *Reviews of Modern Physics*, 86, 995–1036 (2014).
- [2] E. Conti, F. C. MacKintosh, *Physical Review Letters*, 102, 088102 (2009).
- [3] Janmey et al., *Nature Materials*, 6, 48-51 (2007).
- [4] Kang et al., *The Journal of Physical Chemistry B*, 113, 3799-3805 (2009).
- [5] M. L. Gardel, *Science*, 304, 1301–1305 (2004).
- [6] Lieleg et al., *Biophysical Journal*, 96, 4725-4732 (2009).
- [7] Chaudhuri et al., *Nature*, 445, 295-298 (2007).

## P9 - DYNAMICS OF EPITHELIAL TISSUES ON HETEROGENEOUS SUBSTRATES

Diogo E. P. Pinto,<sup>1,\*</sup> Gonca Erdemci-Tandogan,<sup>2</sup> M. Lisa Manning,<sup>2</sup> and Nuno A. M. Araújo<sup>1</sup>

<sup>1</sup>Centro de Física Teórica e Computacional, Universidade de Lisboa, Campo Grande, Lisboa, Portugal.

<sup>2</sup>Department of Physics, Syracuse University, Syracuse, New York, USA.

\*Corresponding Author: dpinto@alunos.fc.ul.pt

Many biological processes are governed by the motion of cells in dense tissues. Examples range from embryonic development to cancer metastasis. Following the growing interest on this subject, extensive experimental studies have been performed. To help understanding the experimental results, researchers have developed different theoretical and numerical models, with different levels of detail. Arguably, the most promising one for the study of confluent tissues is the Self-Propelled Voronoi model, which is able to capture the epithelial tissue geometry and dynamics in the limit of a single monolayer [1, 2]. Most studies with this model focus on idealized conditions, when the tissues are resting on liquid beds, neglecting any interaction with the substrate. But, in reality, most controlled experiments are performed on a substrate where cells can adhere, grow, and proliferate. Here, we study the role of the substrate on the dynamics of the tissue. We show that when a substrate can alter the properties of the tissue cells, it forces the tissue to reorganize and, depending on how long the cells take to adapt to the substrate, a motility induced phase separation can be observed. This mechanism would allow for the compartmentalization of the tissue which might have implications in the development of artificial organs.

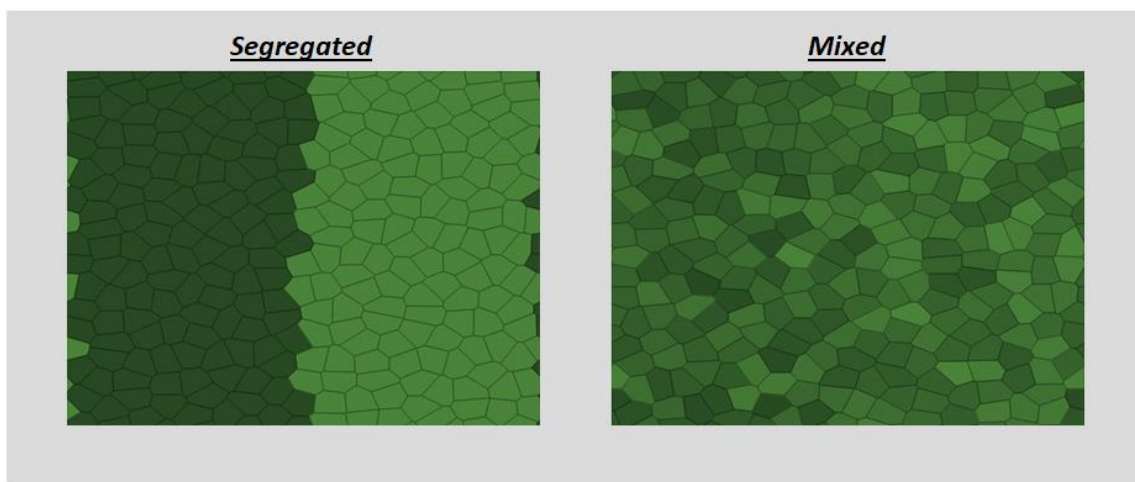


Figure 1. Two possible stationary states of the tissue. On the left-hand side the tissue remains compartmentalized because cells adapt quickly to the substrate. While, on the right-hand side, cells take too long to adapt, which promotes complete mixing.

## References

- [1] Dapeng Bi et al., *Physical Review X* 6, 021011 (2016).
- [2] Jin-Ah Park et al., *Nature Materials* 14, 1040 (2015).

## P10 - ELECTRONIC PROPERTIES OF TWISTED BILAYER GRAPHENE IN THE PRESENCE OF A MAGNETIC FIELD

M. C. M. Quintela, J. C. C. Guerra, S. M. João, J. M. B. Lopes dos Santos

Departamento de Física e Astronomia, Universidade do Porto, Rua do Campo Alegre 4169-007, Porto, Portugal.

\*Corresponding Author: mfcmmquintela@fc.up.pt

In AA-stacked twisted bilayer graphene, the presence of a constant magnetic field opens a gap in the density of states, as well as creating Landau levels. The Kernel Polynomial Method (KPM) can be used to study optical and electronics properties.

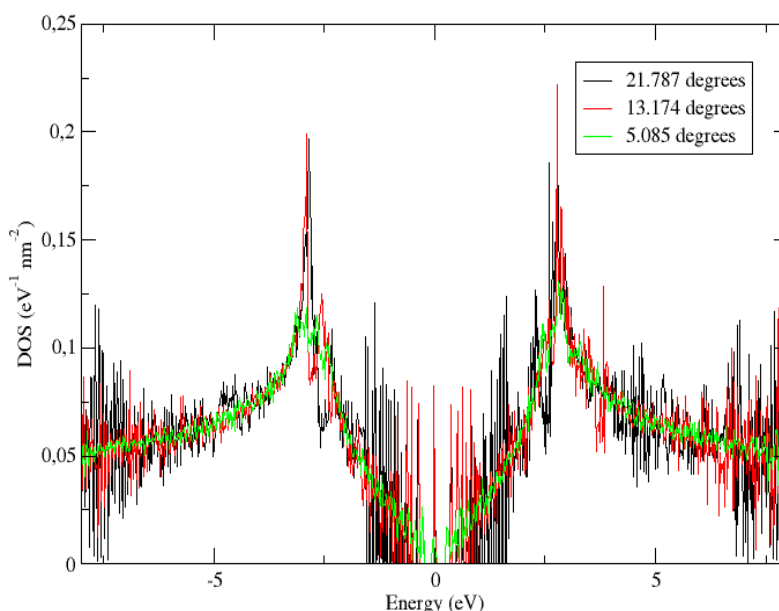


Figure 1. Density of States for different commensurable angles

Using KITE, an open-source software developed in our group, it is possible to calculate the density of states for several commensurable angles, as well as the optical conductivity and the local density of states. The aim of this work is to analyze how the features of these quantities change with the twist angle in the presence of a uniform magnetic field.

### References

- [1] Weisse, A., Wellein, G., Alvermann, A., *Reviews of Modern Physics* 78, 275 (2016).
- [2] Lopes dos Santos, J., Peres, N., Castro Neto, A., *Physical Review B* 86, 155449 (2012).
- [3] Lopes dos Santos, J., Peres, N., Castro Neto, A., *Physica Review Letters* 99, 256802 (2007).
- [4] Anh Le, H., Nam Do, V., *Physical Review B* 97, 125136 (2018).

## P11 - ENERGY LOSS BY FAST-TRAVELING CHARGED PARTICLES TRAVERSING TWO-DIMENSIONAL MATERIALS

Jaime E. Santos,<sup>1,\*</sup> Mikhail I. Vasilevskiy,<sup>1</sup>, Nuno M. R. Peres,<sup>1</sup> and Antti-Pekka Jauho<sup>1</sup>

<sup>1</sup>Centro de Física and Departamento de Física, Universidade do Minho, P-4710-057 Braga, Portugal.

<sup>2</sup>DTU Nanotech, Department of Micro and Nanotechnology Ørsted Plads, Building 345C, DK-2800 Kgs. Lyngby, Denmark.

\*Corresponding Author: jaime.santos@fisica.uminho.pt

We consider the problem of the radiation losses by fast-traveling particles traversing two-dimensional materials or thin films. After reviewing the problem of screening of electromagnetic fields by two-dimensional conducting materials, we apply the results to obtain the energy loss by a fast particle traversing such a film. In particular, we discuss the pattern of radiation emitted by mono-layer graphene treated within a hydrodynamic approximation [1]. These results are compared with recent published results using similar approximations [2,3] and we discuss how one can improve on the signals obtained by using different materials.

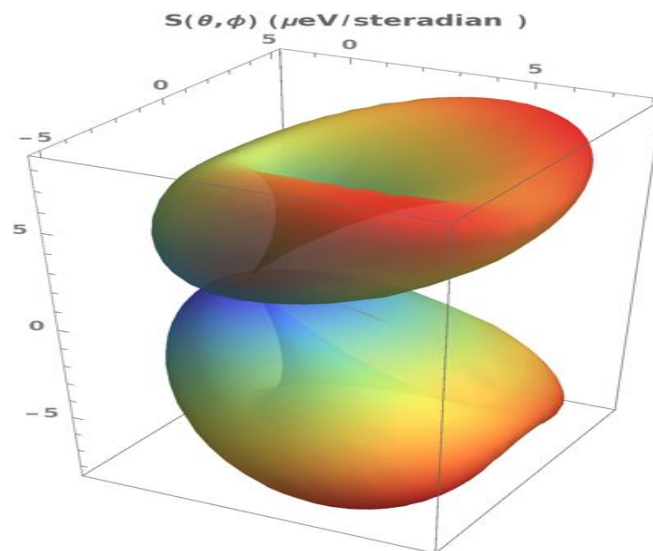


Figure 1. Energy emitted per steradian for an ultra-relativistic electron traversing a sheet of mono-layer graphene at a 30° angle from the vertical.

### References

- [1] Jaime E. Santos, Mikhail I. Vasilevskiy, Nuno M. R. Peres, and Antti-Pekka Jauho, in preparation.
- [2] Z. L. Miskovic, S. Segui, J. L. Gervasoni, and N. R. Arista, Phys. Rev. B 94, 125414 (2016).
- [3] K. Akbari, S. Segui, Z. L. Miskovic, J. L. Gervasoni, and N. R. Arista, Phys. Rev. B 98, 195410 (2018).

## P12 - ENHANCED LOCALIZATION AND PROTECTION OF TOPOLOGICAL EDGE STATES DUE TO GEOMETRIC FRUSTRATION

L. Madail,<sup>1,\*</sup> S. Flannigan,<sup>2</sup> A. M. Marques,<sup>1</sup> A. J. Daley,<sup>2</sup> and R. G. Dias<sup>1</sup>

<sup>1</sup>Department of Physics & I3N, University of Aveiro, 3810-193 Aveiro, Portugal

<sup>2</sup>Department of Physics & SUPA, University of Strathclyde, Glasgow G4 0NG, United Kingdom

\*luisamadail@ua.pt

Topologically non-trivial phases are linked to the appearance of localized modes in the boundaries of an open insulator. On the other hand, the existence of geometric frustration gives rise to degenerate localized bulk states. The interplay of these two phenomena may, in principle, result in an enhanced protection/localization of edge states. In this paper, we study a two-dimensional Lieb-based topological insulator with staggered hopping parameters and diagonal open boundary conditions. This system belongs to the  $C_{2v}$  class and sustains 1D boundary modes except at the topological transition point, where the  $C_{4v}$  symmetry allows for the existence of localized (0D) corner states. Our analysis reveals that, while a large set of boundary states have a common well defined topological phase transition, other edge states reflect a topological non-trivial phase for any finite value of the hopping parameters, are completely localized (compact) due to destructive interference and evolve into corner states when reaching the higher symmetry point. We consider the robustness of these compact edge states with respect to time-dependent perturbations and indicate ways that these states could be prepared and measured in experiments with ultracold atoms.

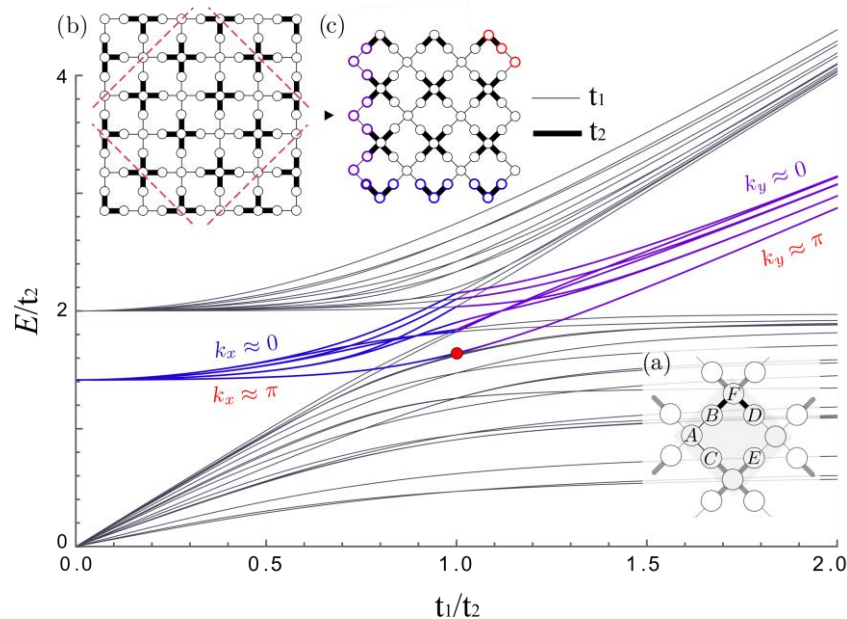


Figure 1. Boundary states of the Lieb rotated lattice. In the top-left, we schematize the creation of the rotated lattice with unit cell of (a) from the two-dimensional Lieb model (b) where the boundaries belong to a  $\pi/4$  rotated x-y reference frame (c). The energy spectrum as a function of the hopping parameters is plotted for the rotated Lieb lattice with  $5 \times 5$  plaquettes and  $t_2 = 1$ . We identify the different types of states according to their localization in the lattice: bulk (black line), vertical (purple line), horizontal (blue line) and corner (red dot) states. This last state appears only for  $t_1 = t_2$ , when  $C_4$  rotation symmetry is restored.

## P13 - EQUATION OF STATE OF ACTIVE COLLOIDAL PARTICLES

J. Viana\*, M. Tasinkevych

1 - Departamento de Física, Faculdade de Ciências, Universidade de Lisboa, 1749-016 Lisbon, Portugal.

2 - Centro de Física Teórica e Computacional, Universidade de Lisboa, 1749-016 Lisbon, Portugal.

\*Corresponding Author: fc49547@alunos.fc.ul.pt

Active colloids represent a new class of non-equilibrium soft condensed matter in which energy harvesting and conversion take place at the level of individual constituents. They reveal novel types of self-assembly not accessible in traditional condensed matter systems, such as “living crystals” [1]. A basic question in such non-equilibrium systems is whether it is possible to characterize the system by conventional macroscopic parameters such as, e.g., pressure or an effective temperature, and if yes does there exist an equation of state relating these parameters. We perform here extensive Langevin dynamics simulations to address this issue for a suspension of active colloidal particles. Each of the particles spins with a given frequency  $f$  about an axis perpendicular to a plane, with the plane slightly tilted to cause sedimentation down the plane. This is the classic geometry used to find the equation of state. Experimentally such system can be realized by a suspension of slightly magnetic colloidal particles driven by an in-plane rotating magnetic field [2].

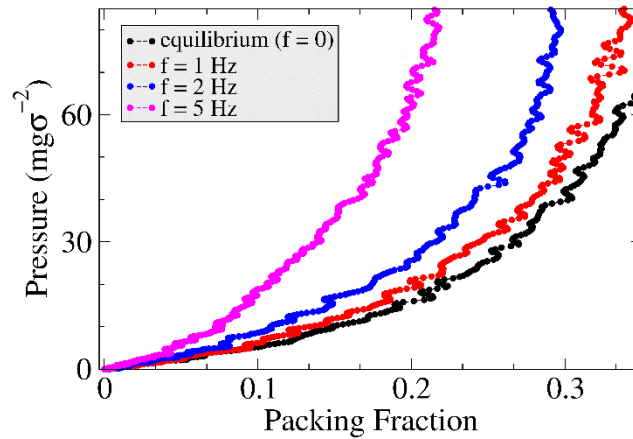


Figure 1. Osmotic pressure  $P$  of a suspension of spherical particles, spinning about an axis perpendicular to a plane, with the plane slightly tilted to cause sedimentation down the plane, as a function of the packing fraction  $\phi$ .  $mg$  is the component of the gravity force on the particle parallel to the plane,  $\sigma$  is the particle diameter.

In the simulations, the particles interact via a soft-core repulsive potential and via rotation-induced hydrodynamic interactions. The later are assumed to be pairwise additive and are calculated using a point-particle approximation. At steady state, the buoyant weight of particles above any height is balanced by the osmotic pressure  $P$  at that height. A calculation of the packing fraction  $\phi$  versus height permits estimation of  $P$  as a function of  $\phi$ , as shown in figure 1. These results demonstrate that one cannot achieve data collapse by simply rescaling the vertical axis by a constant (different for each  $f$ ). This observation indicates that the effective temperature model is not applicable for this system: the effective temperature would depend on the packing fraction. Additionally, we find that the simulation results approximately obey the scaling relation  $P - P_{eq} \propto f^2 \phi^4$ , where  $P_{eq}$  is the equilibrium pressure of passive (not spinning) particles. This relation can be rationalized by using a simple scaling argument. The numerical simulations highlight the importance of hydrodynamic interactions in this non-equilibrium system and demonstrate that one cannot characterize steady state of the system in terms of the effective temperature.

#### References

- [1] J. Palacci et al., *Science* 339, 936 (2013).
- [2] M. Driscoll et al., *Nature Physics* 13, 375 (2017).



**P14 - EXCITATION OF GRAPHENE PLASMONS BY QUANTUM EMITTERS**Beatriz A. Ferreira,<sup>1,\*</sup> Nuno MR Peres<sup>1</sup><sup>1</sup>International Iberian Nanotechnology Laboratory and Center of Physics of the University of Minho and the University of Porto.

\*Corresponding Author: beatriz.ferreira@inl.int

In this work we study three different structures made from graphene. We use these structures to show that is possible to excite the optical and acoustic plasmons in the case of the double graphene layer and the screen plasmon in the graphene near a metal due to the presence of a quantum emitter. This classic calculation are obtain through the dyadic Green Functions. We also quantize the electromagnetic field in order to calculate the transition rate through the Fermi Golden Rule and we show that we obtain the same results of the classic transition.

**References**

- [1] Frank HL Koppens, et al., Nano letters, 11(8):3370–3377, 2011.
- [2] Mark S Tame, et al., Nature Physics, 9(6):329, 2013.
- [3] Mauro Cuevas, Journal of Optics, 18(10):105003, 2016.
- [4] Paulo A. D. Gonçalves and Nuno MR Peres, An introduction to graphene plasmonics. World Scientific, 2016.
- [5] Alexandre Archambault, et al., Physical Review B, 82(3):035411, 2010.
- [6] EA Hinds, Advances in Atomic, Molecular, and Optical Physic ,28:237–289, 1990.

# P15 - HOLE LOCALIZED STATES IN INTERACTING GEOMETRICALLY FRUSTRATED SYSTEMS

F. D. R. Santos, R. G. Dias

Department of Physics & I3N, University of Aveiro, Campus Universitario de Santiago, 3810-193 Aveiro, Portugal.

\*filipedrsantos@ua.pt

Many-body localized states are shown to exist in geometrically frustrated lattices if the interacting Hamiltonian generates a network of transition matrix elements between many-body Wannier states with bubble-like structures. We show that such structures occur in the  $U/t = \infty$  Hubbard model on the Lieb and Kagome lattices and hole localized eigenstates of these models are standing waves in these bubbles. In the particular case of one hole in a Lieb cluster with arbitrary spin configuration, these bubbles are the fundamental cycles of the network. These bubble-like standing waves constitute an interesting many-body generalization of the concept of most compact localized state. The full set of hole localized states of the  $U/t = \infty$  Hubbard model on the Lieb and Kagome lattices is constructed and the general expression of the number of one-hole localized states with one flipped spin is given for clusters with arbitrary shape. A numerical approach is described for the case of a large number of holes in a large cluster.

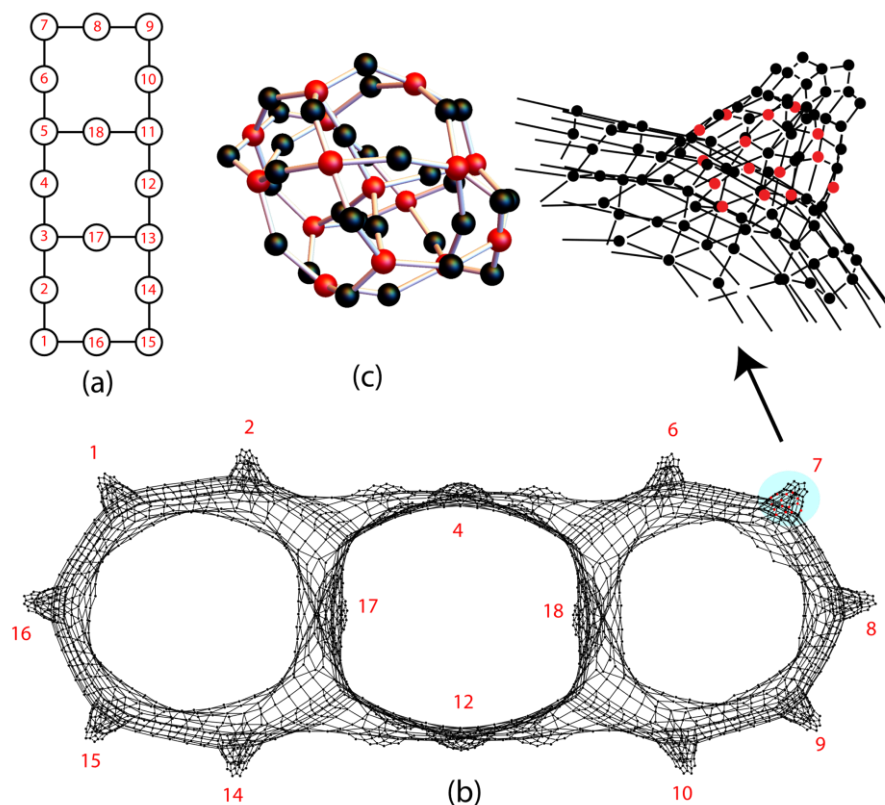


Figure 1. (a) Lieb-1  $\times$  3 cluster with indexed sites. (b) Network corresponding to the Lieb-1  $\times$  3 cluster with two holes and one flipped spin. In (a) and (b), the localized states are standing waves in a bubble, shown in (c), which is a set of interlocked rings in the network. The small bubbles in (b) generate localized states with a fixed flipped spin at the site indicated by the number next to the bubble, according to the labeling shown on the top diagram.

## P16 - MAGNETIC BEHAVIOR IN MULTI-SEGMENTED NANOWIRES OF FE/CU WITH DIFFERENT NUMBER OF LAYERS

Suellen Moraes<sup>1</sup>, David Navas<sup>1</sup>, Mariana P. Proenca<sup>1,2</sup>, Célia T. Sousa<sup>1</sup> and João P. Araújo<sup>1</sup>

<sup>1</sup> IFIMUP and IN-Institute of Nanoscience and Nanotechnology and Dep. Física e Astronomia, Universidade do Porto, Rua do Campo Alegre 687, 4169-007 Porto, Portugal.

<sup>2</sup> Instituto de Sistemas Optoelectrónicos y Microtecnología, Universidad Politécnica de Madrid, Avda. Complutense 30, E-28040 Madrid, Spain.

Ferromagnetic nanostructures with complex and controlled magnetic behavior have been extensively studied during the last years. The need for low-energy technologies and the recent advances in chemical and self-assembly synthesis techniques have boosted the growth of 3D nano-objects. This capacity to control size and shape, not only in the plane but also along the vertical direction, leads to the appearance of new effects in spin configurations. This potential is of great interest for a wide range of applications, such as spintronics and novel magnetic sensors, chemical and biological sensors, drug delivery systems and medical treatment by hyperthermia [1].

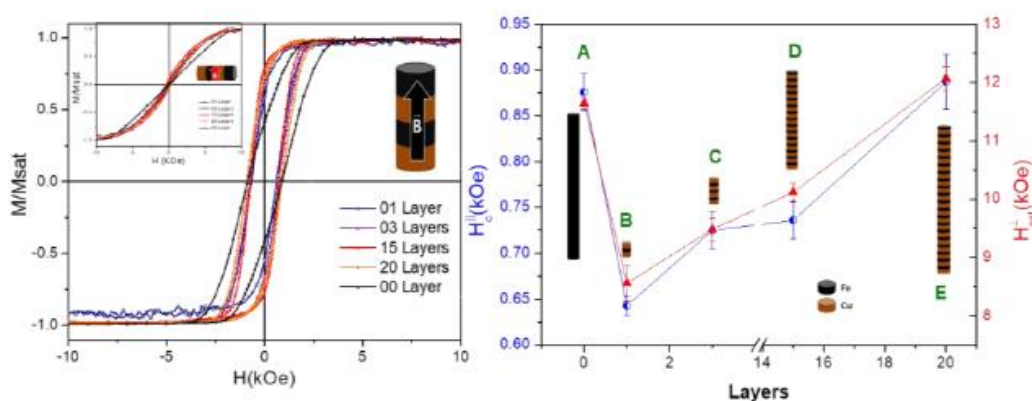


Figure 1. Magnetic hysteresis loops  $[M(H)]$  recorded for the Fe/Cu NWs (left), and study of the parallel coercivity field and perpendicular saturation field (right).

In this work, Fe/Cu nanowires (NWs) were prepared with different thickness ( $L$ ) and varying the number of layers. Figure 1 shows the magnetic hysteresis loops  $[M(H)]$  recorded for the Fe/Cu NWs with  $L_{Fe}=300$  nm and  $L_{Cu}=170$  nm varying the number of layers between 0 and 20, with the applied magnetic field parallel ( $\parallel$ ) and perpendicular ( $\perp$ ) to the NWs long axis. The results illustrate a magnetic anisotropic behaviour for Fe/Cu NWs with the easy magnetization axis lying parallel to the wire axis, arising from the competition between the magnetocrystalline anisotropy and the shape anisotropy factors [2]. Analyzing the behaviour of the parallel coercivity in Figure 1, a drastic reduction of  $H_c$  is observed when non-magnetic layers are introduced in the Fe magnetic NWs. This is due to the generation of nucleation points of new magnetic domain walls leading to an easier magnetization reversal, as predicted by Allende et al. using Monte Carlo calculations [3]. For the length of this segment of Fe and Cu, the Fe/Cu multisegmented nanowire acts like a collection of non-interacting magnetic entities along the NW (intrawire interactions), which leads us to conclude that the increase in  $H_c$  occurs due to the sum of the individual contribution of each segment [1]. Moreover, Figure 1 shows the saturation field as a function of the number of layers, evidencing a behaviour similar to the one observed for  $H_c$ .

### References:

- [1] Moraes S.; Navas D.; Béron F.; Proenca M.P.; Pirota K.P.; Sousa C.T.; Araújo J.P., *Nanomaterials*, 8(7), 490, 2018.
- [2] Susano, M.; Proenca, M.P.; Moraes, S.; Sousa, C.T.; Araújo, J.P., *Nanotechnology*, 27, 335301, 2016.
- [3] Núñez, A.; Pérez, L.; Abuin, M.; Araujo, J.P.; Proenca, M.P., *J. Phys. D: Appl. Phys.* 50, 155003, 2017.

# P17 - MAGNETIC STUDIES OF MONOCLINIC $\text{Cu}_4\text{O}(\text{SeO}_3)_3$ , A COPPER-OXO-SELENITE DERIVATIVE

J. F. Malta,<sup>1,2,\*</sup> M. S. C. Henriques<sup>1</sup>, J.A. Paixão<sup>1</sup>, A. P. Gonçalves<sup>2</sup>

<sup>1</sup> CFisUC, Department of Physics, University of Coimbra, Portugal.

<sup>2</sup> C2TN, Department of Nuclear Science and Engineering, Instituto Superior Técnico, Portugal.

\*Corresponding Author: josemalta@ctn.tecnico.ulisboa.pt

$\text{Cu}_4\text{O}(\text{SeO}_3)_3$ , a copper-oxo-selenite derivative belonging to the  $\text{Cu}_x\text{O}(\text{SeO}_3)_{x-1}$  family containing the celebrated skyrmionic chiral magnet  $\text{Cu}_2\text{OSeO}_3$ , crystallises in two different polymorphs with monoclinic and triclinic structures [1]. Their crystal structures have been reported and this compound was found as contaminant of  $\text{Cu}_2\text{OSeO}_3$ , but is otherwise poorly known. It can be obtained during the copper selenite decomposition in air at high temperatures [2] or by reacting  $\text{CuO}$  and  $\text{SeO}_2$  in a typical solid state reaction [3]. In this work, we obtained high quality monoclinic  $\text{Cu}_4\text{O}(\text{SeO}_3)_3$  single crystals through a chemical vapour transport reaction in evacuated sealed quartz tubes. The presence of the monoclinic form was confirmed by single-crystal and powder XRD. The magnetic properties were not been previously investigated, and the present studies show a typical antiferromagnetic behaviour, with a Néel temperature of  $\sim 58$  K, similar to that of the cubic chiral magnet  $\text{Cu}_2\text{OSeO}_3$ . A fit of the magnetic susceptibility to a modified Curie-Weiss law gave a value of the effective magnetic moment per magnetic atom of  $1.84 \mu_B$ , close to the expected theoretical value for  $\text{Cu}^{2+}$ . Figure 1 shows the Zero-Field Cooling (ZFC)  $M(T)$  curves for  $\text{Cu}_4\text{O}(\text{SeO}_3)_3$  measured in a small single crystal. In addition to the main transition, an anomaly at 13 K is observed for values of applied magnetic fields above 1000 Oe, corresponding to a canting of the Cu magnetic moments into a ferrimagnetic state. Above 13 K, and below  $T_N$ , a very small remanence is observed in the hysteresis cycles. The low-temperature  $M(H)$  curves, represented in figure 2, show a spin-flop transition starting at  $H_{c1} \sim 280$  Oe, likely from a helical into a conical ferromagnetic intermediate phase, and a second transition at  $H_{c2} \sim 730$  Oe, possibly into a collinear ferrimagnetic phase, as above  $H_{c2}$  the induced moment increases linearly with applied field. The induced ferromagnetic component in a 9 T field is  $0.86 \mu_B/\text{Cu}$  at 1.8 K and attains a maximum value of  $0.98 \mu_B/\text{Cu}$  at 13 K, larger than observed in  $\text{Cu}_2\text{OSeO}_3$ .

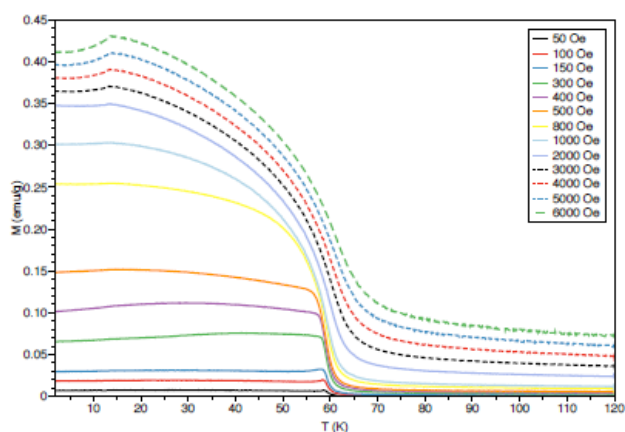


Figure 1. Zero-Field Cooling (ZFC) Magnetisation Curves ( $M(T)$ ) for the  $\text{Cu}_4\text{O}(\text{SeO}_3)_3$  in the single crystal form.

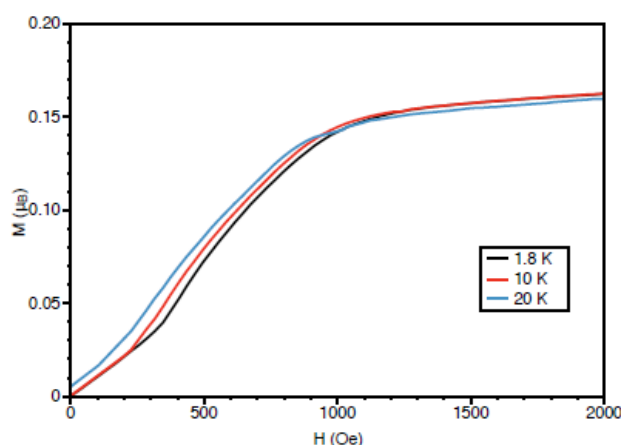


Figure 2. Magnetic-field dependence of the magnetisation ( $M(H)$ ) for 1.8 K, 10 K and 20 K.

## References

- [1] H. Effenberger et al., *Monatshefte fuer Chemie* 117, vol. 117, pp. 887–896, 1986.
- [2] J. F. Malta, et al., *J. Magn. Magn. Mater.*, vol. 474, , pp. 122–126, 2019.
- [3] J. R. Panella, et al., *Cryst. Growth Des.*, vol. 17, p. 4944, 2017.

**P18 - MEASURING NANOSCALE INTERACTIONS WITH FORCE FEEDBACK MICROSCOPY**M. V. Vitorino,<sup>1,2,\*</sup> and M. S. Rodrigues<sup>1,2</sup><sup>1</sup>Department of Physics, University of Lisboa, Campus Faculdade de Ciências da Universidade de Lisboa, Edifício C8, Piso 4, Campo Grande, 1749-016 Lisboa, Portugal.<sup>2</sup>University of Lisboa, Faculty of Sciences, BioISI – Biosystems and Integrative Sciences Institute, Lisboa, Portugal.

\*Corresponding Author: mvvitorino@fc.ul.pt

Atomic force microscopes (AFMs) have been key instruments in the exploration of the nanoscale for the past decades. Their capability to image molecules in almost any environment, but also to touch, manipulate and measure interactions at the nanometer level have turned these instruments into molecular toolboxes. However, significant problems still undermine the use of the instrument, in particular when studying soft matter, where the application and measurement of pN-level forces is a requirement. The AFM is based on the deflection of a spring (called the cantilever), in which a nanometric tip is attached. The fact that the tip-sample force is obtained from the angular deflection of the cantilever, introduces stability problems, increases the uncertainty of force measurements and prevents the spectroscopic investigation of the interactions under study [1,2].

The force feedback microscope (FFM) attempts to solve some of these issues by including a feedback element in the conventional AFM [2]. My PhD work has been focused on the development of this new type of microscopy and demonstration of its advantages and drawbacks in comparison with the conventional AFM scheme. In addition to the feedback mechanism that stabilizes the tip position, the developed FFM also features an improved detection mechanism, which makes it sensible to the position of the cantilever, and not to its angular deflection. This enables the measurement of interactions with much lower uncertainty and their investigation at different timescales. The microscope has been developed using a modular 3D-printing strategy, allowing to reduce significantly its production cost.

We have demonstrated that this manufacturing strategy and the added instrumentation does not decrease the imaging performance of the instrument, allowing simultaneously a more precise measurement of forces. The FFM was used to perform indentation curves on soft materials, such as cells, to establish their mechanical properties, earning an order-of-magnitude lower uncertainty when compared to the conventional AFM experiment. Additionally, the increased tip stabilization allowed the study of the nucleation of capillary water bridges, which was inaccessible to the conventional instrument [3]. The added force sensitivity also enabled the study of the effects of friction in harmonic oscillators [4]. Finally, our FFM experimental setup also enabled the application of a new non-contact measurement strategy to study the viscoelasticity of soft matter.

In conclusion, the FFM technique has emerged as a consistent and reliable alternative to study interactions at the molecular scale, in particular showing an improved performance when addressing soft matter studies. In this talk I will give a broad view into the main instrumental issues and highlight some key scientific results obtained during my PhD work.

**References**

- [1] H.J. Butt, B. Capella, M. Kappl, *Surface science reports*, 59, 1-152 (2005).
- [2] M.S. Rodrigues et al., *Applied Physics Letters*, 101, 203105 (2012).
- [3] M.V. Vitorino, A. Vieira, M.S. Rodrigues, *Scientific reports*, 7, 3726 (2017).
- [4] M.V. Vitorino, et al., *Scientific reports*, 8, 13848 (2018).

**P19 - MICROMAGNETIC STUDY OF THE VORTEX STATE IN SUB-MICRON IRON DISCS**L. Peixoto<sup>\*1</sup>, C.T. Sousa<sup>1</sup>, D. Navas<sup>1</sup>, J.P. Araújo<sup>1</sup><sup>1</sup>IFIMUP and DFA, Faculdade de Ciências da Universidade do Porto, Rua do Campo Alegre 1021/1055, Porto, Portugal<sup>\*</sup>Corresponding Author: ludgero.peixoto@fc.up.pt

Magnetic nanostructures are, currently, the focus of several research fields, such as data storage, sensing and biomedicine. One subset of these nanostructures are discs that present a magnetic vortex state in remanence. These discs are used for data storage [1] and for a cancer therapy, magneto-mechanically induced cell death [2].

In this work, micromagnetic simulations of sub-micron iron discs are performed for different aspect ratios (diameter/thickness) and normalized inter-dot distance (distance/diameter). The simulations were performed using mumax3 and were divided in two subsets. The first group of simulations were based on treated SEM (Scanning electron microscope) images of real samples, disc-shaped nanostructures with intrinsic shape anisotropy. Here the thickness was varied from 20 nm to 100 nm as the diameter was fixed by the real sample. The other group of simulations were based on circular discs, to eliminate the anisotropy of the real disc. Different combinations of diameter and thickness were used with the resulting aspect ratio ranging between 2 and 25.

For both sample-sets the magnetic susceptibility, the nucleation and the annihilation fields were determined and studied with respect to the varied parameters.

The vortex state was found in discs with aspect ratios between 5 and 15, consistent between both subsets of data. When the inter-dot distance is greater or equal to the diameter of the disc, the interactions between discs were found to be negligible and the disc can be considered isolated.

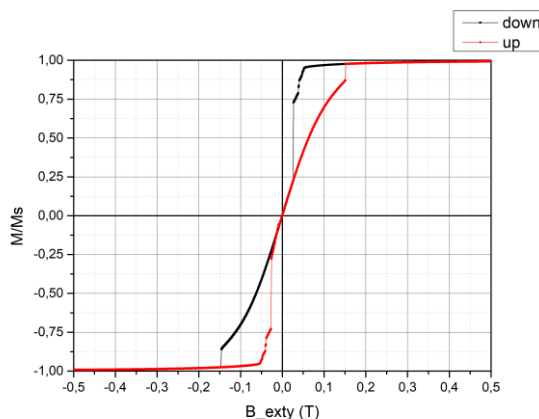


Figure 1. Simulated hysteresis loop a 30 nm-thick iron disc.

## References

- [1] Bohlens, S.; Krüger, B.; Drews, A.; Bolte, M.; Meier, G. & Pfannkuche, D., Applied Physics Letters 93, 142508 (2008).
- [2] Yu Cheng, Megan E. Muroski, Dorothée C.M.C. Petit, Rhodri Mansell, Tarun Vemulkar, Ramin A. Morshed, Yu Hana, Irina V. Balyasnikova, Craig M. Horbinski, Xinlei Huang, Lingjiao Zhangc, Russell P. Cowburn, Maciej S. Lesniak, Journal of Controlled Release 223, 75 (2016).

**P20 - MIXED-ORDER SYMMETRY-BREAKING QUANTUM PHASE TRANSITION FAR FROM EQUILIBRIUM**

T. O. Puel,<sup>1,2</sup> Stefano Chesi<sup>1</sup>, S. Kirchner<sup>3</sup>, and P. Ribeiro<sup>2,1\*</sup>

<sup>1</sup>Beijing Computational Science Research Center, Beijing 100193, China.

<sup>2</sup>CeFEMA, Instituto Superior Técnico, Universidade de Lisboa Av. Rovisco Pais, 1049-001 Lisboa, Portugal.

<sup>3</sup>Zhejiang Institute of Modern Physics, Zhejiang University, Hangzhou, Zhejiang 310027, China.

\*Corresponding Author: Ribeiro.pedro@gmail.com

We study the current-carrying steady-state of a transverse field Ising chain coupled to magnetic thermal reservoirs and obtain the non-equilibrium phase diagram as a function of the magnetization potential of the reservoirs. Upon increasing the magnetization bias we observe a discontinuous jump of the magnetic order parameter that coincides with a divergence of the correlation length. For steady-states with a non-vanishing conductance, the entanglement entropy at zero temperature displays a bias dependent logarithmic correction that violates the area law and differs from the well-known equilibrium case. Our findings show that out-of-equilibrium conditions allow for novel critical phenomena not possible at equilibrium.



**P21 - MODELING OF WOUND CLOSURE IN EPITHELIAL TISSUE**

G. M. Carvalho,<sup>1,2,3,\*</sup> A. S. Nunes,<sup>1,2</sup> L. Carvalho,<sup>4</sup> A. Jacinto,<sup>4</sup> P. Patrício<sup>2,5</sup> and N. A. M. Araújo<sup>1,2</sup>

<sup>1</sup>Departamento de Física, Faculdade de Ciências, Universidade de Lisboa, 1749-016 Lisbon, Portugal.

<sup>2</sup>Centro de Física Teórica e Computacional, Universidade de Lisboa, 1749-016 Lisbon, Portugal.

<sup>3</sup>Instituto Federal de Educação, Ciência e Tecnologia Catarinense, 89283-064 São Bento do Sul, Brazil.

<sup>4</sup>Centro de Estudos de Doenças Crônicas, Faculdade de Ciências Médicas, Universidade NOVA de Lisboa, 1169-056 Lisbon, Portugal.

<sup>5</sup>ISEL - Instituto Superior de Engenharia de Lisboa, Instituto Politécnico de Lisboa, 1959-007 Lisbon, Portugal.

\*Corresponding Author: genilson.carvalho@ifc.edu.br

Wound healing is essential in the recovery of living organisms upon injury [1]. Understanding the mechanisms that underlie wound closure would be beneficial to improve the efficiency and timescale of the process. It is known that intercellular junctions play an important role in the tissue stability and response to mechanical perturbations. In particular, it was shown experimentally that the function of occluding junctions is essential in the healing of the embryonic epithelium of *Drosophila*. The lack of functional occluding junctions affects not only the time of wound closure, but also the maximum area of the wound as cells conform to the tension redistribution after a cut is performed [2]. It has also been proposed that an actomyosin cable formed in the cells around the injured area is partially responsible for the contraction of the tissue that leads to the closure of the wound [3]. Here, we present a model of a two-dimensional tissue, capable of reproducing the healing process. Cells are represented by nodes that interact with neighbors. We consider two mechanisms: the occluding junctions in cell-cell cohesion and the formation of an actomyosin cable around the cut. To model the first, we use elastic elements. For the second, we introduce a second type of elastic elements with a time-dependent spring parameter connecting the cells around the cut, that is related to the timescale for the formation of the cable. We investigate how the evolution of the area of the wound depends on the strength of the interaction of occluding junctions and the timescale of formation of the actomyosin cable and find that the results are compatible with experiments.

### References

- [1] M. Takeo et al., Cold Spring Harbor Perspectives in Medicine, 5, 1 (2015).
- [2] L. Carvalho et al., Journal of Cell Biology, 217, 12 (2018).
- [3] Y. Matsubayashi et al., Journal of Cell Biology, 210, 3 (2015).

## P22 - MUON IMPLANTATION EXPERIMENTS IN SEMICONDUCTOR FILMS: CHARACTERIZATION OF DEPTH RESOLUTION

A. F. A. Simões,<sup>1,\*</sup> H. V. Alberto,<sup>1</sup> R. C. Vilão<sup>1</sup>, J. M. Gil<sup>1</sup>, A. Weidinger<sup>2</sup>, P. M. P. Salomé<sup>3,4</sup>, P. A. Fernandes<sup>3,4,5</sup>, T. Prokscha<sup>7</sup>, A. Suter<sup>7</sup> and Z. Salman<sup>7</sup>.

<sup>1</sup>CFisUC, Department of Physics, University of Coimbra, Coimbra, Portugal.

<sup>2</sup>Helmholtz-Zentrum Berlin für Materialien und Energie, Berlin, Germany.

<sup>3</sup>I3N and Department of Physics, University of Aveiro, Portugal.

<sup>4</sup>International Iberian Nanotechnology Laboratory, Braga, Portugal.

<sup>5</sup>CIETI and Department of Physics, Instituto Superior de Engenharia do Porto, Porto, Portugal.

<sup>6</sup>Ångström Laboratory, Ångström Solar Center, Uppsala University, Uppsala, Sweden.

<sup>7</sup>Laboratory for Muon Spin Spectroscopy, Paul Scherrer Institut, Villigen, Switzerland.

\*Corresponding Author: afa.simoes96@gmail.com

Muon spin spectroscopy using slow muons is an extremely useful tool for probing the surfaces of solids and depth-resolved properties [1-3]. In the experiments the muons are generated in the target of an accelerator with a kinetic energy of 4 MeV. In order to probe the surfaces and interfaces of solids, they are subsequently moderated and accelerated towards the sample with kinetic energies in the range 3-25 keV. The average muon stopping depth (typically in the order of tens of nanometers) is a function of the muon implantation energy and of the density of the material, but the stopping range extends over a broad region (also in the order of tens of nanometers). Therefore, a simulation procedure is required in order to extract the depth-dependence of the experimental parameters. In this poster we will present the method used to extract depth-resolved information from the dependence of the experimental parameters with implantation energy.

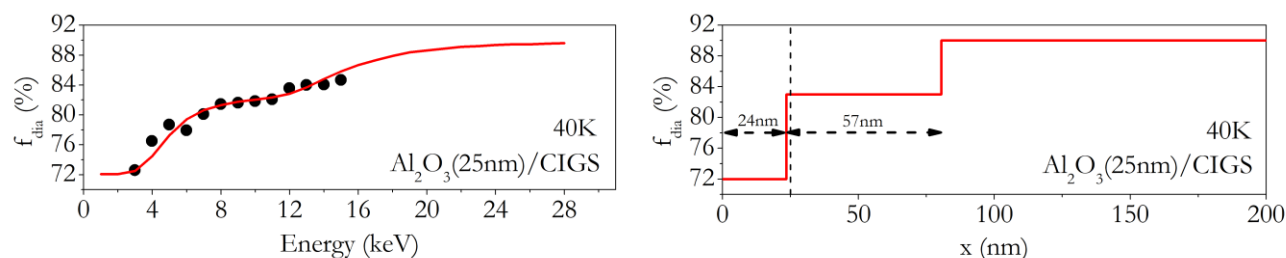


Figure 1. **Left** : Diamagnetic fraction as a function of muon implantation energy,  $f_{dia}(E)$  at 40 K. The red curve is the predicted behaviour of  $f_{dia}(E)$  assuming a depth dependence of the fraction,  $f_{dia}(x)$ , as shown in the corresponding graph at **right**.

### References

- [1] E. Morenzoni et al., *J. Phys.: Condens. Matter*, 16, S4583 (2004)
- [2] F. Al Ma'Mari et al., *Nature*, 524, 69 (2015)
- [3] H. V. Alberto et al., *Phys. Rev. Materials*, 2, 025402 (2018)

P23 -  $\text{Na}_2\text{Ti}_3\text{O}_7$  NANOTUBES BY HYDROTHERMAL METHOD

F. X. Nobre,<sup>1,3\*</sup> A. Almedia,<sup>3</sup> P. B. Tavares,<sup>5</sup> J. Agostinho Moreira,<sup>3</sup> R. S. da Silva,<sup>4</sup> Y. L. Ruiz,<sup>2</sup> W. R. Brito<sup>1</sup> and P. R. C. Couceiro<sup>1</sup>

<sup>1</sup>Department of chemistry, Federal University of Amazon, Octávio Hamilton Botelho Mourão, Manaus, Brazil.

<sup>2</sup>Department of Materials Engine., UFAM, Octávio Hamilton Botelho Mourão, Manaus, Brazil.

<sup>3</sup>Department of Physis and Astronomy, FCUP, Campo Alegre, Porto, Portugal.

<sup>4</sup>Departament of Physis, UFS, AV. Marechal Rondon, Sergipe, Brazil.

<sup>5</sup>Department of Chemistry, UTAD, Quinta de Prados, Vila Real, Portugal.

\*Corresponding Author: xavier.nobre.ufpi@gmail.com

The development of energy storage devices has intensified studies related to the procurement and application of semiconductors [1]. In this context, sodium titanate polymorphs are considered promising in the manufacture of solid state batteries [2]. In this study sodium titanate nanotubes (nTiNa) were synthesized using the phase mixture (anatase and brookite), previously obtained using the sol-gel method at 65 °C for 6h, as synthesis pretreatments using the hydrothermal method (pH = 11) at 160 °C for 72 h. The obtained materials were washed several times with distilled water and dried at 100 °C for 12 h. The synthesized sodium titanate nanotubes were characterized structurally by X-ray diffraction (XRD), Raman vibration microscopy and Transmission electron microscopy (TEM). In parts of Figure 1 the diffraction pattern (Fig. 1a) and the images obtained by TEM (Fig. 1b) for the nanotubes are presented.

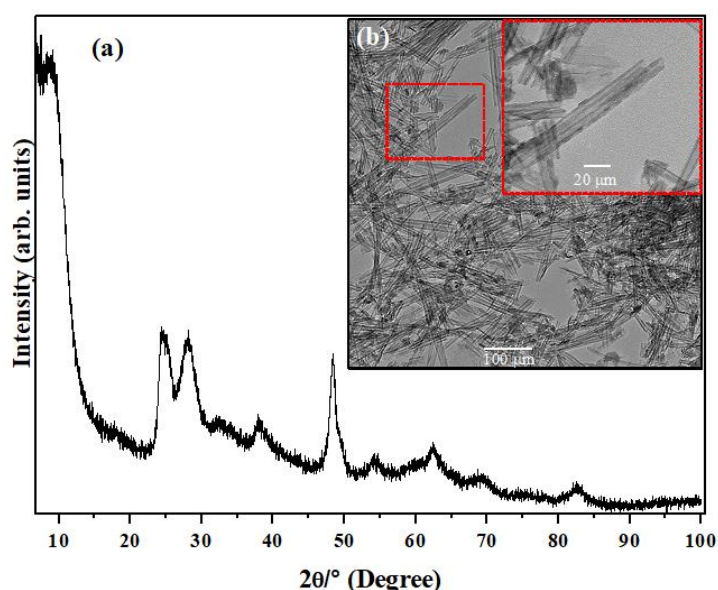


Figure 1. (a) XRD pattern and (b) TEM image of nTiNa.

After the crystallographic indexation of all peaks present in the XRD pattern for sodium titanates synthesized were confirmed the monoclinic phase (JCPDS no. 72-0148) with the formula  $\text{Na}_2\text{Ti}_3\text{O}_7$  [1]. The profile and intensity of the diffraction peaks suggest a tubular structure for material with nanometric dimensions with tube-like morphology. In Figure 1(b) shows the TEM images, thus confirm the information presented in the X-ray diffraction analysis [2]. As also, it can possible to verify nanotubes with an average length of 115 nm and an average width of 12 nm.

#### References

- [1] P. Slamep, W.B. Widayatno, A. Subhan, B.Prihandoko, *Materials Science and Engineering*, 432, 1-5 (2018).
- [2] A. Rudola, K. Saravanan, C.W. Mason, P. Balaya, *J. Mater. Chem. A*, 1, 2653-2662 (2013).

## P24 - NONLINEAR OPTICAL CONDUCTIVITY OF GRAPHENE IN THE INDEPENDENT ELECTRON APPROXIMATION

D. J. Passos,<sup>\*</sup> G. B. Ventura, J. M. Viana Parente Lopes and J. M. B. Lopes dos Santos

<sup>1</sup>Centro de Física do Porto, Universidade do Porto, 4169-007, Portugal.

<sup>\*</sup>Corresponding Author: passos.djs@gmail.com

There has been a recent surge of interest on the nonlinear optical properties of monolayer graphene since it was realised that its unique linear dispersion near the Dirac points led to high optical susceptibilities or conductivities. These conductivities show resonant behavior near frequencies which match the “effective gap” set by the chemical potential[1]. When considering the tunability of the chemical potential in graphene by an applied voltage or chemical doping, one sees a great potential on the use of graphene on optical devices[1]. Bilayer graphene shows a similar promise with recent work showing the existence of strong optical nonlinearities[2] and with the added tunability of the band gap, a feature unique to bilayer graphene [3]. In this talk, we will address the spectrum of the linear and nonlinear optical conductivity monolayer and bilayer graphene, within the independent electron approximation, using numerical and analytical tools that our group recently developed [4,5].

### References

- [1] J. L. Cheng, N. Vermeulen, and J. E. Sipe, *New Journal of Physics*, 16, 053014, (2014)
- [2] Wu, S., Mao, L., Jones, A. M., Yao, W., Zhang, C., & Xu, X., *Nano letters*, 12(4), 2032-2036, (2012)
- [3] Eduardo V Castro, KS Novoselov, SV Morozov, NMR Peres, JMB Lopes Dos Santos, Johan Nilsson, F Guinea, AK Geim, and AH Castro Neto, *Physical Review Letters*, 99(21):216802, (2007)
- [4] G. B. Ventura, D. J. Passos, J. M. B. Lopes dos Santos, J. M. Viana Parente Lopes, and N. M. R. Peres, *Physical Review B*, 96, 035431, (2017)
- [5] D. J. Passos, G. B. Ventura, J. M. V. P. Lopes, J. M. B. L. dos Santos, and N. M. R. Peres, *Physical Review B*, 97, 235446, (2018)

## P25 - THE KERNEL POLYNOMIAL APPROXIMATIONS OF THE THOULESS FORMULA

N.A. Khan,\* J.P. Santos Pires, J.M. Viana Parente Lopes, and J.M.B. Lopes dos Santos

Centro de Física das Universidades do Minho e Porto,  
Departamento de Física e Astronomia, Faculdade de Ciências,  
Universidade do Porto, 4169-007 Porto, Portugal

\*Corresponding Author: nak@fc.up.pt

We report the kernel polynomial approximations of the localization length for a onedimensional non-interacting electronic system with different models of disorder at zero temperature. In particular, we implement the **Kernel Polynomial Method (KPM)** [1] for the simulations of the famous Thouless formula [2], which has an  $O(L)$  computational complexity, where  $L$  is the linear size of the system. In the context of tight-binding Anderson model, we find an excellent agreement with the perturbative result [3] in the limit of large system, confirming the validity of the kernel polynomial procedure.

Our main purpose is to investigate the disorder induced metal-insulator transition in a non-interacting tight-binding system with power-law correlated disorder model (de Moura-Lyra Model [4]). The KPM estimates of the localization length diverge as  $(1 - \alpha)^{-1}$ , indicating the delocalization transitions at  $\alpha = 1$ , where  $\alpha$  is the correlation exponent of the spectral density. In addition, we confirm our numerical results by comparing with the perturbative result [4].

#### References

- [1] A. Weibe, G. Wellein, A. Alvermann, and H. Fehske. Rev. Mod. Phys., 78:275, 306,(2006).
- [2] D J Thouless. Journal of Physics C: Solid State Physics, 5(1):77, (1972).
- [3] F. M. Izrailev and A. A. Krokhin, Phys. Rev. Lett. 82, 4062 (1999).
- [4] J.P. Santos Pires, N.A. Khan, J.M. Viana Parente Lopes, and J.M.B. Lopes dos Santos  
arXiv:1903.02335v3.

## P26 - NON-LINEAR OPTICAL RESPONSE OF HEXAGONAL BORON NITRIDE WITH A MAGNETIC FIELD

J.C.C. Guerra\*, S.M. João, J.M.V.P. Lopes

Centro de Física das Universidades do Minho e do Porto and Departamento de Física e Astronomia, Faculdade de Ciências, Universidade do Porto, Rua do Campo Alegre, 4169-007 Porto, Portugal.

\*Corresponding Author: up201204726@fc.up.pt

The study of the optical properties of 2D crystals, both linear and non-linear, has been subject of much attention as of late. This is mainly due to the vast array of phenomena that arise in these materials, especially in graphene, such as high non-linear optical conductivity [1-4], four-wave mixing [1,2,5], Faraday rotation [6,7,8], third harmonic generation [2,3], Kerr effects [2,3], fractional quantum Hall effect and magnetoplasmons [6,9]. In this work, we calculate numerically the linear and second-order conductivity of the hexagonal Boron Nitride (h-BN) in a magnetic field and compare these results with analytical expressions obtained using the Dirac approximation [11]. Furthermore, we also discuss the problem of the constraints on a magnetic field in a system with periodic boundary conditions. The numerical calculation of the conductivity of h-BN is done using the expressions obtained in [10], which, by taking into account all the bands in the first Brillouin Zone, give us accurate results. These calculations are carried out by the KITE software [12]. For the linear conductivity, we observe the peaks that correspond to transitions between Landau Levels, as expected by the analytical expression [11]. However, for the second-order conductivity, the analytical expression yields zero, which clearly differs from the obtained results. This means that the Dirac approximation isn't enough to describe the second-order conductivity of the h-BN.

### References

- [1] X. Yao and A. Belyanin, Giant optical nonlinearity of graphene in a strong magnetic field, *Physical Review Letters*, 2012
- [2] Cheng, J. L. Guo, C., Nonlinear magneto-optic effects in doped graphene and in gapped graphene: A perturbative treatment, *Physical Review B*, 2018
- [3] Cheng, J. L. Vermeulen, N. Sipe, J. E.; Third order optical nonlinearity of graphene; *New Journal of Physics*; 2014
- [4] M. Tahir, K. Sabeeh, Gap opening in the zeroth Landau level in gapped graphene: Pseudo-Zeeman splitting in an angular magnetic field, *Journal of Physics: Condensed Matter* (2012)
- [5] König-Otto, Jacob C.; Wang, Yongrui; Belyanin, Alexey; Berger, Claire De; Heer, Walter A.; Orlita, Milan; Pashkin, Alexej; Schneider, Harald; Helm, Manfred; Winnerl, Stephan; Four-Wave Mixing in Landau-Quantized Graphene, *Nano Letters*, 2017
- [6] Bludov, Yu V.; Vasilevskiy, M. I.; Peres, N. M.R.; Magnetic field assisted transmission of THz waves through a graphene layer combined with a periodically perforated metallic film, *Physical Review B*, 2018
- [7] Yumoto, Go; Matsunaga, Ryusuke; Hibino, Hiroki; Shimano, Ryo; Ultrafast Terahertz Nonlinear Optics of Landau Level Transitions in a Monolayer Graphene, *Physical Review Letters*, 2018
- [8] Crassee, Iris Levallois, Julien Walter, Andrew L. Ostler, Markus Bostwick, Aaron Rotenberg, Eli Seyller, Thomas van der Marel, Dirk Kuzmenko, Alexey B.; Giant Faraday rotation in single- and multilayer graphene; *Nature Physics*; 2010
- [9] Moradi, Afshin; Energy density and energy flow of surface waves in a strongly magnetized graphene; *Journal of Applied Physics*; 2018
- [10] S.M. João, J.M.V.P. Lopes, Non-linear optical response of non-interacting systems with spectral methods (arXiv:1810.0373)
- [11] J.C.C. Guerra, Magneto-Optical Properties of 2-Dimensional Lattices, Master Thesis (2018)
- [12] J.V. Lopes, S.M. João, A. Ferreira, L. Covaci, M. Andelkovic, and T. Rappoport. 2018. Quantum KITE. Website: <https://quantum-kite.com/>

## P27 - NON-STEADY FLOWS IN POROUS MEDIA

A.F.V. Matias,<sup>1,2,\*</sup> R.C.V. Coelho,<sup>1,2</sup> and N.A.M. Araújo<sup>1,2</sup><sup>1</sup>Departamento de Física, Faculdade de Ciências, Universidade de Lisboa, 1749-016 Lisbon, Portugal.<sup>2</sup>Centro de Física Teórica e Computacional, Universidade de Lisboa, 1749-016 Lisbon, Portugal\*Corresponding Author: [afmatias@fc.ul.pt](mailto:afmatias@fc.ul.pt)

In many natural and technological processes, ranging from oil to coffee extraction, groundwater transport, and filtering, a fluid flows through an intricate network of channels (porous medium) that significantly constrains the fluid dynamics [Coelho, 2016; Giro, 2017]. The fluid/structure interaction may lead to erosion, deposition, and fracturing, triggering instabilities (e.g. clogging and cavitation) which in turn feedback in the flow [Jäger, 2017; Sampaio Filho, 2016]. In particular, during coffee extraction there are three critical mechanisms: **i)** swelling [Mateus, 2007], **ii)** erosion and deposition, and **iii)** transport of suspended particles [Jäger, 2018]. We perform numerical simulations using the Lattice Boltzmann method to study the impact of swelling on the instantaneous flux and on the permeability. For a regular BCC lattice of particles, we determine that the permeability of the medium decreases with time due to particle swelling, as seen in Fig. 1. This behavior agrees with experimental observations [Corrochano, 2015] and analytical calculations [Pan, 2006]. We also study the impact of particle shape and configuration. These results improve our understanding on flows through non-static porous media like in the coffee extraction process.

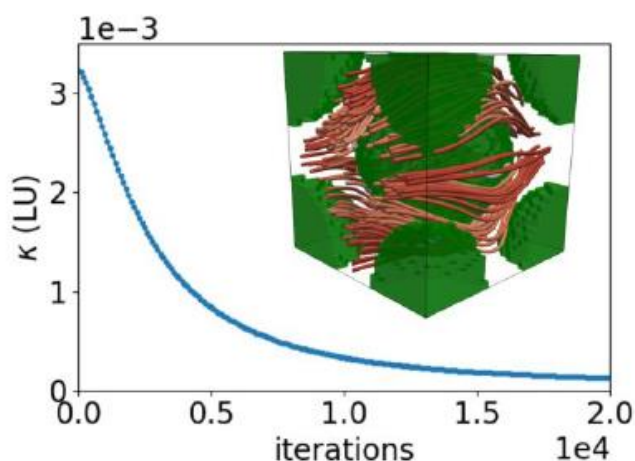


Figure 1. Plot of the permeability, in lattice units, as function of number of iterations. The flow (red tubes) around the particles (in green) is represented on the inset. The particles are arranged in a BCC lattice and their volume increases due to swelling with the number of iterations.

### References

- [Coelho, 2016] R.C.V. Coelho, and R.F. Neumann, *European Journal of Physics* **37**, 055102 (2016).  
 [Corrochano, 2015] B.R. Corrochano, J.R. Melrose, A.C. Bentley, P.J. Fryer, S. Bakalis, *Journal of Food Engineering* **150**, 106-116 (2015).  
 [Giro, 2017] R. Giro, P.W. Bryant, M. Engel, R.F. Neumann, and M.B. Steiner, *Scientific Reports* **7**, 46317 (2017).  
 [Jäger, 2017] R. Jäger, M. Mendoza, and H.J. Herrmann, *Physical Review Letters* **119**, 124501 (2017).  
 [Jäger, 2018] R. Jäger, M. Mendoza, and H.J. Herrmann, *Physical Review Fluids* **3**, 074302 (2018).  
 [Mateus, 2007] M.L. Mateus, M. Rouvet, J.C. Gummy, and R. Liardon, *Journal of Agricultural and Food Chemistry* **55**, 2979 (2007).  
 [Pan, 2006] C. Pan, L.S. Luo, C.T. Miller, *Computers & Fluids* **35**, 898-909 (2006).  
 [Sampaio Filho, 2016] C.I.N. Sampaio Filho, A.A. Moreira, N.A.M. Araújo, J.S. Andrade Jr, and H.J. Herrmann, *Physical Review Letters* **117**, 275702 (2016).



## P28 - NUMERICAL SIMULATION OF NON-EQUILIBRIUM STATIONARY CURRENT THROUGH NANO-SCALE 1D CHAINS

J. P. Santos Pires,<sup>1,\*</sup> B. Amorim,<sup>2</sup> and J. M. Viana Parente Lopes<sup>1</sup>

<sup>1</sup>Centro de Física das Universidades do Minho e Porto, Universidade do Porto, Porto, Portugal

<sup>2</sup>CeFEMA, Instituto Superior Técnico, Universidade de Lisboa, Lisboa, Portugal

\*Corresponding Author: up201201453@fc.up.pt

Calculating the DC electric conductivity of a quantum system is an important issue in Condensed Matter Physics. Commonly, the steady-state current is calculated using the Kubo Formula for linear response [1]. For infinite systems there is generally a well-defined steady-state regime, while for finite systems a phenomenological relaxation must be introduced in order to reach such state. However, for nanoscale systems, a different approach, called Landauer-Büttiker [2,3] is usually taken, where the sample is put into contact with two perfectly conducting leads. These leads act as particle reservoirs with different values of the chemical potential, mimicking a difference of electric potential between the contacts. In this approach, there is no need of any relaxation mechanism, even the system being small, since the infinite leads provide the continuum spectrum needed for a steady-state DC response. But how crucial are the infinite leads? Addressing this question is the main purpose of this work. In this work, we explore the possibility of observing a stationary electric current traversing a small one-dimensional chain coupled to perfectly conducting finite leads [4,5], by propagating in time all of the initially occupied electron states. The model we study is a nearest-neighbor tight-binding chain with open boundaries, where the sample stands for the few sites in the middle section shown in red (which may hold an on-site disordered potential as well). We considered two initial conditions for the system: **1)** The system is initially in thermodynamic equilibrium, with states filled up to  $E_F = 0$ , and a ramp-like electrostatic potential is turned-on at  $t = 0$  – the non-partitioned setup; **2)** The system is tripartite with the potential ramp is in place, and at  $t = 0$  the boundary hoppings are connected – the partitioned setup. We implemented an efficient algorithm [6] to time-evolve the occupied electron state for both setups and measured the instantaneous current crossing the central bond of the sample.

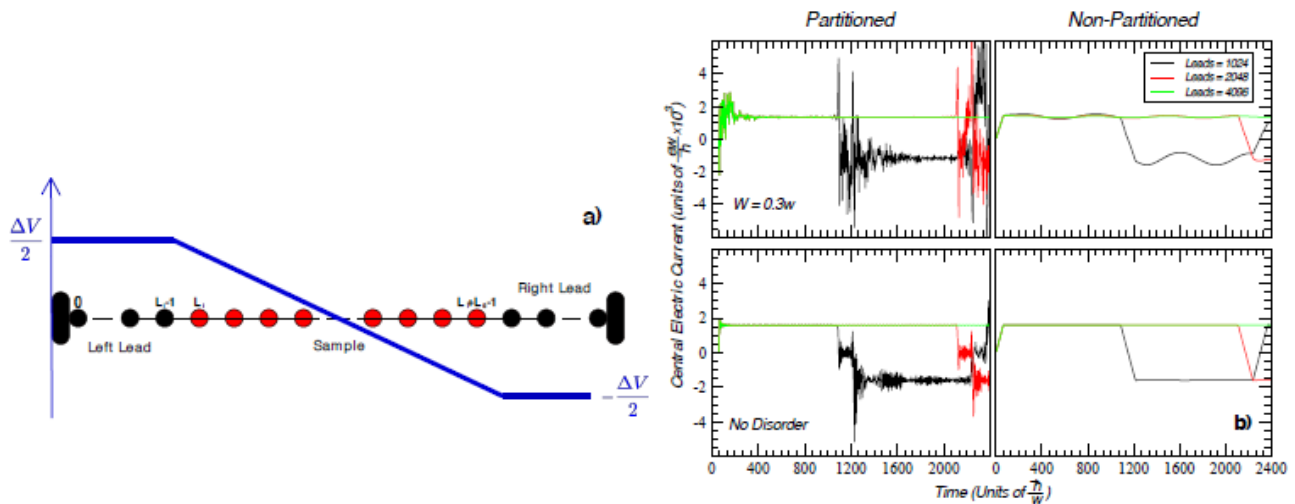


Figure 1. **a)** Scheme of the system including the profile of the applied electrostatic potential; **b)** Electric current crossing the center of the sample, as a function of time and for different sizes of the leads. The left panels correspond to the partitioned setup and the right panels to the non-partitioned case. The sample length was 256 sites and  $\Delta V = 0.01$  (in units of the hopping).

The main conclusion is that in both setups, we obtain the same stationary current across the sample for times that are large enough for transients to die away, but small when compared to the time of the first-reflection on the boundaries (we call this the Quasi-Stationary Transport Scale - QSTS). This time scale is

shown to be proportional to the size of the leads, or equivalently to the level-spacing of the lead's spectrum. Moreover, the finite size of the leads also give rise to further minor finite-size effects on the QSTS, which show up as oscillations with an amplitude decreasing with the lead's size. These effects are inexistent or very small, if the sample is ordered. As a conclusion, we show that the non-equilibrium current achieved with both approaches is the same and has the value given by the Landauer Formalism, apart from the observed finite-size effects. These results agree with the published work of Stefanucci et al [7].

**References**

- [1] R. Kubo, J. Phys. Soc. Jpn. 12, 570-586 (1957).
- [2] R. Landauer, Phil. Mag. 21, 863 (1970).
- [3] A.-P. Jauho, N. S. Wingreen, and Y. Meir, Phys. Rev. B 50, 5528 (1994).
- [4] P. P. Pal, S. Ramakrishna, T. Seideman, J. Chem. Phys. 148, 144707 (2018).
- [5] B. S. Popescu, A. Croy, Phys. Rev. B 95, 235433 (2017).
- [6] H. Tal-Ezer and R. Kosloff, J. Chem. Phys. 81, 3967 (1984).
- [7] G. Stefanucci, C.-O. Almbladh, Phys. Rev. B 69 195318 (2004).

**P29 - PERTURBED ANGULAR CORRELATION STUDIES ON FERROELECTRIC  $\text{Ca}_3\text{Ti}_2\text{O}_7$** 

Tiago Leal<sup>1</sup>, Pedro Rocha-Rodrigues<sup>1</sup>, Ricardo Moreira<sup>1</sup>, Gonalo N. P. Oliveira<sup>1</sup>, Joo G. Correia<sup>2</sup>, Armandina M. L. Lopes<sup>1</sup>, Joo P. Araujo<sup>1</sup>

<sup>1</sup>IFIMUP and IN—Institute of Nanoscience and Nanotechnology, Departamento de Fsica e Astronomia da Faculdade de Cincias da Universidade do Porto, Rua do Campo Alegre, 687, Porto 4769-007, Portugal.

<sup>2</sup> C2TN, Centro de Cincias e Tecnologias Nucleares, Instituto Superior Tcnico, Universidade de Lisboa, Estrada Nacional 10, 2695-066 Bobadela LRS, Portugal.

E-mail de contacto: tiagoleal06@gmail.com

A key issue in materials science is the search for new multifunctional materials that fulfil the goal of miniaturization and increased efficiency [1,2]. The discovery of improper ferroelectricity [3] in artificial superlattices of  $\text{SrTiO}_3\text{:PbTiO}_3$  unveiled an approach to design novel ferroelectric materials which lead to an increasing curiosity on similar naturally layered perovskites Ruddlesden-Popper (R.P.) phases. The outstanding physical properties in these systems arises from its the lattice distortions. In this work, we find  $\text{Ca}_3\text{Ti}_2\text{O}_7$ , a member of the (RP) series  $\text{A}_{n+1}\text{B}_n\text{O}_{3n+1}$ , with  $n=2$ , having a predicted tetragonal  $I4/mmm$  structure at higher temperatures that undergoes a structural transition to a orthorhombic structure  $A2_1am$  at about  $\sim 1035\text{K}$  [4]. In this work we present a  $\text{Ca}_3\text{Ti}_2\text{O}_7$  hyperfine characterization using perturbed angular correlation (PAC) spectroscopy. This local characterization was performed in an extensive range of temperatures from 10K to 1220K. The structure analysis is possible using the hyperfine characterization technique, perturbed angular correlation (PAC) spectroscopy. Here, the use of a local probe enables us to follow octahedral distortions of the R.P. series, namely the tilt and rotation mechanisms responsible for the establishing of the room temperature polar structure. Information on local lattice properties can be extracted by studying the electric field gradient (EFG) tensor. The EFG in the vicinity of the probe atom, which is due to the local charge distribution, allows reconstructing the atomic and electronic environment of the atomic probe in the material. This information can assist in the study of the system phase transitions. Our local probe latest results will be presented and discussed.

#### References

- [1]. N. A. Benedek, J. M. Rondinelli, H. Djani, P. Ghosez, and P. Lightfoot, "Understanding ferroelectricity in layered perovskites: New ideas and insights from theory and experiments", *Dalton Trans.*, **44**, 10543-10558 (2015).
- [2] A. B. Harris, "Symmetry analysis for the Ruddlesden-Popper systems  $\text{Ca}_3\text{Mn}_2\text{O}_7$  and  $\text{Ca}_3\text{Ti}_2\text{O}_7$ ", *Phys. Rev. B*, **84**, 064116 (2011).
- [3] Bousquet E, Dawber M, Stucki N, Lichtensteiger C, Hermet P, Gariglio S, Triscone JM, Ghosez P. "Improper ferroelectricity in perovskite oxide artificial superlattices", *Nature* (2008) Apr 10;452(7188):732-6.
- [4] B. Gao, F. Huang, Y. Wang, J. Kim, L. Wang, S. Lim, and S. Cheong, "Interrelation between domain structures and polarization switching in hybrid improper ferroelectric  $\text{Ca}_3(\text{Mn,Ti})_2\text{O}_7$ " *Applied Physics Letters*, **110**, 222906 (2017).

**P30 - PERTURBED ANGULAR CORRELATION STUDY OF  $\text{SRMNGe}_2\text{O}_6$  AND  $\text{CAMNGe}_2\text{O}_6$** 

Ricardo Moreira<sup>1</sup>, Tiago Leal<sup>1</sup>, Pedro Rocha-Rodrigues<sup>1</sup>, Gonalo N. P. Oliveira<sup>1</sup>, Lei Ding<sup>6</sup>, Claire V. Colin<sup>4,5</sup>, Céline Darie<sup>4,5</sup>, Céline Goujon<sup>5</sup>, Murielle Legendre<sup>5</sup>, J. G. Correia<sup>2,3</sup>, João P. Araújo<sup>1</sup>, Armandina M.L. Lopes<sup>1</sup>

<sup>1</sup>IFIMUP and IN—Institute of Nanoscience and Nanotechnology, Departamento de Física e Astronomia da Faculdade de Ciências da Universidade do Porto, Rua do Campo Alegre, S/N, Porto 4169-007, Portugal.

<sup>2</sup>CERN EP, CH 1211 Geneva 23, Switzerland

<sup>3</sup>C2TN, Centro de Ciências e Tecnologias Nucleares, Instituto Superior Técnico, Universidade de Lisboa, Estrada Nacional 10, 2695-066 Bobadela LRS, Portugal

<sup>4</sup>Univ. Grenoble Alpes, Inst NEEL, F-38042 Grenoble, France

<sup>5</sup>CNRS, Inst NEEL, F-38042 Grenoble, France

<sup>6</sup>ISIS Pulsed Neutron Facility, Rutherford Appleton Laboratory, Harwell Oxford, Didcot OX11 0QX, UK

*\* Corresponding author: up201202493@fc.up.pt*

Multiferroic materials have been under the spotlight due to their fundamental scientific interest and for potential applications in technology. Among these interesting materials are the group of compounds belonging to the Pyroxene family with general chemical formula  $\text{AM}(\text{Si,Ge})_2\text{O}_6$ . More specifically,  $\text{SrMnGe}_2\text{O}_6$  and  $\text{CaMnGe}_2\text{O}_6$  are isostructural, crystallizing with monoclinic C2/c symmetry and are characterized by zigzag chains of  $\text{MnO}_6$  octahedra linked by edge-sharing, separated by  $\text{GeO}_4$  tetrahedra chains along the same axis, linked by corner-sharing. Due to this arrangement these systems present a rich diversity of low-dimensional magnetic properties. The existence and possible interplay of low dimensionality and magnetic frustration results in multiferroic and/or magnetoelectric properties.

Since these properties might arise from local structural features that are not well described by methods based on long-range average structural models, the use of local probe studies is essential. In this context, hyperfine methods, such as perturbed angular correlation (PAC) spectroscopy where the study of the electric field gradient (EFG) in the vicinity of a probe atom, allows reconstructing of the atomic and electronic environment of the probe in the material, helps to clarify the origin of the properties exhibited in these systems. In this work a temperature dependent EFG study will be presented and discussed, guided by EFG simulation results using ab-initio Wien2k, attempting to clarify the experimental observation of two different local environment for in  $\text{SrMnGe}_2\text{O}_6$ , as opposed to only one in  $\text{CaMnGe}_2\text{O}_6$ .

**P31 - PHASE SEPARATION OF ACTIVE BROWNIAN SYSTEMS**

P. D. Neta\*, C. S. Dias, N. A. M. Araújo, and M. M. Telo da Gama

Departamento de Física, Faculdade de Ciências, Universidade de Lisboa, P-1749-016 Lisboa, Portugal, and  
Centro de Física Teórica e Computacional, Universidade de Lisboa, P-1749-016 Lisboa, Portugal.

\*Corresponding Author: pedro.neta@alunos.fc.ul.pt

From swarms of unicellular organisms to complex tissues, active matter stuns with its ability to self-organize. Swimming unicellular organisms, such as bacteria, are known to accumulate close to substrates, forming a non-equilibrium growing interface, where scale invariance and universal scaling laws are expected [1]. The morphology of the interface may also affect the system's dynamical response. It is desirable to relate the interfacial morphology to the microscopic dynamical rules. Previous studies suggest that, for a range of activity and density of cells, swarms of swimming cells separate into a dense fluid and a gas phase [1-2]. This phase separation occurs even in the absence of attractive interactions or aligning mechanisms, and the nature of these transitions, known as motility-induced phase transitions (MIPT), is not yet fully understood.

In this work, we simulate one simple model that exhibits MIPT. We perform kinetic Monte Carlo simulations of active particles on a square lattice. We observe phase separation between high- and low-density phases of active particles and compute the coexistence line. We show that this phase separation is dependent on both the activity and the density of particles. When a flat wall is introduced, aggregates of active particles are formed near the wall. We characterized these aggregates and their dependence on the particles activity.

#### References

- [1] J. Bialké et al., *Physical Review Letters*, 115, 098301 (2015).
- [2] C. F. Lee, *Soft Matter*, 13, 376 (2017).

## P32 - PIEZOELECTRIC RESPONSE TAILORING OF $K_{0.5}Na_{0.5}NbO_3$ USING DIFFERENT SINTERING METHODS

M. M. Gomes<sup>1\*</sup>, R. Vilarinho<sup>1</sup>, R. Pinho<sup>2</sup>, A. Almeida<sup>1</sup>, P. Vilarinho<sup>2</sup> and J. Agostinho Moreira<sup>1</sup>

<sup>1</sup>IFIMUP-IN, Institute of Nanoscience and Nanotechnology, Department of Physics and Astronomy of Faculty of Sciences, University of Porto, Portugal

<sup>2</sup>CICECO, Center for Research in Ceramics and Composite Materials, Department of Materials and Ceramic Engineering, University of Aveiro, Portugal

\*up201402744@fc.up.pt

The substitution of lead-based materials is important to assure sustainability. Though lead-based materials have higher piezoelectric values, there are other promising friendly environment compounds, namely  $K_xNa_{(1-x)}NbO_3$ . For  $x=0.5$  (0.5KNN), the high-temperature cubic symmetry changes to a non-symmetric ferroelectric tetragonal structure at  $T_3=693$  K. At  $T_2=491$  K it becomes orthorhombic, stabilizing in a rhombohedral symmetry below  $T_1=165$  K. Recently, theoretical calculations have predicted piezoelectric response enhancement whether  $T_3$  and  $T_2$  become closer. Moreover, it has been suggested that sintering conditions and microstructure can act significantly on the magnitude of that temperature interval. To unravel the effect of sintering conditions in 0.5KNN, ceramics were prepared by conventional sintering (CS), spark plasma sintering (SPS), and spark plasma texturing (SPT). XRD data at room conditions revealed that the two latter methods yield 0.08 and 0.16 GPa of internal stresses, respectively. It is worth emphasizing, that the emergence of these stresses have strong repercussions on the values of the piezoelectric coefficient  $d_{33}$ , increasing from 50 to 125 pC.N<sup>-1</sup> for SPS and SPT samples, respectively.

In this work, we present a detailed, temperature dependent, lattice dynamic study of 0.5KNN ceramics produced by the three methods referred to above, using Raman spectroscopy. For the three types of sintered samples, we have observed clear critical temperature shifts, and specific different modes behaviors at  $T_1$ ,  $T_2$  and  $T_3$ . To corroborate this outcome, the temperature dependence of the polar and dielectric properties of the SPT sample was also studied using pyroelectric current and dielectric techniques. The obtained experimental results will be discussed towards disentangling how the sintering methods tailor the piezoelectric response, in order to provide competitive, lead-free materials.

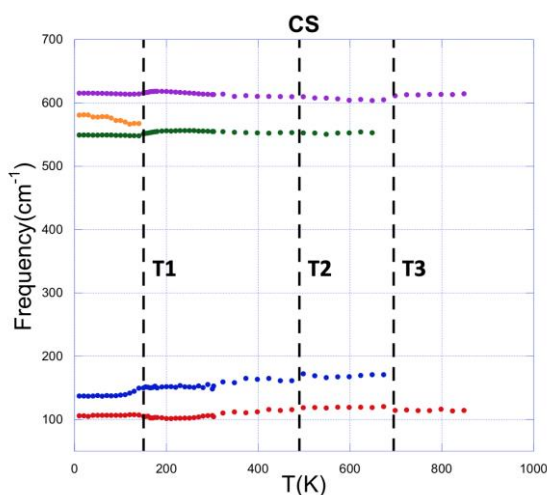


Figure 1. Frequency of representative Raman modes vs temperature for a CS sample

### References

- [1] E. Buixaderas et al, *Ferroelectrics*, 391, 51-57 (2009)
- [2] B. Orayech et al, *J. Appl. Cryst.*, 48, 318-333 (2015)
- [3] R. Pinho et al., *to be submitted*.

### P33 - PROBING THE STRUCTURAL PROPERTIES OF A SOLAR-CELL P-N INTERFACE USING IMPLANTED POSITIVE MUONS

H. V. Alberto,<sup>1,\*</sup> R. C. Vilão<sup>1</sup>, A. F. Simões<sup>1</sup>, J. M. Gil<sup>1</sup>, A. Weidinger<sup>2</sup>, P. M. P. Salomé<sup>3,4</sup>, P. A. Fernandes<sup>3,4,5</sup>, T. Prokscha<sup>7</sup>, A. Suter<sup>7</sup> and Z. Salman<sup>7</sup>

<sup>1</sup>CFisUC, Department of Physics, University of Coimbra, Coimbra, Portugal

<sup>2</sup>Helmholtz-Zentrum Berlin für Materialien und Energie, Berlin, Germany

<sup>3</sup>IN and Department of Physics, University of Aveiro, Portugal

<sup>4</sup>International Iberian Nanotechnology Laboratory, Braga, Portugal

<sup>5</sup>CIETI and Department of Physics, Instituto Superior de Engenharia do Porto, Porto, Portugal

<sup>6</sup>Angström Laboratory, Angström Solar Center, Uppsala University, Uppsala, Sweden

<sup>7</sup>Laboratory for Muon Spin Spectroscopy, Paul Scherrer Institut, Villigen, Switzerland

\*Corresponding Author: lena@fis.uc.pt

It is well known that the performance of a solar cell depends critically on the quality of its p-n interface. Solar cells based on  $\text{Cu}(\text{In}_{1-x}\text{Ga}_x)\text{Se}_2$  (CIGS) semiconductors are a successful technology, with energy conversion efficiency values exceeding 22.8%[1]. However, its defect system and structural properties are quite complex, limiting the available information and modelling of the interface properties. In this work, we describe the use of implanted positive muons as a probe to obtain depth-resolved information in a p-n interface. Experiments are performed in the Low Energy Muon Facility (LEM) at the Paul Scherrer Institut (PSI), Switzerland, where the energy of the incoming positive muons can be controlled in the eV to keV range, adequate to study thin films as a function of implantation depth, in the tens of nanometer scale. The results obtained for different solar cell heterostructures using CIGS as absorber are presented, showing that the muon probe can be used to measure the width of a defect layer formed at the p-n interface [2]. The microscopic origin of the defect layer detected by the muon is discussed.

#### References

- [1] M. A. Green, K. Emery, Y. Hishikawa, W. Warta, E. D. Dunlop, Solar cell efficiency tables (version 48), *Prog. Photovolt: Res. Appl.* 24, 905 (2016).
- [2] H.V. Alberto, R.C. Vilão, R.B.L. Vieira, J.M. Gil, A. Weidinger, M.G. Sousa, J.P. Teixeira, A.F. da Cunha, J.P. Leitão, P.M.P. Salomé, P.A. Fernandes, T.Törndahl, T Prokscha, A. Suter, Z. Salman, *Physical Review Materials* 2, 025402 (2018).



## P34 - SELF-PROPELLED MOTION OF FLEXIBLE PARTICLES THROUGH TORTUOUS CHANNELS

D. P. F. Silva,<sup>1,2\*</sup> R. C. V. Coelho,<sup>1,2</sup> M. M. Telo da Gama,<sup>1,2</sup> and N. A. M. Araújo<sup>1,2</sup>

<sup>1</sup>Centro de Física Teórica e Computacional, Faculdade de Ciências, Universidade de Lisboa, Campo Grande, 1749-016 Lisboa, Portugal

<sup>2</sup>Departamento de Física, Faculdade de Ciências, Universidade de Lisboa, Campo Grande, 1749-016 Lisboa, Portugal

\*Corresponding Author: fc53534@alunos.fc.ul.pt

Active matter consists of particles that can collect energy from their surrounding and convert it into self-propelled motion [1]. Here, we study the motion of active particles through tortuous channels. Previous models of active particles have mostly considered them rigid, with invariant shape and size. However, when the size of the channels is comparable to the size of the particles, shape changes need to be considered. To model that, we develop a numerical two-component fluid model, based on the Lattice Boltzmann method, with short and midrange interactions. In this model, one of the fluids represents the flexible particle and the other the surrounding medium. The self-propelled motion is then modeled as a persistent random walk of one of the fluids. We show that the active particle can self-propel through the channel and that its motion can be rectified by the channel [Fig. 1]. Our results suggest that properties of the flexible particles such as surface tension and viscosity affects its effective velocity across the channel. We also investigate the relation between activity and effective velocity.

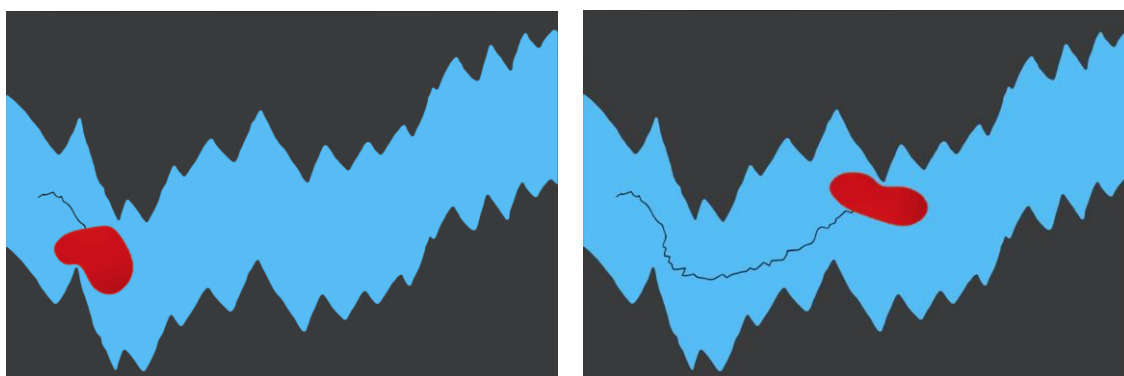


Figure 1. Cell moving through a tortuous path at two different instants of time.

### Reference

[1] Bechinger, C. *et al. Reviews of Modern Physics* 88, 045006 (2016).

## P35 - SIMULATION OF THE FORMATION AND SWELLING OF POLYURETHANE-BASED NANOGELS

V. Lenzi<sup>1,\*</sup> and L. Marques<sup>1</sup>

<sup>1</sup>CFUM-UP, University of Minho, Campus de Gualtar, Braga, Portugal.

\*Corresponding Author: veniero.lenzi@fisica.uminho.pt

Micro- and nanogel beads, ranging from 10 nm to 100  $\mu\text{m}$  in size, constitute an important class of polymer networks. Due to their promising applications[1,2], there is growing interest in understanding the mechanism controlling their properties and formation process[3].

In this work, we show the results of Dissipative Particle Dynamics simulations of the formation process of polyurethane nanogels, obtained from the crosslinking of end-functionalized chains, and their swelling behaviour.

The crosslinking reaction has been modelled using a distance-based algorithm, which includes a reversible dimerization step. Different reaction conditions, such as explicit solvent presence and confinement into a spherical region, have been considered and their impact on the bead's swelling properties and gel's topological properties has been investigated. Explicit solvent simulations have been used to compute the swelling curves, obtained as the radius of gyration of the nanogels in function of the gel-solvent Flory-Huggins interaction parameter.

Our model is capable to reproduce all the observed relevant features of nanogels, and can be used study more complex systems, such as Janus gel nanoparticles, gels obtained from incompatible polymer precursors, interpenetrating networks.

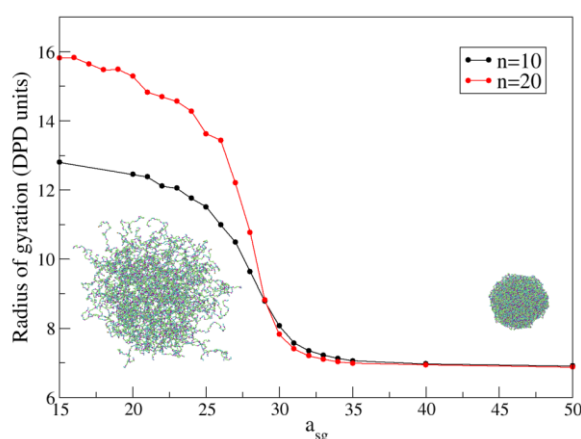


Figure 1: Swelling curves for nanogel beads made from  $n=10$  (black) and  $n=20$  (red), reported as the radius of gyration in function of the Flory-Huggins interaction parameter  $a_{sg}$  between solvent and the gel beads. The quality of the solvent decreases as  $a_{sg}$  increases, and  $a_{sg}=25$  is the theta solvent condition. A representation of the  $n=10$  nanogel in the collapsed and swollen state is also shown.

### References

- [1] P. Grossen et al., *Journal of Controlled Release*, 260:46-60 (2017).
- [2] L. P. Fonseca et al., *International Journal of Pharmaceutics*, 546:106-114 (2018).
- [3] L. Rovigatti et al., *Soft Matter*, 15:1108-1119 (2019).

**P36 - SPECTRAL AND STEADY-STATE PROPERTIES OF RANDOM LIOUVILLIANS**

Lucas Sá,<sup>1,\*</sup> Pedro Ribeiro,<sup>1,2</sup> and Tomaž Prosen<sup>3</sup>

<sup>1</sup>CeFEMA, Instituto Superior Técnico, Universidade de Lisboa Av. Rovisco Pais, 1049-001 Lisboa, Portugal.

<sup>2</sup>Beijing Computational Science Research Center, Beijing 100193, China.

<sup>3</sup>Department of Physics, Faculty of Mathematics and Physics, University of Ljubljana, Ljubljana, Slovenia

\*Corresponding Author: lucas.seara.sa@tecnico.ulisboa.pt

We investigate the properties of generic open quantum systems with Markovian dissipation addressing a class of stochastic Lindblad operators which consists of a random Hamiltonian and a set of independent dissipative channels, acting on the density matrix of the open system.

As a function of the dissipation strength, we find a rich set of regimes regarding global spectral features, the spectral gap, ruling the asymptotic long-time decay, and steady-state properties. Each regime is characterized by finite-size scaling exponents. For two or more dissipation channels, the spectral gap is finite and increases with the system size. The steady-state spectrum is Poissonian distributed at low dissipation strength and resembles that of a random matrix once the dissipation is sufficiently strong. Our results can help understand the long-time dynamics and steady-state properties of generic dissipative systems.

# P37 - SQUARE-ROOT TOPOLOGICAL INSULATORS: AN EXAMPLE USING ULTRACOLD ATOMS

A. M. Marques,<sup>1,\*</sup> G. Pelegrí,<sup>2</sup> R. G. Dias<sup>1</sup>, A. J. Daley<sup>3</sup>, J. Mompart<sup>2</sup> and V. Ahufinger<sup>2</sup>

<sup>1</sup>Department of Physics and I3N, University of Aveiro, 3810-193 Aveiro, Portugal.

<sup>2</sup>Department of Physics, Autonomous University of Barcelona, E-08193 Bellaterra, Spain.

<sup>3</sup>Department of Physics and SUPA, University of Strathclyde, Glasgow G4 0NG, United Kingdom.

\*Corresponding Author: [anselmomagalhaes@ua.pt](mailto:anselmomagalhaes@ua.pt)

We study the single-particle properties of a system formed by ultracold atoms loaded into the manifold of  $l=1$  Orbital Angular Momentum (OAM) states of an optical lattice with a diamond chain geometry, depicted in Fig. 1 [1,2]. The OAM degree of freedom induces a complex phase in some tunneling amplitudes of the tight-binding model that translates as an intrinsic magnetic flux through the plaquettes, leading to the appearance of topological edge states and to Aharonov-Bohm caging when there is a  $\pi$ -flux threading each plaquette, where all energy bands are flat. This model is shown to constitute an example of the recently discovered class of Square-Root Topological Insulators [3,4].

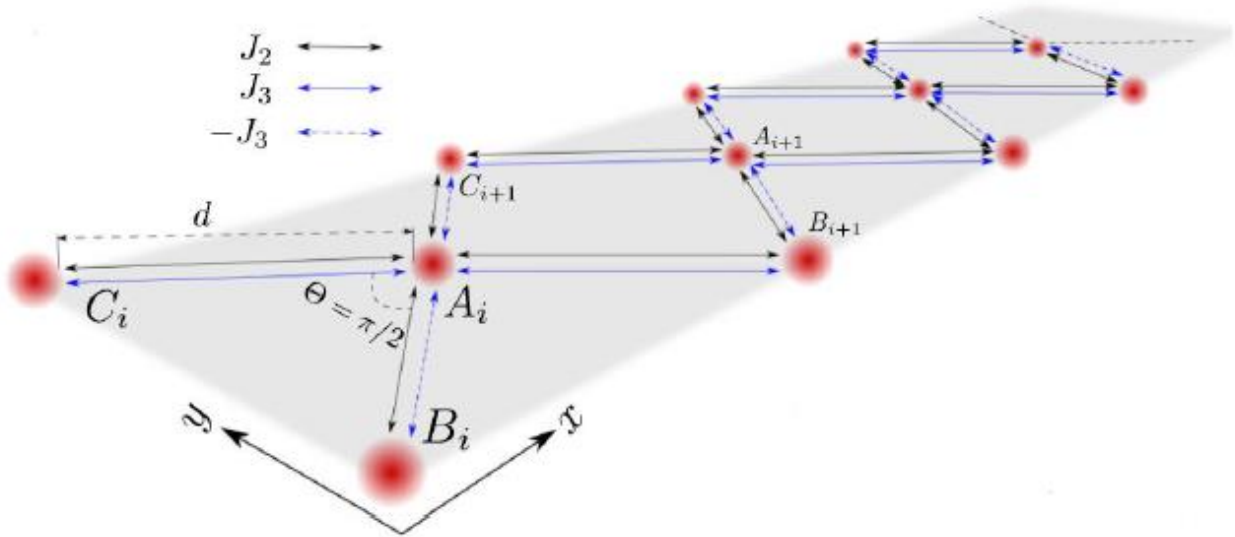


Figure 1. Schematic representation of the diamond chain with two states per site, corresponding to the symmetric winding numbers  $n=\pm 1$  of the excited  $l=1$  OAM. (From [1]).

## References

- [1] G. Pelegrí, A. M. Marques, R. G. Dias, A. J. Daley, J. Mompart, V. Ahufinger, *Phys. Rev. A*, 99, 023613 (2019).
- [2] G. Pelegrí, A. M. Marques, R. G. Dias, A. J. Daley, J. Mompart, V. Ahufinger, *Phys. Rev. A*, 99, 023612 (2019).
- [3] J. Arkinstall *et al.*, *Phys. Rev. B*, 95, 165109 (2017).
- [4] M. Kremer *et al.*, *arXiv pre-prints*, *arXiv:1805.05209* (2018).

# P38 - STRUCTURAL AND MAGNETIC PROPERTIES OF CA AND MN CO-SUBSTITUTED MULTIFERROIC BIFEO<sub>3</sub> NEAR THE MPB REGION

B. Manjunath,<sup>1,2\*</sup> P. A. Joy,<sup>2</sup> and J. Agostinho Moreira<sup>2</sup>

<sup>1</sup>Physical and Materials Chemistry Division, CSIR-National Chemical Laboratory, Pune -411008, India

<sup>2</sup>IFIMUP-IN, Institute of Nanoscience and Nanotechnology, Department of Physics and Astronomy of Faculty of Sciences, University of Porto, Portugal

\*mbalagopalan@fc.up.pt

Magnetoelectrics, due to their coupled magnetic and electric order parameters, have potential applications in the areas of data storage, sensors and actuators, etc. There are very few room temperature magnetoelectrics, and BiFeO<sub>3</sub> (BFO) belongs to this category. Though BFO can show high ferroelectric properties, due to the poor magnetic parameters, the magnetoelectric coupling is very low. To improve the magnetoelectric properties, magnetic properties of BiFeO<sub>3</sub> need to be improved. Pure BFO has very low magnetoelectricity because of its antiferromagnetic character and the spiral spin cycloidal structure with an incommensurate wavelength of 63 nm. BFO nanoparticles with particle size below 63 nm show ferromagnetic behaviour which results in enhanced magnetoelectric properties. Similarly, substitution at the Bi site or Fe site has been reported to show improved magnetic and electric properties due to the suppression of spin periodicity. There are reports on the divalent alkaline earth metal substitution at Bi site which shows enhanced magnetic properties [1,2]. In this work, we report studies on the structural and magnetic properties of Ca and Mn simultaneously substituted at the Bi and Fe sites, respectively, in the multiferroic oxide BiFeO<sub>3</sub>.

Compounds with the formula Bi<sub>1-x</sub>Ca<sub>x</sub>Fe<sub>1-x</sub>Mn<sub>x</sub>O<sub>3</sub> with 0 ≤ x ≤ 0.4 were prepared by the solid-state reaction method by taking stoichiometric amounts of Bi<sub>2</sub>O<sub>3</sub>, Fe<sub>2</sub>O<sub>3</sub>, Mn<sub>2</sub>O<sub>3</sub> and CaCO<sub>3</sub>. Powder X-ray diffraction studies showed that compounds with x ≤ 0.1 have a rhombohedral structure (*R3c*) and compounds with x > 0.2 are orthorhombic (*Pbnm*), and the in-between compositions show a mixed phase of *R3c* and *Pbnm*. The magnetization of the samples increased with increasing the percentage of co-substitution, showing a maximum remanence and coercivity at the MPB region, x = 0.175 as shown in figure 1. Dielectric properties showed a maximum at x = 0.15 and magnetodielectric data showed a maximum at x = 0.1. Changes in the various structural parameters like Fe-O-Fe bond angle, rhombohedral angle, tilt angle, etc., around the MPB region could be leading to the enhanced properties in this region. The higher magnetic, dielectric and magnetodielectric parameters around the MPB region suggest possible magnetoelectric coupling.

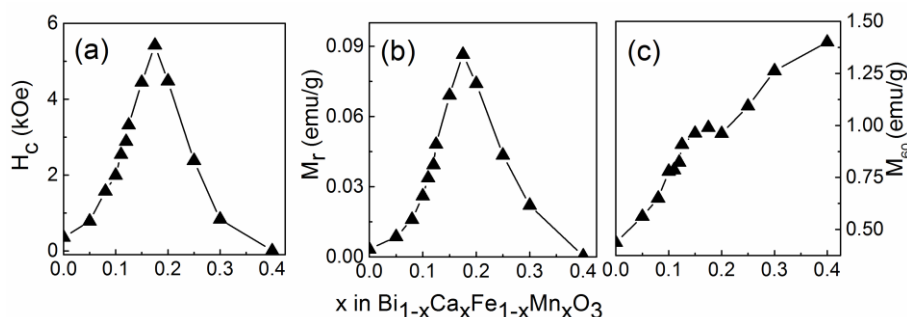


**Figure 1.** (a) Coercivity ( $H_c$ ), (b) remanent magnetization ( $M_r$ ), and (c) magnetization at 60 kOe ( $M_{60}$ ), at 300 K, as a function of  $x$  in  $\text{Bi}_{1-x}\text{Ca}_x\text{Fe}_{1-x}\text{Mn}_x\text{O}_3$

## References

- [1] V. A. Khomchenko et al J. Appl. Phys. 103 024105 (2008).
- [2] D. Tzankov et al, J. Phys. Condens. Matter **17** 4319 (2005).

## P39 - STUDY OF SPIN-VALVE SENSORS GROWN ON POLYMERIC SUBSTRATES

M. V. Ferreira,<sup>1,2,\*</sup> V. Silverio,<sup>1,2</sup> S. Cardoso,<sup>1,2</sup> and D. C. Leitao<sup>1,2</sup><sup>1</sup> INESC-MN, Rua Alves Redol 9, 1000-029 Lisboa, Portugal<sup>2</sup> Instituto Superior Técnico (IST), Universidade de Lisboa, Av. Rovisco Pais, 1000-029 Lisboa, Portugal

\*Corresponding Author: mafalda.ferreira@tecnico.ulisboa.pt

In recent years, the need for functional flexible electronic devices with intrinsic shaping capability has increased considerably. [1] A highly integrative solution consists in using magnetoresistive (MR) sensors showing high field sensitivity and spatial resolution, thus enabling highly accurate detection of surrounding magnetic fields. [2] As so becomes essential to thoroughly understand how sensor performance is affected as we extend the present well-establish cleanroom fabrication methods to flexible polymeric substrates.

Here we report the characterization of spin-valve (SV) sensors fabricated onto laminated 25  $\mu\text{m}$  Polyethylene terephthalate (PET) substrates (courtesy of Adhesives Research). A top-pinned SV stack was deposited by ion beam deposition with the following structure: Ta 2/ Ni<sub>80</sub>Fe<sub>20</sub> 2.5/ Co<sub>80</sub>Fe<sub>20</sub> 2.8/ Cu 2.8/ Co<sub>80</sub>Fe<sub>20</sub> 2.6 / Mn<sub>75</sub>Ir<sub>25</sub> 7/ Ta 5 (thickness in nanometer and target alloy compositions in percentage). Top-pinned SV sensors usually have no need for magnetic annealing treatments, advantageous for temperature sensitive substrates. The SV sensors were then microfabricated by optical lithography and ion beam milling steps, with a nominal dimension of 2 x 100  $\mu\text{m}^2$ . Electrical contacts of Al<sub>98.5</sub>Si<sub>1.0</sub>Cu<sub>0.5</sub>/Ti<sub>10</sub>W<sub>90</sub> were defined by lift-off. SV performance was evaluated at room temperature. Fig. 1(A) shows the magnetic behavior of an unpatterned stack, obtained with Vibrating Sample Magnetometry. The magnetotransport curves of micropatterned structures are shown in Fig. 1(B). Analytical calculations considering the Stoner-Wolfarth model were also performed.

Upon patterning, an increase of the coercivity and saturation field ( $H_{\text{sat}}$ ) of the SV transfer curves were observed, suggesting the presence of a non-negligible magnetostrictive term in the overall energy function of the system. [3] MR ratio reduction and increase in the offset field of the transfer curves were also noticed most likely correlated to an increase of surface roughness. Fig.1 (C) shows AFM measurements of a patterned SV sensor fabricated on laminated PET, with a root-mean-square roughness ( $R_q$ ) value of  $(0.77 \pm 0.05)$  nm, considerably larger than their rigid counterparts,  $(0.29 \pm 0.03)$  nm. Overall, PET films demonstrated to be a promising and viable substrate alternative for MR sensors. Tailoring of magnetostriction anisotropy becomes essential to achieve high-performance linear and non-hysteretic sensors.

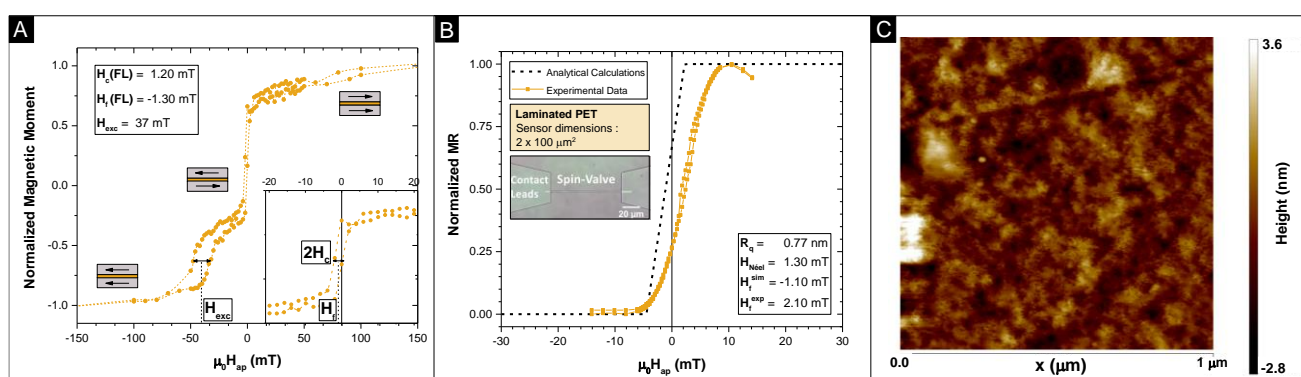


Figure 1. (A)  $M(H)$  behavior of a top-pinned stack grown on laminated PET. Inset shows detail on the free-layer reversal. (B) Normalized experimental MR curves and analytical calculations. (C) AFM characterization of a patterned SV sensor fabricated on laminated PET.

## References

- [1] Cañón Bermúdez et al., *Sci. Adv.*, 4,1, (2018).
- [2] Freitas, et al., *Proceedings of the IEEE*, 104, 10, 1894 – 1918 (2016).
- [3] L. Baril, et al., *J. Appl. Phys.*, 85, 8, 5139–5141 (1999).

# P40 - STUDY OF SUB-VOLUME ACTIVATION IN COFEB/MGO MEMORY DEVICES NEAR SPIN REORIENTATION TRANSITION

J. Fidalgo,<sup>1,2\*</sup> H. Lv,<sup>1,2</sup> A. V. Silva,<sup>1,2</sup> D. Leita<sup>1,2</sup> T. Kämpfe,<sup>3</sup> J. Langer,<sup>4</sup> J. Wrona,<sup>4</sup> O. Berthold<sup>4</sup> and S. Cardoso<sup>1,2</sup>

<sup>1</sup>INESC-MN and IN, Rua Alves Redol 9, 1000-029 Lisboa, Portugal

<sup>2</sup>Instituto Superior Técnico (IST), Universidade de Lisboa, Av. Rovisco Pais, 1000-029 Lisboa, Portugal

<sup>3</sup>Fraunhofer Institute for Photonic Microsystems IPMS, 01099 Dresden, Germany

<sup>4</sup>Singulus Technologies AG, 63796 Kahl am Main, Germany

\*Corresponding Author: joao.fidalgo.da.silva@tecnico.ulisboa.pt

Nanometric magnetic tunnel junctions (MTJs) for spin transfer torque (STT) based memory devices require simultaneously low critical current and high thermal stability. Perpendicular magnetic anisotropy (PMA) materials such as CoFeB/MgO interfaces fulfill these requirements in theory when compared to in-plane (IMA) materials [1]. However, fundamental questions relating to the spin reorientation transition between IMA and PMA are still open.

In this work, we study the STT behavior of CoFeB/MgO based MTJs, with a free layer (FL) thickness near the spin reorientation transition [2], and provide evidence of sub-volume activation through an estimate of the activation volume [3]. The MTJ stacks are deposited by Singulus and have the structure (Å): seed/[Co(5)/Pt(2)]x6/Co(6)/Ru(8)/Co(6)/[Pt(2)/Co(5)]x3/Pt(2)/reference layer separation/CoFeB(10)/MgO/CoFeB(13)/FL enhancement/MgO/cap. The stacks are fabricated into nanopillars at INESC-MN using a previously described process [4], and are electrically characterized through 4-point probe measurements. The effective diameter is extracted from the resistance  $R$  of unannealed samples dependence on nominal diameter (Fig. 1.a), with the model  $R=RA/(\pi(d+d_0)^2/4)$ , where  $RA=12.63 \Omega\mu\text{m}^2$  is taken from current in plane tunneling (CIPT) measurements and  $d_0=119\pm 4 \text{ nm}$  is the extracted correction to the effective diameter. The  $R(I)$  curves of samples, annealed at 300°C without magnetic field, show multiple stable  $R$  states (Fig. 1.b). The activation volumes are estimated from the critical current taken from the  $R(I)$  curves, and are shown to be consistently smaller than the effective volume of the FL (Fig. 1.c).

Evidence is shown throughout the present work that magnetization reversal mechanisms near the spin reorientation transition are quite complex, including multiple resistance states and estimated activation volumes pointing towards sub-volume activation of the free layer. However, this behavior is promising for multi-memory applications such as neuromorphic computing [5].

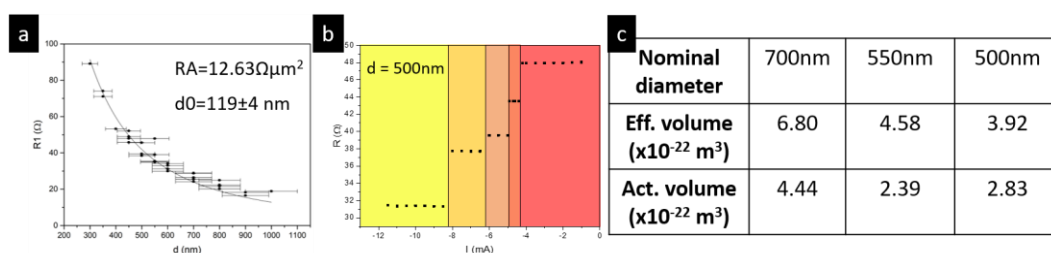


Figure 1.a. Fitting of  $R(d)$  model to resistance measurements and fitting parameters. b.  $R(I)$  curve for sample w/ FL thickness 1.3 nm, annealed at 300 °C without magnetic field, with multiple stable  $R$  states. c. Activation volume estimates compared with effective volume of the FL, in sample w/ FL thickness 1.3 nm, annealed at 300 °C without magnetic field.

## References

- [1] S. Ikeda *et al.*, *SPIN*, 2(3), 1240003 (2012).
- [2] S. Ikeda *et al.*, *Nature Materials*, 9(9), 721-724 (2010).
- [3] W. Wernsdorfer *et al.*, *Physical Review Letters*, 77(9), 1873-1876 (1996).
- [4] B. Pires *et al.*, *Journal of Manufacturing Processes*, 32, 222-229 (2018).
- [5] H. Mulaosmanovic *et al.*, *ACS Appl. Mater. Interfaces*, 9(4), 3792-3798 (2017).



## P41 - TERAHERTZ FREQUENCY COMB IN GRAPHENE FIELD-EFFECT TRANSISTORS

P. Cosme<sup>1,2</sup>, H. Terças<sup>1,2</sup><sup>1</sup>Instituto de Plasmas e Fusão Nuclear<sup>2</sup>Instituto Superior Técnico, Av. Rovisco Pais 1, 1049-001 Lisboa, Portugal

\*Corresponding Author: hugo.tercas@tecnico.ulisboa.pt

Field-effect transistors (FETs) are excellent candidates for all-electric, low-power radiation sources and detectors based on integrated circuit technology [1]. Thanks to the high electronic mobility, graphene FETs are well suited for low consumption devices. In this work, we show that a hydrodynamic instability can be explored (the Dyakonov-Shur instability [2]) to excite the graphene plasmons in a doped system. The instability can be sustained with the help of a source-to-drain current and controlled with the help of a gate voltage. It is shown that the plasmons radiate a frequency comb in the Terahertz (THz) range. We further compute the far-field radiation pattern and coherence, showing that a fairly coherent THz radiation is produced in the process. We argue how this can pave the stage for a new generation of low power THz laser sources in integrated-circuit technology [3].

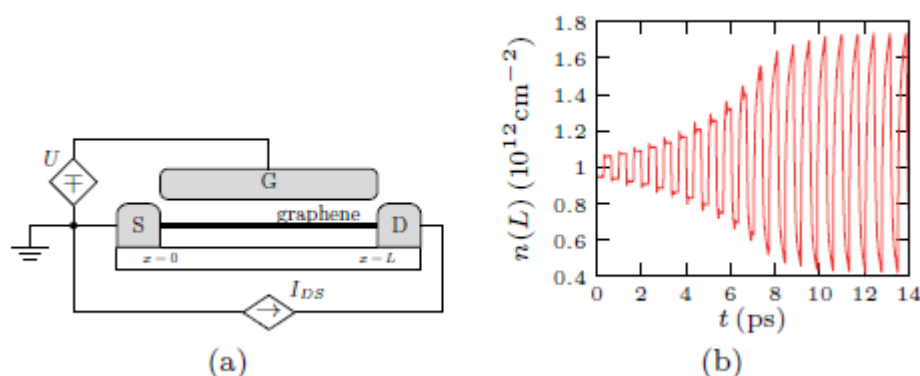


Figure 1. (a) Schematics of a graphene field-effect transistor and the asymmetric feedback boundary condition. A dc current is kept constant at the drain (D), while a constant electronic density is kept at the source (S). (b) Numerical simulation of the electronic density at the drain after the onset of the Dyakonov-Shur instability.

## References

- [1] D. Yadav, G. Tamamushi, T. Watanabe, J. Mitsushio, Y. Tobah, K. Sugawara, A. A. Dubinov, A. Satou, M. Ryzhii, V. Ryzhii, and T. Otsuji, *Nanophotonics* **7**, 741 (2018).
- [2] M. Dyakonov and M. Shur, *Physical Review Letters* **71**, 2465 (1993).
- [3] P. Cosme and H. Terças, (in preparation).

## P42 - THE SHAPE OF LIQUID BRIDGES

P. I. C. Teixeira<sup>1,2,\*</sup> and M. A. C. Teixeira<sup>3</sup><sup>1</sup>ISEL - Instituto Superior de Engenharia de Lisboa, Instituto Politécnico de Lisboa,  
Rua Conselheiro Emídio Navarro 1, 1959-007 Lisbon, Portugal.<sup>2</sup>Centro de Física Teórica e Computacional, Faculdade de Ciências da Universidade de Lisboa,  
Campo Grande, Edifício C8, 1749-016 Lisbon, Portugal.<sup>3</sup>Department of Meteorology, University of Reading, Earley Gate, PO Box 243,  
Reading RG6 6BB, United Kingdom.

\*Corresponding Author: piteixeira@fc.ul.pt

We have studied a single vertical liquid bridge spanning the gap between two flat, horizontal solid substrates of given wettabilities. For this simple geometry, the Young-Laplace equation can be solved (quasi-)analytically to yield the equilibrium shape, under gravity, of the two-dimensional bridge. We establish the range of gap widths (as described by a Bond number  $Bo$  for which the liquid bridge can exist, for given contact angles at the top and bottom substrates ( $\theta_c^t$  and  $\theta_c^b$ , respectively). We also obtain the minimum value of the cross-sectional area of such a liquid bridge, as well as the positions of any inflection points on its surface. This generalises our earlier work in which it was assumed that the gap is spanned by a liquid film of zero thickness.

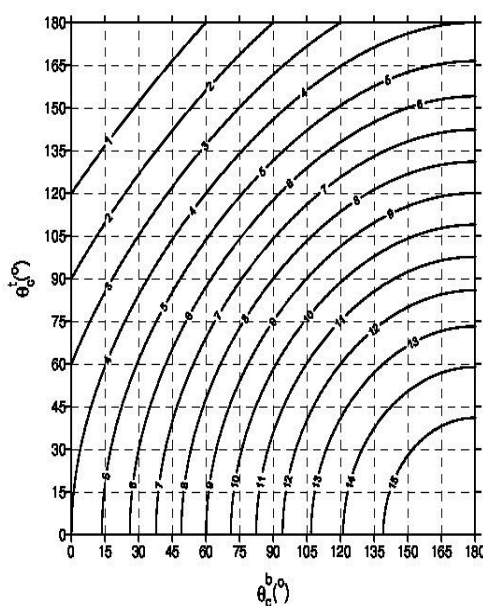


Figure 1. Maximum Bond number for which a liquid bridge can exist, for given contact angles at top and bottom substrates.

**P43 - TRANSPORT THROUGH PERIODICALLY DRIVEN SYSTEMS**Pedro Ninhos<sup>1,\*</sup><sup>1</sup>Department of Physics, Instituto Superior Técnico, Avenida Rovisco Pais, Lisboa, Portugal.\*Corresponding Author: [pedro.correia.ninhos@tecnico.ulisboa.pt](mailto:pedro.correia.ninhos@tecnico.ulisboa.pt)

Periodic drives have been receiving renewed attention as the building blocks of new phases of matter such as topological non-trivial states and time crystals. The dynamics of these new non-equilibrium phases is quite different from their equilibrium counterparts. When isolated, the evolution is strongly dependent on its initial condition. Yet, it is hard to imagine that such a regime can be experimentally probed in electronic systems, due to their short decay-times. In practice, it is expected that the state created after a long period of driving will be determined by the system's environment. We will consider electronic systems whose main thermalization mechanism is due to the contact with metallic leads. We will use this setup to probe transport through periodically driven systems in particular when the Floquet band structure acquires a non-trivial topology.

**P44 - M-THERMOELECTRIC DEVICES BASED ON HYBRID  $\text{Bi}_2\text{Te}_3$ /PVA COMPOSITES**

A. L. Pires<sup>1\*</sup>, I. F. Cruz<sup>1</sup>, J. Silva<sup>2</sup>, G. N. P. Oliveira<sup>1</sup>, S. Ferreira-Teixeira<sup>1</sup>, A. M. L. Lopes<sup>1</sup>, J. P. Araújo<sup>1</sup>, J. Fonseca<sup>2</sup>, C. Pereira<sup>3</sup>, and A. M. Pereira<sup>1</sup>

<sup>1</sup>IFIMUP and IN - Institute of Nanoscience and Nanotechnology, Departamento de Física e Astronomia, Faculdade de Ciências, Universidade do Porto, 4169-007 Porto, Portugal.

<sup>2</sup>CeNTI-Centre for Nanotechnology and Smart Materials, Rua Fernando Mesquita 2785, 4760-034 Vila Nova de Famalicão, Portugal

<sup>3</sup>REQUIMTE/LAQV, Departamento de Química e Bioquímica, Faculdade de Ciências, Universidade do Porto, 4169-007 Porto, Portugal.

\*Corresponding Author: up201510425@fc.up.pt

Thin and flexible micro thermoelectric generators ( $\mu$  –TEGs) are being envisaged as alternative power sources in the last decade. They constitute a new business opportunity for the packaging industry such self-powered wearable mobile electronics and/or to be used on remote places for low power consumption devices [1]. One approach to achieve this goal are by producing thin films using composite pastes composed by inorganic material and polymeric matrix to fix onto the flexible substrate. This strategy is the one that unveil better achievements in the last few years and more promising due to low cost production and the easy to scale up to the market. Nevertheless, although a thorough search is being under pursuit, the results unveil to be always smaller than the direct inorganic material thin films.  $\text{Bi}_2\text{Te}_3$  has been recognized as a prime TE material with the best performance values for near-room temperature applications and the most suitable material to fabricate devices. The current challenge is the combination of  $\text{Bi}_2\text{Te}_3$  materials with a polymeric matrix towards the production of a printable paste without loss of TE properties. Thus, the main goal of this work is to conceive a flexible and easy printed TEG prototype for energy harvesting [2]. Towards this goal,  $\text{Bi}_2\text{Te}_3$  TE material was synthesized by solid-state reaction using a close quartz-tube in a  $\text{N}_2$  atmosphere. The achieved material was submitted to a ball milling process to reduce the mean particle size down to  $50\text{ }\mu\text{m}$  and a pure phase of  $\text{Bi}_2\text{Te}_3$  was achieved after an acid treatment. Also, in this work, we report the use of ion-conductive polymer to produce flexible thermoelectric composites. A full study to obtain the best ratio between the inorganic and organic materials was addressed. The organic material used in this work allows to produce, in one hand, a flexible TE material and in the other hand if we used a concentration between 20-30 wt. % allows to increase the initial Seebeck coefficient of the  $\text{Bi}_2\text{Te}_3$  ( $\sim 156\text{ }\mu\text{V K}^{-1}$ ) in 14% leading to a power factor around  $0.0026\text{ }\mu\text{W K}^{-2}\text{ m}^{-1}$ . Finally, in this work it will be presented a flexible  $\mu$ -TEG produced with the best ratio of polymeric organic-based material as well as validated the power output achieved for a different bench of temperature gradients.

#### Reference:

- [1] M. Haras, T. Skotnicki, Nano Energy. 54 (2018) 461–476.
- [2] A. L. Pires, I.F. Cruz, J. Silva, G.N.P. Oliveira, S. Ferreira-Teixeira, A.M.L. Lopes, J.P. Araújo, J. Fonseca, C. Pereira, A.M. Pereira, ACS Appl. Mater. Interfaces. 11 (2019) 8969–8981.

## P45 - TUNING THE MAGNETOELECTRIC COUPLING IN $\text{TbMnO}_3$ BY FE-CHEMICAL SUBSTITUTION

A. Maia,<sup>1,\*</sup> R. Vilarinho,<sup>1</sup> M. Mihalik jr.,<sup>2</sup> M. Zentková,<sup>2</sup> M. Mihalik,<sup>2</sup> M. M. Cruz,<sup>3</sup> M. Godinho,<sup>3</sup> A. Almeida,<sup>1</sup>  
and J. Agostinho Moreira<sup>1</sup>

<sup>1</sup>IFIMUP, Physics and Astronomy Department, Faculty of Sciences, University of Porto, Rua do Campo Alegre 687, s/n- 4169-007 Porto, Portugal

<sup>2</sup>Institute of Experimental Physics of the Slovak Academy of Sciences, Watsonova 47, Košice, Slovak Republic

<sup>3</sup> Physics Department, Faculty of Sciences, University of Lisbon, Campo Grande, 1749-016 Lisboa, Portugal

\*Corresponding Author: up201405379@fc.up.pt

Magnetoelectric multiferroics, such as orthorhombic rare-earth manganites, where both magnetic and ferroelectric orders are coupled, have attracted great interest as they are crucial to magnetoelectric devices processing. In the case of  $\text{TbMnO}_3$ , an incommensurate sinusoidal collinear order of the Mn spins occurs at  $T_N = 41\text{K}$ , wherein the Mn spins lie in the  $bc$ -plane ( $Pbnm$  setting). Below  $T_{\text{lock}} = 28\text{K}$ , a magnetic transition occurs into a commensurate cycloidal spin order with Mn spins rotating in  $bc$ -plane, compatible with the stabilization of an improper ferroelectric polarization along the  $c$ -axis [1, 2]. Furthermore, it is possible to magnetically control the polarization, as a magnetic field along the  $b$ -axis rotates the cycloidal spin order to the  $ab$ -plane, and thus the electric polarization to the  $a$ -axis [1]. One way to tune the magnetoelectric coupling is by chemical substitution in  $\text{TbMnO}_3$ . The studies in ceramics show that the substitution of  $\text{Mn}^{3+}$  by small amounts of  $\text{Fe}^{3+}$  profoundly changes the magnetic structure, altering the magnetoelectric coupling [3]. However, as these studies were done in ceramics, anisotropic effects such as the flop of the cycloidal plane with an applied magnetic field cannot be ascertained. In this work, oriented single crystals of  $\text{TbMn}_{1-x}\text{Fe}_x\text{O}_3$  with  $x = 2, 4$  and  $6\%$  were used to measure polar, dielectric and magnetoelectric properties versus temperature and magnetic field along the crystallographic directions. The obtained results will be presented emphasizing the effect of temperature and magnetic field on their physical properties for different  $x$ -values.

### References

- [1] T Kimura et al, Phys. Rev. B, **71**(22), 224425 (2005).
- [2] M Mochizuki et al, Phys. Rev. B, **80**(13), 134416 (2009).
- [3] R. Vilarinho et al, JMMM, **439**, 167 (2017).

# P46 - BROADBAND THIRD-HARMONIC GENERATION IN MULTILAYER GRAPHENE FOR THE CHARACTERIZATION OF NEAR SINGLE-CYCLE ULTRASHORT LIGHT PULSES

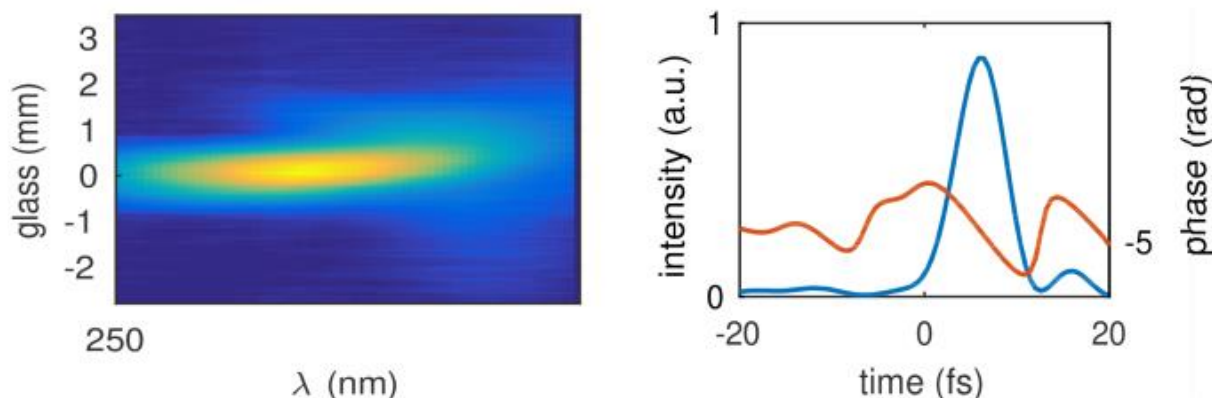
Tiago dos Santos Gomes<sup>1</sup>, Miguel Canhota<sup>1</sup>, Bohdan Kulyk<sup>2</sup>, Alexandre Carvalho<sup>2</sup>, Guilherme Gaspar<sup>2</sup>,  
António José Fernandes<sup>2</sup>, Florinda Costa<sup>2</sup>, Helder Crespo<sup>1</sup>

<sup>1</sup>IFIMUP-IN and Dep. de Física e Astronomia, Fac. de Ciências, Universidade do Porto, Portugal

<sup>2</sup> I3N-Aveiro, Dep. de Física, Universidade de Aveiro, Portugal

Email: [up201504587@fc.up.pt](mailto:up201504587@fc.up.pt)

Graphene - a single atomic layer of carbon atoms - is a very promising material in optics, mainly due to its extremely high broadband nonlinear optical susceptibility [1] and the possibility of occurrence of interband transitions at all optical frequencies. Ultrafast third-harmonic generation (THG) in graphene allows not only to characterize the used ultrashort pulses but also to study the dynamics of the charge carriers in graphene. Additionally, the possibility of obtaining an enhanced nonlinear signal when using multi-layer graphene [2] provides an additional interest to this work. The new technique of dispersion-scan developed by Miranda et al. [3] enables characterizing ultrashort light pulses using an unprecedentedly simple and fully inline optical setup. In this method, the spectrum of a nonlinear signal, such as second-harmonic generation (SHG) (or, in this case, THG), is recorded for different amounts of dispersion applied to a light pulse. It results in a 2D d-scan trace from which the spectral phase of the pulse can be retrieved and, therefore, by inverse Fourier transform, provides the exact temporal intensity profile of the pulse. The most common nonlinear signal for d-scan has been SHG, which can be a problem when using octave-spanning lasers, due to overlap between the SHG and the fundamental spectra. In these cases, it is helpful to use higher-order nonlinearities, like THG [4]. Here we will present several examples of THG d-scan measurements of broadband few-cycle laser pulses obtained in graphene films produced by different growth methods [5]. This enables the characterization of the used ultrashort pulses while providing insight of the electronic dynamics in graphene (a typical THG d-scan trace and the corresponding retrieved femtosecond pulse are shown below).



## References

1. E. Hendry *et al.*, Phys. Rev. Lett. **105**, 97401 (2009).
2. S.A. Mikhailov, Physica E **44**, 924-927 (2012).
3. M. Miranda *et al.* Opt. Express **20**, 688-697 (2012).
4. F. Silva *et al.*, in Conference on Lasers and Electro Optics (CLEO) (OSA, 2013), paper CW1H.5.
5. Bohdan Kulyk *et al.*, in Graphene Week 2018, San Sebastian, Spain.

## P47 - EPR AND AB-INITIO STUDIES OF ERBIUM(III) SIMS

Dorsa Komijani,<sup>1</sup> Maria Susano,<sup>2\*</sup> Manuela Ramos Silva,<sup>2</sup> Hélène Bolvin,<sup>3</sup> Laura C.J. Pereira,<sup>4</sup> Pablo Martín-Ramos,<sup>5</sup> Joana T. Coutinho,<sup>4</sup> Jesús Martín-Gil,<sup>6</sup> Manuel Almeida,<sup>4</sup> Stephen Hill<sup>1</sup>

<sup>1</sup>Department of Physics, Florida State University, National High Magnetic Field Laboratory, 1800 E. Paul Dirac Drive, Tallahassee, FL 32310, USA.

<sup>2</sup>CfisUC, Department of Physics, University of Coimbra, P-3004-516 Coimbra, Portugal.

<sup>3</sup>Laboratoire de Chimie et Physique Quantiques, Université Toulouse III, 118 route de Narbonne, 31062 Toulouse, France.

<sup>4</sup>C<sup>2</sup>TN, IST, Universidade de Lisboa, 2695-066 Bobadela LRS, Portugal.

<sup>5</sup>EPS, Universidad de Zaragoza, Carretera de Cuarte s/n, 22071, Huesca, Spain.

<sup>6</sup>Adv. Mat. Lab., ETSIIAA, Univ.Valladolid, Avda. Madrid, 44. 34004 Palencia, Spain.

\*Corresponding Author: maria.susano@gmail.com

Complexes of lanthanides, the 4f-block series elements, are the most promising candidates for Single-Ion Magnets (SIMs) that can retain their magnetization at practical temperatures. Their unquenched orbital moment promotes anisotropic magnetic properties in a ligand field, leading to magnetic hysteresis and slow relaxation of magnetization that can thus be observed in isolated, non-interacting lanthanide complexes [1]. In this work, we investigate the magnetism and the magnetization blocking barriers of two  $\beta$ -diketonate  $\text{Er}^{3+}$  compounds through *ab-initio* calculations, magnetization and EPR measurements.

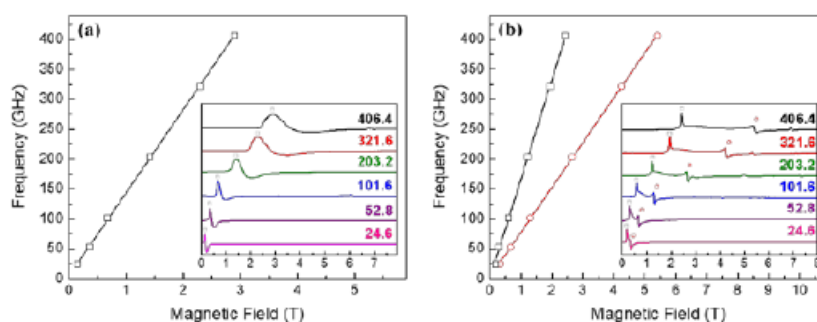


Figure 1. Frequency dependence of resonance magnetic fields collected for constrained powder samples of 1 (a) and 2 (b), at a temperature of 5 K. Insets show the respective powder EPR spectra, with the frequencies indicated above each trace in GHz. The solid lines result from the linear fit to the data points with the parameters  $g_1=9.9$  for 1 (a), and  $g_1=11.9$ ,  $g_2=5.4$  for 2 (b). The resonances marked with  $\square$  and  $\circ$  in the insets correspond, respectively, to the  $g_1$  and  $g_2$  positions of the  $\text{Er}^{3+}$  spectra; the unmarked resonances correspond to molecular oxygen.

Spin-orbit coupling was evaluated as a state interaction between all CASSCF (Complete Active Space Self-Consistent Field) wave functions by the RASSI (Restricted Active Space State Interaction) method, using the MOLCAS78 suite of programs [2]. Spin-Orbit (SO) integrals were evaluated within the AMFI approximation. Electron paramagnetic resonance measurements were carried out in powder samples, at a temperature of 5 K, frequencies ranging from 25 to 406 GHz, and with a magnetic field up to 15 T (Figure 1). The temperature dependence of the AC magnetic susceptibility was measured in the 10-10000 Hz frequency range at zero and 1000 Oe DC magnetic fields. Additional isothermal AC susceptibility measurements,  $\chi_{AC}=f(\omega)$ , were performed in the 10-10000 Hz frequency range, at a temperature of 1.7 and 7 K. All results will be presented, compared and discussed.

## References

- [1] Joana T. Coutinho, Bernardo Monteiro, Laura C.J. Pereira. "Ln(III)-based SIMs" Lanthanidebased multifunctional materials: From OLEDs to SIMs, edited by Pablo Martín-Ramos and Manuela Ramos Silva, Elsevier, 2018.
- [2] F. Aquilante et al., MOLCAS 7: The Next Generation, J. Comput. Chem., 31, 224-247, 2010.



**P48 - SYNTHESIS OPTIMIZATION OF ZN-MN FERRITES FOR FERROFLUID APPLICATIONS**

André Horta<sup>1,\*</sup>, F. Mohseni<sup>1</sup>, C. O. Amorim<sup>1</sup>, J. H. Belo<sup>1,2</sup>, J. S. Amaral<sup>1</sup>

<sup>1</sup>Departamento de Física and CICECO – Aveiro Institute of Materials, Universidade de Aveiro, Portugal

<sup>2</sup>IFIMUP and Department of Physics and Astronomy, Faculty of Sciences, Porto, Portugal

\*Corresponding Author: [andre.horta@ua.pt](mailto:andre.horta@ua.pt)

Zinc-Manganese ferrite nanoparticles have been the subject of increasing research due to their desired properties for hyperthermia applications. These properties include nanometer particle size, tunable magnetic behavior, and high saturation magnetization, providing these ferrites with the necessary requirements for cancer treatment via magnetic hyperthermia. During this ongoing research, we have synthesized and characterized Zn-Mn ferrite powders, aiming to optimize their structural and magnetic properties for further application in a ferrofluid [1].

In this work, samples were synthesized via the sol-gel auto-combustion and hydrothermal methods. As-burnt powders were characterized in XRD, SQUID, SEM and TEM. The XRD diffractograms and Rietveld refinement analysis unveiled the presence of ZnO secondary phase. In order to reduce ZnO phase content a thorough study of the synthesis conditions and parameters is underway. SEM reveals the agglomeration of the ferrite nanoparticles, as can be seen in figure 1, while TEM shows a wide particle size distribution ranging from 10 to 100 nm. Magnetization measurements reveal Curie temperatures above 400K for all samples and a varying blocking temperature, from 140 to 400K, together with a slow decrease in magnetization in ZFC curves for temperatures below the blocking temperature, which can be correlated the presence of particles with larger size, [2].

More recent efforts have been focused on using the hydrothermal method in order to decrease the particle size and its distribution, leading to a better control of the magnetic properties, such as blocking and Curie temperatures.

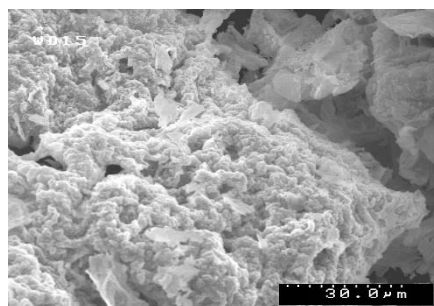


**Figure 4** – SEM image of Mn-Zn ferrite in the form of agglomerated nanoparticles.

#### References

- [1] N. Zhu et al, IEEE Trans. on Applied Superconductivity ASEM18-8265.
- [2] P. H. Nam et al, Physica B: Condensed Matter 550 (2018) 428-435.